

Check for updates

Material Design Strategies for Recovery of Critical Resources from Water

Omar A. Kazi, Wen Chen, Jamila G. Eatman, Feng Gao, Yining Liu, Yuqin Wang, Zijing Xia, and Seth B. Darling*

Population growth, urbanization, and decarbonization efforts are collectively straining the supply of limited resources that are necessary to produce batteries, electronics, chemicals, fertilizers, and other important products. Securing the supply chains of these critical resources via the development of separation technologies for their recovery represents a major global challenge to ensure stability and security. Surface water, groundwater, and wastewater are emerging as potential new sources to bolster these supply chains. Recently, a variety of material-based technologies have been developed and employed for separations and resource recovery in water. Judicious selection and design of these materials to tune their properties for targeting specific solutes is central to realizing the potential of water as a source for critical resources. Here, the materials that are developed for membranes, sorbents, catalysts, electrodes, and interfacial solar steam generators that demonstrate promise for applications in critical resource recovery are reviewed. In addition, a critical perspective is offered on the grand challenges and key research directions that need to be addressed to improve their practical viability.

1. Introduction

The production of many important technologies and commodities, such as batteries, electronics, chemicals, and fertilizers, is dependent on a stable supply of critical minerals and resources. For example, most lithium-ion batteries utilize cathode materials

O. A. Kazi, W. Chen, J. G. Eatman, F. Gao, Y. Liu, Y. Wang, Z. Xia, S. B. Darling
Chemical Sciences and Engineering Division
Argonne National Laboratory
Lemont, IL 60439, USA
E-mail: darling@anl.gov
O. A. Kazi, W. Chen, J. G. Eatman, Y. Liu, Y. Wang, Z. Xia, S. B. Darling
Pritzker School of Molecular Engineering
University of Chicago
Chicago, IL 60637, USA

The ORCID identification number(s) for the author(s) of this article can be found under https://doi.org/10.1002/adma.202300913

© 2023 UChicago Argonne, LLC. Advanced Materials published by Wiley-VCH GmbH. This is an open access article under the terms of the Creative Commons Attribution-NonCommercial-NoDerivs License, which permits use and distribution in any medium, provided the original work is properly cited, the use is non-commercial and no modifications or adaptations are made.

DOI: 10.1002/adma.202300913

containing cobalt, which has been classified as a critical mineral by the U.S. Geological Survey (USGS).[1] While the production of lithium-ion batteries for consumer electronics, electric vehicles, and renewable energy storage systems continues to surge, global cobalt reserves are placed under increasing strain. Geopolitical concerns further complicate the extraction of this resource, as ≈70% of global cobalt production is concentrated in the Democratic Republic of the Congo where child labor is allegedly used in mining operations.^[2,3] In addition to cobalt, there are dozens of other material resources necessary for essential products and services that have been deemed "critical" due to vulnerabilities in their supply chains with significant economic or security-related consequences. Many of these resources are represented through the list of critical minerals published by the USGS, including rare-earth elements (REEs) and metals used in batteries

(e.g., lithium, cobalt, nickel), catalysts (e.g., cerium, platinum, palladium), and other indispensable applications.^[1] Thus, there is an urgent demand for the development of sustainable recycling processes and extraction techniques to promote a more secure circular economy for critical resources.

It should be noted that there is no consensus on a universal method to quantify the "criticality" of a resource, in part due to the complexity of factors such as political, social, economic, geographical, and technological problems that may be unique to specific supply chains. In addition, a lack of abundant, accessible data fully encapsulating these factors and varying interests and goals of the stakeholders in studies on critical resources further complicate the quantification of resource criticality.^[4] Thus, minerals excluded from the USGS list such as phosphorus^[5] or copper^[6] could still be considered valuable to recover by other stakeholders. Thus, for the purpose of this article, we will not focus on the details of whether a specific resource is universally considered to be critical. When referring to critical resources, we specifically refer to material resources such as metals, minerals, and nutrients, excluding energy and fuels from the category.

Critical resources can be found in a variety of water streams including both anthropogenic sources (e.g., municipal water treatment, industrial wastewaters, acid mine drainage) and natural reservoirs (e.g., geothermal brines, seawater), presenting an opportunity to couple resource recovery with water treatment





processes.^[7,8] For example, lithium is another critical resource for energy storage technologies with significant quantities of its reserves being in geothermal brines in Chile.^[9] However, the arid Chilean deserts suffer from water scarcity issues that are exacerbated by the water intensiveness of regional mining operations.^[10] The development of separation technologies that can simultaneously extract resources like lithium while also generating clean water can substantially alleviate the stress on shared water reservoirs while also bolstering the supply of a vital critical resource. Combined resource recovery and water treatment processes can further promote a circular water economy by generating fit-for-purpose streams from nonfreshwater sources.

Aside from lithium, there are many other critical resources that can be found in water sources at concentrations suitable for recovery. However, the environmental and chemical conditions can vary drastically across different streams and resources (e.g., temperature, pH, dissolved species), necessitating the development of different technologies to selectively target specific resources over other interferent species. In municipal wastewaters, nutrients such as nitrogen and phosphorous are typically the resources of interest for recovery due to their value in fertilizer production and potential for eutrophication in effluent waterways. However, the presence of biological species and organic matter can cause fouling and interfere with the selectivity of materialbased separation technologies such as membranes or sorbents. Other resources in municipal wastewater, such as dissolved organics, cellulose, and metals, may also be valuable to recover depending on their concentrations and the efficiency of the recovery process.[11] In seawater and brines, the interest is typically more focused on recovering metals (e.g., lithium, heavy metals, REEs) due to their high value and limited supply in land-based ores.^[12] However, these metals are often present in much lower concentrations than other ions in saline waters such as Na⁺, K⁺, Ca²⁺, and Mg²⁺. This presents a paramount challenge of designing materials with properties that interact differently with cations based on their valence, size, hydration energy, or other distinguishable chemical properties. The compositions of industrial wastewaters are more unpredictable and can vary substantially depending on their source, but can also contain a variety of critical resources.^[13] The resources across all of these streams can exhibit starkly different physical and chemical properties (e.g., size, charge, solubility, volatility), requiring the development of robust separation technologies suited to recover targeted resources in their respective aqueous environments.

As the effects of climate change and rapid population growth continue to increase the strain on global supplies of both freshwater and critical resources, there is a growing need for separation technologies that can effectively address these intrinsically coupled problems. Material science and engineering can play a crucial role in developing those technologies by designing materials with surface and structural properties optimized to control their interactions with critical resources in water for their facile recovery. One of the key technical challenges in resource recovery from water is achieving a high selectivity, which requires materials that can screen dissolved resources from interferent species, often by tailoring their interactions at the solid–liquid interface. Fouling by particulates or biological media also presents a major challenge for separation processes in water as it can inhibit resource extraction by covering the surfaces of materials and phys-

ically damaging them. The cost, energy efficiency, and environmental impact of both the resource recovery process as well as the fabrication of the required materials must also be evaluated via technoeconomic and life cycle analyses to determine their viabilities for practical and sustainable deployment. There exists a vast space of material parameters that have been explored to address these challenges, including chemical composition, surface functionalization, morphology, hydrophilicity, zeta potential, and many others.

While there are several published reviews that focus on resource recovery, many of these exclusively discuss a specific subset of material classes, water sources, or critical resources. [11,14–25] To the best of our knowledge, there remains a need for reviews that comprehensively assess the key material-based technologies that have been developed for critical resource recovery from water. In this review, we discuss the recent advances in membranes, sorbents, catalysts, electrodes, and interfacial solar steam generators (ISSGs) that are of relevance to systems for critical resource recovery from water. Each of these fields possess an incredible depth of history and scientific literature that cannot be addressed in a single review. Instead, we seek to highlight how the different material compositions, structures, and properties that have been reported in the literature can be engineered to modulate the mechanisms and performance of these five separation technologies for resource recovery applications. The materials covered in this review include those that have been used directly for the recovery of different critical resources, as well as those that have been used for noncritical separations, which may be relevant to understand and adapt for applications in critical resource recovery from water. We believe both are important to discuss, especially as attention toward this research field grows rapidly. There are also many other separation processes that are relevant to resource recovery but are not driven by the properties of material technologies and consequently will not be discussed in this review, such as hydrometallurgy [26,27] (e.g., solvent extraction, chemical precipitation), coagulation/flocculation, [14] and biochemical processes.[28]

2. Membranes

2.1. Membrane Separation Principles

Membrane technologies have been used intensively in water treatment for decades because of their high efficiency, low cost, and energy-friendly character. Membranes are typically classified by their pore-size distributions. Nanoscale membranes with average pore sizes below 10 nm predominate in applications for critical resource recovery. In the context of resource recovery, the simultaneous presence of various types of solutes (e.g., metal ions, organic molecules, particulates) in water necessitates the design of membranes with selectivity for target resources. Effectively separating species with similar physical or chemical properties is a considerable challenge to both industrial applications and fundamental studies. The separation mechanisms and interactions between solutes and membrane surfaces play significant roles in solving such challenges.^[29] The three primary mechanisms of separation in membranes are size exclusion (steric hindrance). dielectric exclusion, and Donnan exclusion, each of which will be discussed. Membrane distillation crystallization, liquid-liquid



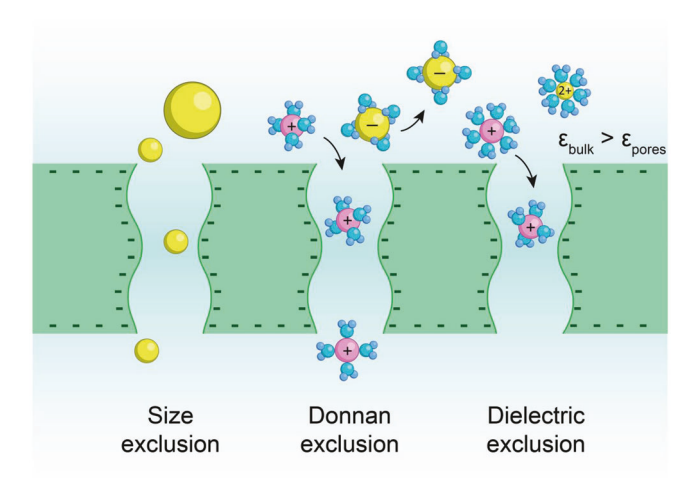


Figure 1. Schematic representation of the three primary membrane separation mechanisms: size exclusion, Donnan exclusion, and dielectric exclusion.

extraction, and electrodialysis have specific separation mechanisms that will be discussed separately.

Size exclusion separates solutes based on geometrical confinement, where solutes that are larger than the pore size are rejected by the pore opening (Figure 1). Depending on the target resource, the solute sizes can vary from a few angstroms (e.g., ions) to nanometers. When any charged species dissolves in water, it forms a surrounding electric field that attracts water molecules toward its surface to reduce the overall electric potential. Therefore, after being stabilized and hydrated by water molecules, the size of the charged species becomes larger than its static size. For example, the static ionic radius for a lithium ion (Li⁺) is \approx 0.07 nm, but its hydrodynamic ionic radius reaches \approx 0.34 nm.^[30] The interactions between ions and water molecules are relative weak, so water molecules can be either rearranged or removed when ions transfer across pores.[31] Membrane separation technologies apply size-exclusion extensively, but they lose the ability to distinguish solutes with similar sizes when the poresize distribution of the membrane is broad.

Most membranes are composed of materials with surface functional groups that can dissociate in aqueous environments to create a charged solid-liquid interface. A charged surface can interact electrostatically with ions in solution to reject them from permeating through a membrane via dielectric exclusion or Donnan exclusion (Figure 1). Due to the confinement effect, a solvation energy barrier is induced by the difference between the dielectric constants of the bulk solution and the solvent in the membrane matrix, preventing ions from passing through a membrane. The energy barrier hinders the transport of both cations and anions, regardless of their charge. This additional rejection mechanism is called dielectric exclusion, which is also influenced by a membrane's pore size, pore geometry, and surface charge. Donnan exclusion is observed in charged membranes (e.g., ion exchange membranes (IEMs)) that are only permeable to oppositely charged ions (counterions) and impermeable to similarly charged ions (coions). Counterions are attracted to the oppositely charged surface and then permeate though the membrane while coions are excluded outside the membrane, forming an

ionic concentration gradient that influences the subsequent diffusion of ions. Eventually, a Donnan equilibrium is formed at the membrane–solution interface where the electrochemical potentials of the permeable components are identical in both environments. The strength of the Donnan exclusion effect varies between ions of different valences, enabling the design of ionselective membranes.

Other membrane separation techniques apply different mechanisms to collect target species, as shown in Figure 2. The liquidliquid extraction technique uses a supported liquid membrane (SLM) containing an organic solvent to strip target molecules from the feed aqueous phase and then release ions to the receiving phase on the other side.^[32] The organic solvent in the membrane dissolves organic extracting agents that can form metalorganic ligand bonds to the target ions selectively in order to extract the ions from the other phase. Membrane distillation crystallization (MDC) employs hydrophobic microporous membranes to form a highly saturated salt solution through solvent evaporation. By creating a temperature difference across the membrane, a vapor pressure gradient is induced that drives solvent evaporation. The solvent vapors are condensed and collected in the cold stream, and the salt-containing solution is concentrated in the hot stream. Electrodialysis (ED) processes utilize alternating cation and anion exchange membranes to drive cationic and anionic migration in opposite directions through selective IEMs under an applied electric field. The targeted ions can then be collected at the corresponding reservoir. Among these three techniques, liquid-liquid extraction processes have not been largely used in the industry because of their low recovery efficiency. MDC is an effective process to recover ions and purify water but typically lacks the ability to separate individual ions. ED can achieve a high separation efficiency of ions with different charges, but further work is necessary to improve the separation performance for ions with the same charge.

2.2. Polymeric Membranes

Polymeric membranes are the most widely adopted membranes in separation industries because they are economical and easy to produce. Polymeric nanofiltration (NF) membranes corresponding to pore sizes of ≈1 nm or molecular weight cutoff (MWCO) of 150-300 Da have shown the ability to selectively reject multivalent ions while allowing monovalent ions to pass. Synthetic homopolymers are the most common materials that have been used to produce such membranes, such as polyethersulfone (PES), [35] polyacrylonitrile (PAN),[36] and polyimide.[37] Phase inversion is a traditional method to prepare membranes by controlling their immersion in a nonsolvent and the evaporation of a volatile solvent in a cast polymeric solution. It produces integrated asymmetric membranes with a dense skin layer on top providing selectivity and a thick but more open layer underneath providing mechanical stability. It is hard to control the formed pore size under the NF regime with phase inversion, so it has not been widely applied in producing NF membranes.

Interfacial polymerization is a common technique to produce NF membranes by polymerizing monomers on a porous support to form a thin but dense polymer barrier layer. Such membranes have shown potential advantages in multi-/monovalent ion



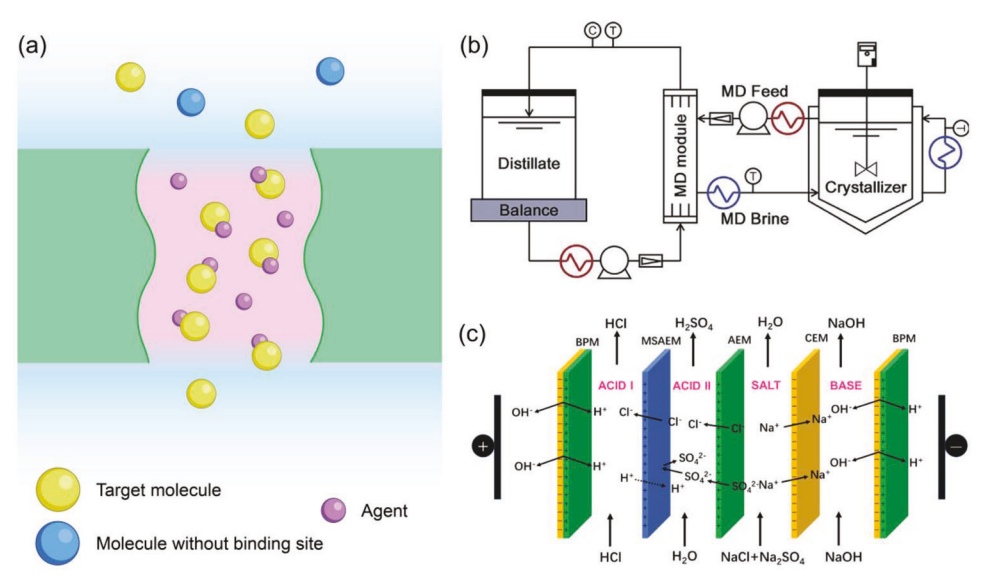


Figure 2. Separation mechanisms of membrane: a) liquid–liquid extraction; b) distillation crystallization; c) Electrodialysis. a,b) Reproduced with permission. [33] Copyright 2018, Elsevier. c) Reproduced under the terms of the CC-BY Creative Commons Attribution 4.0 International license (https://creativecommons.org/licenses/by/4.0). [34] Copyright 2020, The Authors, published by MDPI.

separations. For example, Shi et al.^[38] applied interfacial polymerization on a polyvinyl chloride hollow fiber membrane to form separation layers by moderately amplifying pore size, yielding an efficient Na₂SO₄/NaCl selectivity factor of 10.0. Thin-film composite (TFC) membranes with polyamide (PA) as the effective layer are a predominant type of commercial NF membrane prepared by interfacial polymerization. For example, NF270 is a common commercial TFC membrane with a polyester support matrix, microporous polysulfone interlayer, and polyamide barrier layer that shows high sulfate/chloride separation efficiency.^[39] The design of TFC membranes has been achieved through selection of monomer,^[40] manipulation of the membrane structure,^[41] regulation of the active layer network,^[42] and modification of electrical properties.^[43]

Renewable biomass is a valuable alternative material for producing NF membranes due to its abundance and biocompatibility, using sources such as polyphenol^[44] and chitosan. ^[45] For example, Zhou et al. ^[45] prepared a composite NF membrane from chitosan via a surface coating and chemical cross-linking method that exhibited a decreased salt rejection to different inorganic electrolyte solutions in the order of Na₂SO₄, NaCl, MgSO₄, and MgCl₂. While NF membranes have small pore sizes and strong electrostatic interactions to achieve ion selectivity, they also often suffer from low permeability, concentration polarization, and membrane fouling.

In contrast to NF membranes, loose nanofiltration (LNF) membranes with relatively large pore size (500 kDa < MWCO < 2000 kDa) can exhibit dye rejection as well as salt permeation, thus expanding the range of separable solutes. Similar to NF membranes, synthetic polymers have been used to fabricate LNF membranes. For example, Ding et al. [46] synthesized sulfonated polyethylenimine (SPEI) to form a loose active layer for LNF membranes. By controlling the degree of sulfonation of SPEI and the concentrations of monomers, a highly permeable NF–SPEI membrane was formed that presented high dye rejections and

low salt rejections. Bioinspired molecules such as polydopamine (PDA) have also been used increasingly as a multifunctional coating for membranes that exhibit desirable effectiveness in wastewater treatment. For instance, Wu et al. Modified basswood surfaces with PDA to obtain 3D wood-based ionic imprinted membranes for the separation of neodymium(III). They were able to achieve perm-selectivity coefficients greater than 10. However, the high cost of dopamine hinders large-scale applications, so alternative bioinspired materials such as gallic acid [50] and tannic acid [51] have been studied to produce LNF membranes.

Homopolymers and traditional fabrication methods lack the ability to precisely control nanostructure at the molecular level. Self-assembled materials represent a class of materials that use interatomic and intermolecular interactions to guide the organization of building blocks, such as block copolymers (BCPs) and liquid crystals. Such materials can form uniform, well-aligned, and ordered nanostructures, which enhance the selectivity. BCPs consist of multiple polymer chains that form characteristic structures at equilibrium in the size range of 5-50 nm. For example, Zhou et al.[52] used cylinder-forming polystyrene-block-poly(methyl methacrylate) as a template to fabricate continuous AlO_x channels with pore sizes from 21 to 16 nm. BCPs can be designed to contain blocks with different chemical properties, so the overall performance is enhanced by taking advantage of each building block. For example, a block copolymer poly(ethylene-b-vinyl alcohol) was used to prepare supported liquid membranes where the ethylene segments provide good chemical resistance and reduce the solvent-induced swelling, while vinvl alcohol units endow hydrophilic domains to create water-swollen ion-transporting channels.^[53] Liquid crystals (LCs) are advanced materials that show long-range order, forming uniform crystals with pore sizes of 0.5-2 nm. They are distinguished based on the forming condition (e.g., lyotropic and thermotropic) and molecular structure (e.g., rod shape, disk shape).^[54] The applications of LCs in membrane separation



ADVANCED MATERIALS

depends on the control of orientational alignment by surface interaction or external forces and mechanical robustness. For example. Bögels et al.[55] used 1.3.5-tris(1H-benzoldlimidazol-2vl)benzene and a polymerizable benzoic acid derivative to form a hydrogen-bonded complex. After self-assembling in a columnar hexagonal mesophase and cross-linking the alkene functionalities in benzoic acid, films with a high density of nanopores were formed and the surface was functionalized with carboxylic acid. The membrane selectively bonded with Na+ and K+ ions over Li⁺, Cs⁺, and ammonium (NH₄⁺), which was attributed to the smaller hydrated radius of Na+ and K+ ions compared to the other tested cations. This example demonstrates the potential of achieving selective separations between similarly charged species by precisely controlling membrane pore structures and uniformity, which is a key facet of the recovery of critical resources that coexist with many interferents in water sources.

Polymeric membranes can also be used in a variety of nonpressure-driven separation processes that can be translated toward applications in critical resource recovery. SLM offers opportunities to recover copper,[56] cobalt,[57] nickel,[58] and many other metal ions. The membrane materials should have chemical stability and permit high solute flux. For example, polyvinylidene difluoride (PVDF) was used as a SLM due to its resistance to harsh chemical conditions. Zante et al.[59] used a PVDF membrane to achieve selectivity for cobalt over nickel with separation factors as high as 218. IEMs inhibit the permeation of coions and promote adsorption of counterions due to the large amount of fixed charged groups within the structural matrix and the high thickness of the membrane. Most IEMs are polymeric membranes. For example, Radmanesh et al. [60] incorporated nanoclays into PES-based heterogeneous cation membranes to obtain selectivity of Na⁺ and Ca²⁺ over Mg²⁺. LNF membranes have also been used as anion-conductive membranes in a LNF-based ED process, which yielded 98.9% desalination efficiency and 99.4% dye recovery.[61] Mixed matrix membranes are made from blending polymers with either other polymers or microporous crystalline materials such as zeolites. Sheng et al. [62] prepared ZSM-5 zeolite/PVA-based mixed matrix membranes by a simple mixing and casting procedure and controlled the amount of ZSM-5 to produce a significant enhancement in both monovalent cation permeability and permselectivity.

Inspired by natural ion channels in cell membranes, research has also been done to create synthetic supramolecular ion channels using artificial compounds. The design principle for such ion channels consists of driving molecular components to self-assemble, employing various noncovalent atomic level forces such as electrostatic hydrogen-bonding and $\pi-\pi$ interactions. Gilles and Barboiul $^{[63]}$ prepared ureido-15-crown-5-ether compounds self-assembling in ion channel H-bonded superstructures within bilayer membranes. They found that channels were selectively responsive to the presence of K+ cations, even in the presence of a large excess of Na+ due to the multivalent sandwichtype binding toward K+ and larger cations. Designing a rational synthetic method for reliable and stable ion channels remains a significant challenge.

Membrane modification is a common and attractive method to either obtain additional functionalities while retaining pristine properties or change original physical/chemical properties to overcome inherent shortcomings. Major problems in membrane materials include undesirable confinement dimensions, fouling, wettability, low mechanical stability, and insufficient surface charge; each of these must be addressed to deliver effective resource-recovery membrane processes. In order to obtain antifouling properties, efforts have been done to minimize attractive interactions between the membrane surface and species. For instance, Yang et al.[64] fabricated conformal coatings of Al₂O₃, SnO₂, TiO₂, and ZnO on the surface of commercial PVDF membranes through atomic layer deposition. The membrane surface was imparted with mechanically rigid hydrophilicity that protected membranes from fouling by crude oil, a common constituent in industrial wastewater streams that may contain critical materials of interest. Cross-linking is a common method to improve chemical resistance and mechanical strength. Chen et al. [65] provided a novel method to prepare hollow fiber nanofiltration membranes through layer-by-layer deposition of polycations and polyanions. They performed cross-linking after each polyelectrolyte deposition, and the obtained membrane enhanced the size-exclusion effect and possessed good durability, performance stability, and acid/alkaline resistance. The surface charge of a membrane strongly affects ion selectivity, so modification of charge density and surface groups is intensively applied for desirable ion selectivity. For example, Yang et al.[66] grafted PEI on a PA surface to convert the original negatively charged surface to a positively charged surface. The PA layer played the role of size exclusion, and the PEI layer produced a strong electrostatic exclusion for the NF membrane to achieve a high separation factor of Li⁺/Mg²⁺. Heavy ion irradiation and UV exposure can be used to generate reactive free radicals and new functional groups for polymers with inert surface, and even create nanopores, [67] but such treatments might also cause surface damage during the radiation process.

Beyond improvement of the membrane structure, incorporating nanoparticles with special properties into membranes is another strategy to enhance membrane properties. For example, zwitterionic materials contain cationic and anionic groups, so they can attract water molecules via both electrostatic and hydrogen bonding interactions, providing a promising method to improve the antifouling property. Ma et al.[68] introduced a novel zwitterionic amine monomer polyethyleneimine-graftsulfobetaine methacrylate to electroneutral NF membranes that forms antifouling surfaces by interfacial polymerization. The addition of nanoparticles can also create extra water-passage channels and increase hydrophilicity, which improves permeability and antifouling properties. Zhang et al. [69] used layer-assembled in situ mineralization to prepare a CaCO₃/polyethyleneiminegallic acid (CaCO₃/PEI-GA) loose NF membrane that exhibited high permeability and fouling resistance due to the hydrophilicity of the CaCO₃/PEI-GA selective layer. The negative surface charge of the membrane also resulted in high rejection of dye molecules and low rejection of salts, which could present a useful strategy for isolating dissolved metal ions from wastewater.

2.3. Nanomaterials

2D materials are crystalline solids with a high ratio between their lateral size ($\approx 1-10~000~\mu m$) and thickness (<1 nm). [70] 2D material NF membranes for resource recovery have attracted



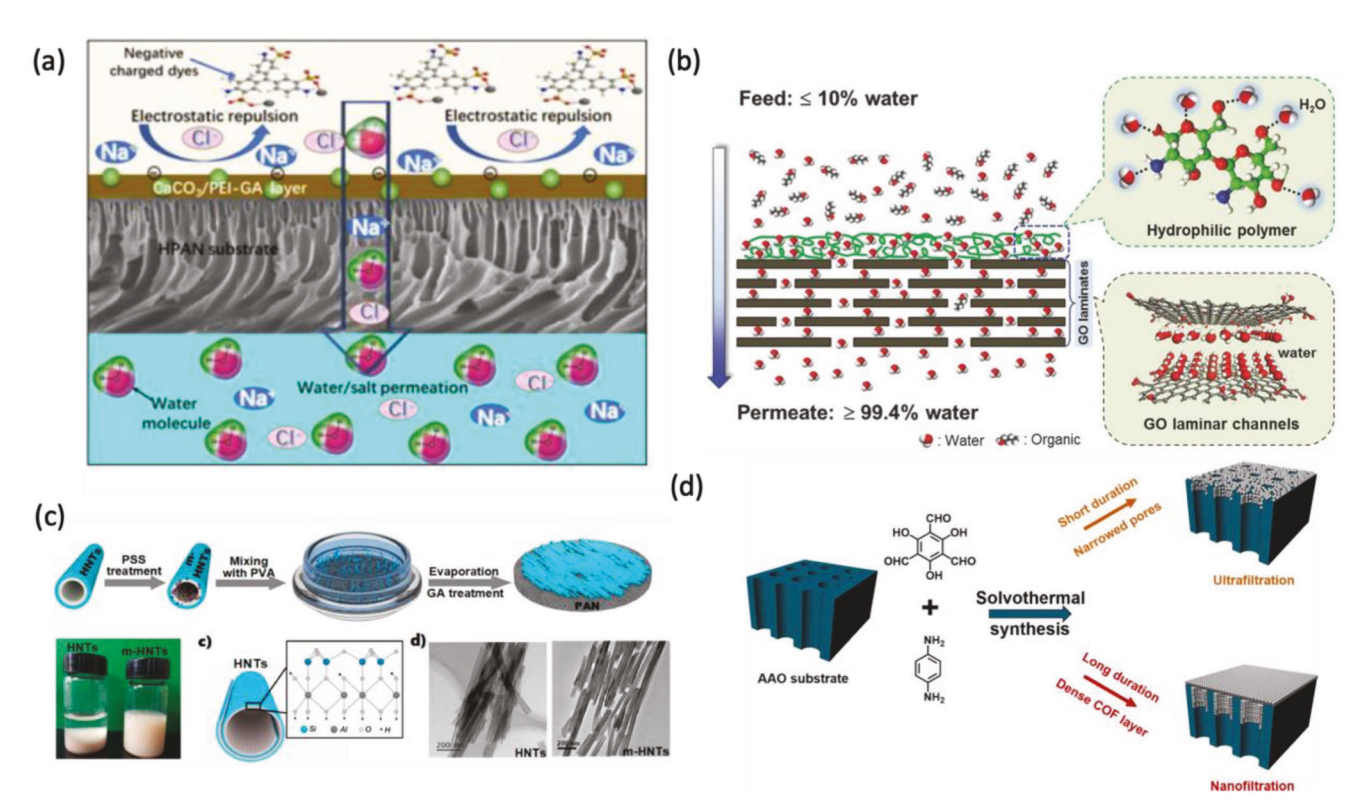


Figure 3. Membranes used for separation. a) A highly permeable loose nanofiltration membrane was prepared to achieve high dye rejection but low salt rejection. Reproduced with permission. Copyright 2019, Elsevier. b) Schematic of the water-organic separation process using the synergistic effect of a hydrophilic polymer and GO laminates. It exhibits two pathways for solute transport: inherent pore size and interlayer spacing. Reproduced with permission. Wiley-VCH. c) Fabrication process of clay nanotube membrane. Reproduced with permission. American Chemical Society. d) Illustration of COF-based membranes with adjustable performances by controlling the growth of COF crystallites on AAO substrates. Reproduced with permission. Copyright 2019, Elsevier.

attention due to their tunable physical confinement dimension, geometry, modifiable chemistry, and mechanical strength. Typical 2D NF membranes include graphene, graphene oxides, metal—organic frameworks (MOFs), and covalent organic frameworks (COFs)—and the categories are still expanding. There are two primary methods to use 2D materials as membranes: a 2D single-layer or a stacked thin-film membrane. For the latter, the inherent pore size and the interlayer spacing together form the physical confinement, as illustrated in **Figure 3**.

Graphene and graphene oxides were the first 2D materials studied for membranes because of their nanoplate structure, large surface area, and robust mechanical properties. Their surface is comprised of reactive oxygen functional groups, so surface functionalization is frequently applied to optimize performance. For example, Zhu et al.[74] grafted poly(sulfobetaine methacrylate) brushes on GO and prepared LNF membranes from mixing the composites with the PES via phase inversion. MOFs are porous materials constructed from organic-inorganic hybrid crystalline networks where metal ions form nodes and organic components form linkers. Guo et al.[75] prepared a polymer/MOF membrane from a linear polymer polystyrene sulfonate (PSS) with ample sulfonate groups to construct a PSS@HKUST-1 membrane and then further introduced sulfonate groups to direct the recognition of alkaline and alkalineearth metal ions. COFs are emerging crystalline polymeric networks in which organic units connect together to form in-plane ordered pores and stack vertically via π - π interactions. Their architectures can be tuned by designing molecular precursors based on reticular chemistry. For example, Zhang et al. [76] prepared a highly crystalline porous 2D cationic COF nanosheets through a Schiff base reaction between ethidium bromide and 1,3,5-triformylphloroglucinol. After performing a layer-by-layer restacking process to assemble a continuous and dense membrane on a nylon 66 support, they achieved selective sieving for ionic molecules of different molecular sizes and charges, along with high solvent permeability. This outlines a method to prepare cationic selective membranes from COFs by understanding and controlling how physical size and electrostatic interactions can collectively be used to target charged resources. Shi et al.^[73] demonstrated a controllable solvothermal synthesis of imine-based COF layers with adjustable pore sizes on anodic aluminum oxide (AAO) substrates, as shown in Figure 3. By controlling the duration of the synthesis, they could modulate the pore sizes of AAO supports till the formation of continuous COF layers, leading to a gradually enhanced selectivity. This further highlights the importance of controlling physical confinement and surface charge to enhance membrane selectivity for resource recovery applications.

Some other 2D materials have also drawn considerable attention for membrane applications. 2D transition-metal



timizing separation efficiency, and efforts to control pore-size distribution and surface chemistry, discover new membrane materials, and modify existing membrane structures continue.

dichalcogenides (TMDs or TMDCs) are a group of atomically thin nanolayers in the form of MX2, with M representing a transition metal atom (Mo or W) and X a chalcogen atom (S, Se, or Te). The MX₂ has the sandwich-like X-M-X structure where a plane of transition metal atoms separates two planes of chalcogen atoms. TMDCs have shown potential in resource recovery. Sun et al.[77] assembled chemically exfoliated tungsten disulfide (WS2) nanosheets into lamellar thin films and obtained an ultrafast separation membrane for small molecules (≈3 nm). Hu et al. [78] modified molybdenum disulfide (MoS₂) nanosheets with tannic acid yielding a superior performance of water flux and rejection of cations/organic dyes. MXenes are a relatively new family of 2D transition metal carbides, nitrides, and carbonitrides, which are formed by selectively etching A-layers from the existing ternary MAX phases, where "M" is a transition metal, "A" is a group IV-V element, and "X" is carbon and/or nitrogen. For example, Fu et al.[79] prepared multilayered oxygen-functionalized Ti₃C₂ (Ti₃C₂O_x) to achieve a highly efficient mercury(II) removal from water with ultrafast kinetics, impressive removal capacity, high selectivity, and strong pH independence.

Aside from those classic 2D materials, other materials with ordered structure can also be used in membranes for resource recovery. Materials with nanosheet, nanoflake, and nanotube morphologies have been investigated for membrane separations such as carbon nanotubes (CNTs),[80] boron nitride nanoflakes,[81] and halloysite nanotubes (HNTs).[82] Phyllosilicate minerals are naturally occurring clays that can be an abundant and low-cost source material for membranes. Xia et al. found that after exfoliation, vermiculite, a hydrous layered aluminosilicate compound, formed a nanosheet structure with a strong negative surface charge. After cross-linking with alkanediamine, the prepared 2D vermiculite membranes exhibited ion diffusivities tuned by the length of the selected diamine molecule. This opens a pathway to systematically tune ionic transport properties to design membranes for selective resource recovery.[83] Nanotube-structured materials can also be used to fabricate mixed matrix membranes or organic-inorganic hybrid membranes by dispersing them within a polymer matrix.^[84] Qin et al.^[72] fabricated composite HNT-based membranes (m-HNTs/PAN) via a simple and efficient evaporation-introduced method, which allows well-aligned nanotubes' composite membranes to show good fouling resistance against dye accumulation. The exploration of clay-based nanomaterials for membranes expands the potential range of material properties that can be controlled for enhanced solute separation and resource recovery systems. Enhancement and modification of these systems is a promising direction for future work.

2.4. Outlook

Application of membranes in wastewater and biomass treatment provides an effective and energy-efficient method for resource recovery. However, high concentration polarization, low chemical resistance, and serious fouling still impede some applications. Highly selective transport of specific molecules also remains a challenge when using current commercial membrane materials. Exploration of operating processes provides opportunities in op-

3. Sorbents

Adsorption technology has played a remarkable role in recovering critical resources from water, such as minerals for energy and catalytic applications, REEs, and nutrients.[19,24,85-87] Adsorption in water occurs at the solid-liquid interface between a sorbent and the solution when an adsorbate transports from the bulk solution to the solid-liquid interface and adsorbs onto the active binding sites. From a surface chemistry perspective, the adsorption mechanisms can be classified into inner sphere complex and outer sphere complex formation. As shown in Figure 4, in inner sphere complexes, the adsorbate is directly interacting with the sorbent interface without involving water molecules in between. This type of adsorption usually involves chemical or hydrogen bonding. Examples of inner sphere complex formation mechanisms include coordination and chelation reactions to form metal complexes,[88-90] surface precipitation of adsorbates onto sorbents,[91,92] and direct ligand exchange between adsorbates and sorbents. Outer sphere complex formation only involves physical interactions without bond formation, such as electrostatic, van der Waals, and hydrophobic interactions. A typical example of outer sphere complex adsorption is ion exchange, wherein an adsorbate replaces a coion at the diffuse double layer of an oppositely charged sorbent surface.

The chemical bonds formed in inner sphere complexes are typically strong, resulting in high adsorption affinity. However, due to the binding strength, inner sphere complex adsorption is typically irreversible, [86] which hinders the recovery of materials and regeneration of sorbents. For resource recovery, the sorbents that have captured the target resources could either be used directly as functional materials like catalysts and fertilizers or regenerated after extracting the resources by an elution process. In a typical elution process, the saturated sorbent is washed by a desorbing agent, although large volumes and high concentrations may be necessary for effective regeneration. For example, acid wash[93,94] or alkaline wash[95,96] elution processes are typically used to recover metal cations and nutrients by regenerating a sorbent via ion exchange with hydrogen or hydroxide ions. For adsorption based on ligand exchange, resource recovery requires desorption agents with stronger binding affinities than the adsorbed resource. A typical example of this is the recovery of metal ions through elution with surfactants to form chelates in bulk solution.[97]

Several figures of merit can be used to evaluate the performance of different sorbents, including adsorption capacity, removal efficiency, adsorption kinetics, selectivity, recyclability, and material and operational costs. The morphology of sorbents also influences their performance and can be characterized by specific surface area, porosity, geometry, and spatial organization. In porous sorbents, adsorbates can diffuse into the pores for adsorption, and the performance can be tuned by modulating the pore size, pore geometry, or overall porosity. The performance of sorbents also depends on conditions like temperature, pH, and operating ranges of adsorbate concentrations, which may govern



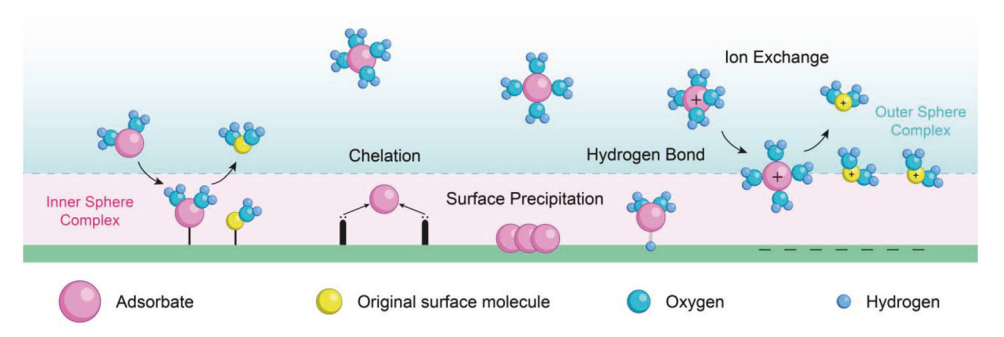


Figure 4. Adsorption mechanisms for capture of solutes on surfaces.

the utility of a sorbent for resource recovery from different water sources.

There are a variety of materials that could be used as sorbents for recovering different resources such as metals (e.g., REEs, precious metals, heavy metals) and nutrients (predominantly N and P). The major classes of sorbents include carbon-based materials, polymers, inorganic materials, organic frameworks, biomass, and composite materials, all of which are discussed in this section. Some examples of sorbent materials are shown in **Figure 5**, which are organized by material geometry. The scope of this content is inherently broad considering the number of material classes and target resources, so it is difficult to fully cover every aspect of adsorption for each material. This review is focused on providing an overview of the characteristics of common sorbent materials and pertinent strategies to improve their performance for resource recovery.

3.1. Carbon-Based Materials

Carbon-based materials represent a large material family that includes activated carbon, biochar, graphene, carbon black, and other carbon nanomaterials. They are the most commonly used sorbent materials in industry and have been extensively studied due to attractive properties for resource adsorption such as high surface area, hierarchical porosity, chemical stability, low toxicity, and availability. Their unique properties enable carbon-based materials to capture a variety of resources like REEs, [24] precious metals, [105] Li, [106] and nutrients. [107]

3.1.1. Activated Carbon

Activated carbon is a highly porous material with hierarchical porosity, large surface area, and abundant active sites, which are favorable for adsorption. Due to its high availability from nature and simple preparation process, activated carbon has been one of the most widely used commercial sorbents in water treatment. However, pristine activated carbon lacks selectivy toward specific adsorbates and requires appropriate surface modification to enhance its performance. For example, Zhang et al. loaded lanthanum oxide onto an activated carbon fiber to enhance the adsorption affinity for P by reacting via ion exchange, Coulomb, and Lewis acid—base interactions. Carboni et al. log fabricated a mesoporous carbon (MC) platform that shows no background adsorption of uranium (U)(VI) as a platform to study the effects of

15 different functional ligands on the adsorption capacity. They found that MC–O–PO(OH) $_2$ demonstrated a high adsorption capacity of >60 mg g $^{-1}$ while the other functionalized MC sorbents all had adsorption capacities <30 mg g $^{-1}$, emphasizing the importance of selecting the appropriate surface chemistry to optimize adsorptive performance.

3.1.2. Biochar

Biochar is a solid material derived from the thermochemical conversion of biomass in an oxygen-limited environment.[110] The chemical composition and properties of biochar depend on the type of biomass feedstock and the thermal treatment methods. Depending on the feedstock materials, biochar can be composed of carbon, hydrogen, oxygen, nitrogen, mineral elements, and nutrients.[111,112] Biochar is attractive as a sorbent due to its low cost, high surface area and porosity, and diverse surface functional groups, and has been demonstrated to be an effective candidate for nutrient recovery.^[20] Some researchers even have considered using biochar as an eco-friendly, low-cost alternative to activated carbon.[19,104] Huggins et al.[104] compared the nutrient recovery performance of granular wood-derived biochar (BC) and granular activated carbon (GAC), and found that BC showed a greater adsorption capacity than GAC at high initial concentrations of PO₄ and NH₄. They attributed the higher adsorption capacity of BC to its macroporous structure compared with the microporous GAC, as shown by scanning electron microscopy (SEM) images (Figure 5g).

Similar to activated carbon, specific surface modification, such as loading metal on biochar, can be desirable to enhance the overall performance. [107] However, a judicious selection of feedstock type is even more important since the properties of biochar mostly depend on the feedstock materials. [20,113] Although numerous surface modification methods of biochar have been reported, it is still difficult to control the properties of biochar precisely due to variabilities between feedstocks, introducing randomness to the production process. Yang et al.[20] have discussed possible strategies to reuse spent biochar sorbents together with the recovered substances, including using them as fertilizers, capacitors, catalysts, or for industrial production and use. Phosphorous is the most widely reported target for biochar-based adsorption in resource recovery due to the viability of the spent sorbent with the adsorbed P for reuse as a slow-release fertilizer.[107,114] In addition to P, examples of recovering other resources using

Figure 5. Examples of sorbent materials organized by material geometry. a) Self-assembled peptide amphiphiles for phosphate recovery. Reproduced with permission. [98] Copyright 2021, American Chemical Society. b) Functionalized magnetite particles for adsorption of noble metal nanoparticles. Reproduced with permission. [99] Copyright 2016, Elsevier. c) An illustration of lithium-ion sieves (LIS) technology. Reproduced with permission. [100] Copyright 2016, Elsevier. d) ZrO₂ for sequential recovery of Cr and V regulated by pH. Reproduced with permission. [101] Copyright 2016, Elsevier. e) UiO-66-NH₂ for the adsorption of Pd(II), Pt(IV), and Au(III) anions. Reproduced with permission. [102] Copyright 2017, Royal Society of Chemistry. f) An ion-cross-linked supramolecular Zn²⁺-poly(amidoxime) (PAO) hydrogel for uranium recovery from seawater. Reproduced with permission. [105] Copyright 2020, Wiley-VCH. g) SEM images of granular-wood-derived biochar (BC) and granular activated carbon (GAC) sorbents used in resource recovery. Reproduced with permission.[104] Copyright 2016, Elsevier.

biochar like precious metals, heavy metals, and REEs have also been reported.[19]

3.1.3. Graphene Family

Materials in the graphene family have demonstrated promising capabilities both for water decontamination and capturing critical resources.[19,87,105,115,116] The graphene family contains multiple materials whose structures are based on graphene, such as graphene nanosheets, GO, and reduced graphene oxide, fullerenes, nanotubes, and 3D graphite. Graphene materials that have been used in resource recovery typically possess features like high specific area, oxygen functionalities, abundant active sites for molecular binding and postmodification, and thermal and chemical stability.^[87] Liu et al.^[117] used graphene oxide nanosheets (GO NSs) as sorbents to capture copper ions in water and reduced them in situ to form copper nanoparticles (Cu NPs).



The resultant nanocomposite (Cu NPs/GO NSs) was shown to have in vitro antibacterial ability against *Escherichia coli*. In contrast to this application, the antibacterial property of graphene oxide and other graphene family materials like carbon nanotubes also raises concerns about unintentionally disrupting microbiota in wastewater during the resource recovery process.^[118] Similar to other carbon-based materials, the selectivity of graphene family materials is generally low but can be improved via surface modification.^[115,119]

3.2. Polymers

Polymers are attractive for resource recovery due to their facile processibility and high tunability in chemical structure and morphology to accommodate different target resources. They are also popular supporting materials for other functional materials in composite sorbents. We will discuss the application of synthetic polymers, natural polymers, and supramolecular receptors as sorbents for the recovery of precious metals, [105,120] nutrients, [87,121] REEs, [122] and other critical resources.

3.2.1. Synthetic and Natural Polymers

Synthetic ion-exchange resins (IERs) have shown great potential in resource recovery, especially for resource extraction and preconcentration, in part due to their commercial availability and their versatility to extract different charged species in water.[123,124] There are various types of mature IER sorbents available in the market with distinct surface properties suitable for different targets.[125] For example, Du et al.[126] used modified-Dowex M4195 resin to remove both phosphate and nitrate from water. Kumar et al.[127] tested the extraction performance of Tulsion CH-96 and T-PAR resins for seven heavy rare earths (HREs) and found that Tulsion CH-96 could directly be applied for binary HRE separations while the pristine T-PAR could not. Pristine commercial IERs do not always have sufficient capacities, kinetics, or selectivity toward specific resources and may require further modification to achieve desirable separation factors. Loading metal onto IERs is a common strategy to improve their selectivity. Clark et al. [128] prepared copper- and zinc-loaded resins to achieve selective recovery of total ammonia nitrogen (TAN) from wastewater. By binding each functional group in the IER with an ammine-complexing transition metal cation, they converted the IER to a ligand exchanger where the transition metals strongly bound anionic functional groups. This deterred competing cations from exchanging ions in the resin while TAN bound to the metal cations.

Hydrogels are another class of synthetic polymers that garnered interest for resource recovery applications. A hydrogel is a 3D cross-linked polymeric network that can swell to imbibe large amounts of water.^[129] Compared to rigid resins, hydrogels are more flexible and can uptake more water. Khan and Lo^[130] summarized the applications of hydrogels in the adsorption of multiple pollutants in water, including some critical resources of interest. They pointed out the advantages of using hydrogels as sorbents such as facile tunability and reusability. They also discussed the potential challenges of evolving hydrogels for practical

applications including stability, limited surface area, slow kinetics, limited selectivity, and difficulty recovering micro-/nanosized hydrogels from bulk solutions. Recently, Yan et al. [103] fabricated an ion-cross-linked Zn²+–poly(amidoxime) (PAO) supramolecular hydrogel (Figure 5f) for ultrahigh U recovery from seawater owing to the hydrophilicity of the hydrogel and the high PAO loading (\approx 96 wt%). High-performance polymer sorbents can also be designed by selecting an appropriate substrate polymer, grafting specific ligands, [131] and precisely designing chemical structures. [132] Selective polymer sorbents can also be prepared via ion imprinting, wherein artificial receptors for target ions are fabricated in the polymer, imitating a lock-and-key mechanism for capturing target resources. [133,134] In addition to surface binding sites, ion imprinted polymers can also exploit steric interactions and size exclusion to improve selectivity.

Natural polymeric sorbents mainly consist of materials extracted from living organisms, such as cellulose, [135] alginate, [136] chitosan, [137] and protein. [138] These materials are advantageous for being biodegradable and abundant in supply. They are often rich in hydroxyl, carboxyl, and amine groups in their structures that can efficiently bind with metal ions through various interaction modes, and therefore are commonly used to recover metal ions.[19,105] Examples of using natural polymer-based sorbents to recover phosphorus have also been reported.[87,136-138] For example, Venkiteshwaran et al.[138] selectively captured phosphate in the presence of arsenate by immobilizing phosphate-binding proteins (natural polymers) on N-hydroxysuccinimide-activated Sepharose 4 Fast Flow beads. Pristine natural polymers often cannot be used directly as sorbents due to their poor intrinsic selectivity for resource extraction. Chemical modification, [139] crosslinking, [137] and compositing [87] with other functional materials are general techniques to improve performance for resource recovery.

3.2.2. Supramolecular Receptors

Supramolecular receptors are organic molecules or supramolecular architectures consisting of molecules that are able to selfassemble into a large construct that offers multiple binding sites for targets. $^{[140,14\tilde{1}]}$ Some of the receptors have cavitary structures enabling host-guest interactions between the receptor and the target ions/molecules. Most of these macrocycles have tunable cavity size and chemistry to accommodate different targets. Some supramolecular receptors are commercially available and abundant in nature like crown ether and cyclodextrins. Crown ether is commonly used as a probe for Li recovery by providing multiple chelating sites for Li ions.[134,142] Cyclodextrins have larger cavities that are more suitable for capturing organic compounds, but can also be adapted to recover metal ions and nutrients. [143] Some artificial macroreceptors have been synthesized and used in the reclamation of phosphate from water like bipyridyl bis(urea)-based anion receptor,[144] cyanstar macrocycles, [145,146] and gadolinium complex, [147] as summarized by Othman et al.[87] Recently, Fowler et al.[98] presented a prototype of a material platform utilizing peptide amphiphiles (PAs) that can self-assemble into wormlike micelles to serve as a solid support for straightforward capture of phosphate from water at a certain pH. By adjusting the pH, they were able to controllably



release the captured phosphate for multiple cycles and demonstrated selectivity over nitrate and nitrite. Their simulation results emphasized the importance of PA packing in phosphate binding and indicated a new multichain phosphate-binding mechanism that was unique to PA micelles, as shown in Figure 5a. There are also examples of specially designed artificial receptors used for metal reclamation such as a primary amide prepared from commercially available ClC(O)CH2CH(Me)CH2/Bu and NH3 for the extraction of gold,[148] synthesized cucurbit[6]uril for gold recovery[149] and platinum recovery.[150] However, the examples of supramolecular receptors used in resource recovery are still limited due to their high cost and complex syntheses. Considering the highly tunable nature of such receptors to achieve outstandexchange ability, and positive surface charge. ing selectivity, there is a need for more exploration of supramolecular receptor-based sorbents in reclaiming critical resources.

3.3. Inorganic Materials

Inorganic sorbents can be classified into two main categories: metal-based materials and Si-containing materials. Metal-based materials include metal oxides, metal hydroxides, and metal sulfides. Metal-based materials designed for specific resource recovery applications like lithium sieves and magnetic nanoparticles will also be discussed. Si-containing materials include mesoporous silica, minerals, and clay. Inorganic materials generally have more ordered, crystalline structures than other sorbent materials, endowing them with unique properties like mechanical strength, stability in water, well-controlled surface properties, low loss of raw material during regeneration, and robust cycle performance.

3.3.1. Metal-Based Materials

Compared to pristine metals that are rare in their pure forms and may not have enough active binding sites for most critical resources, oxidized metal-based materials like metal oxides, hydroxides, and sulfides are more versatile sorbents that have been widely applied in recovering many resources like precious metal, [105] lithium, [151] and phosphate. [87] Various types of metal oxides have been reported as sorbents for resource recovery such as MnO_2 , $^{[152]}Mn_2O_3$, $^{[153]}CeO_2$, $^{[154]}Fe_2O_3$, $^{[155]}TiO_2$, $^{[156]}$ and ZrO2. [101] Metal oxides have often been prepared into nanoparticles to enhance removal efficiency, but aggregation is a common issue with nanoparticle materials. Using a porous supporting matrix like polymers or chelating with surface functional groups are common strategies to overcome this challenge.[105] pH-dependent binding mechanisms are often incorporated to achieve controllable capture and release of certain targets. For example, Wu et al.[101] found that pH had a strong effect on the adsorption and desorption of V(V) and Cr(VI) on a tetragonal ZrO₂ sorbent. By tuning the pH, they controlled the polyatomic ionic states of Cr(VI) and V(V) to achieve a separation factor of 362.05 in a 1:1 V/Cr solution at a pH of 3.5 and recovered each metal at >99.8% purity (Figure 5d).

Compared to metal oxides, metal-sulfide-based sorbents are relatively less explored. Due to the strong soft-soft interactions between sulfur atoms and precious metals, metal sulfides have shown potential for recovering precious metals.^[105] Examples of 2D metal sulfide sorbents including MoS₂, [157] CuS, [158] and 3D metal sulfides like SnS^[159] and WS₂^[160] have been reported. More research is needed to further understand and utilize the special sulfur affinity for capturing specific resources. Metal hydroxides like layered double hydroxides (LDHs) can also be useful sorbents for resource recovery. LDHs such as Mg, Fe-LDH[161] and CaFe-LDH[162] are composed of lamellar structures of divalent and partially substituted trivalent cations, accompanied by anions and water molecules in interlayer spaces to balance the overall charge. They are intensively studied in phosphate recovery due to favorable characteristics like high surface area, basicity, anion

Magnetic nanoparticles like nano zerovalent iron, magnetite (Fe₃O₄), and maghemite nanoparticles have sparked attention as sorbents because they can easily be incorporated into other material systems and be recovered by applying a magnetic field (Figure 5b). [87,92,99,163] Magnetic separation could also lower operation costs and recover sorbents more efficiently than conventional membrane filtration methods. The potential release of metal ions causing secondary contamination is a general concern for utilizing metal-based sorbents. To address this, an evaluation of release rates of metal ions from the sorbents is advisable to ensure that their use does not cause environmental pollution.^[101]

Lithium-ion sieves (LISs) are the most common sorbents for lithium recovery due to their high selectivity, uptake capacity, and cyclability. The main materials used for LISs include lithium manganese oxide (LMO), lithium titanium oxide, aluminum hydroxide, and mixed lithium manganese and titanium oxide, as lithium ions can easily enter nonstoichiometric crystalline networks of manganese and titanium oxides or aluminum hydroxide. [134] LISs are made by introducing template ions via redox or ion-exchange reactions and then eluting them from the crystal structure. The vacancies left by the template removal will selectively bind lithium ions due to ion-screening phenomena and the memory effect. [100,134,164] The mechanism is illustrated in Figure 5c. Yu et al.[151] assessed the adsorption capacity, selectivity, technological maturity, stability, regeneration ability, operating conditions, environmental safety, and cost of Mn-based, titanium (Ti)-based, and Al-based LISs. They summarized that Al-based LISs have the highest technological maturity, stability, cyclability, environmental safety, and the least stringent operating conditions and costs. However, their poor capacity and selectivity may hinder their application. By contrast, Mn-based LISs generally exhibit the highest selectivity, and Ti-based LISs possess the best adsorption capacities. These authors also highlighted the importance of pH in LIS performance owing to the Li-H ionexchange adsorption mechanism. [151] Several other reviews have provided a holistic overview of many important aspects of LIS technology, such as the synthesis, application examples, regeneration methods, advantages and limitations, and possible strategies to overcome the limitations, which will not be discussed here.[100,134,151,164]

3.3.2. Si-Based Materials

Mesoporous silica materials possess homogeneous pore sizes, high surface area, hydrothermal stability, and an abundance





of surface silanol groups enabling simple postfunctionalization. They serve as a rigid material platform with malleability to precisely control pore morphology and implement diverse surface chemistries. [19] Attaching appropriate surface functional probes can overcome the poor efficiency and selectivity of pristine mesoporous silica. For example, Chouyyok et al.[165] anchored both Cu(II)-ethylenediamine (EDA)-complexterminated silanes and Fe(III)-EDA-complex-terminated silanes onto a MCM-41 surface for phosphate adsorption. They found that the Fe(III)-EDA-modified MCM-41 sorbent was more effective than the Cu(III)-EDA-modified MCM-41, showing a higher distribution coefficient and lower silica and metal ion leaching rate in capturing phosphate. Zeng et al.[166] synthesized a 1.4.7.10-tetraazacvclododecane-functionalized mesoporous silica and evaluated its performance in adsorbing Pd(II) in HCl-HNO₃ solution. The results indicated that Pd(II) adsorption was rapid (within 30 min) on this sorbent, and the recovery rate could reach 85% with high selectivity over 16 interfering ions. Silica gel is another commonly used silica-based material in resource recovery with high porosity and is often prepared as nanoparticles. Silica gel is typically composited with polymer matrices^[167] to improve the adsorption affinity or with magnetic nanoparticles [168] to improve the removal efficiency.

Si-containing minerals are also attractive materials due to their natural abundance and low cost. They are also environmentally friendly as their exchangeable ions (Ca2+, Na+, and K+) are relatively benign.^[19] Natural porous minerals like zeolites,^[123,169] diatomite,[170] and palygorskite[171] have frequently been reported for nutrient recovery,[172] among which natural zeolites garner the most interest due to their high cation-exchange capacity and their molecular sieving properties.^[173] Clay minerals like halloysite, kaolinite, bentonite, montmorillonite, muscovite, illite, attapulgite, and modified natural and synthetic clays have also demonstrated their potential for the removal of critical metals.^[19] The primary adsorption mechanisms for mineral sorbents are ion exchange and surface complexation, which often make their adsorption behavior highly pH-dependent.[174,175] Just like the other sorbents discussed above, surface modification with organic ligands,[176] mixing with polymers,[177] or incorporating with metal oxides^[178] may improve the overall adsorption performance of mineral sorbents. Some non-Si minerals like hydroxyapatite may also be used as sorbents for reclaiming critical resources.[179] Despite a variety of natural and synthetic mineral candidates to explore in this field, more research is needed to develop facile and effective surface and bulk treatment methods to address the intrinsic limitations of raw mineral materials like poor selectivity and relatively low adsorption capacity.

3.4. Organic Frameworks (MOFs and COFs)

MOFs and COFs are two novel classes of porous coordination polymers existing in either 2D or 3D forms. Their distinguishing features including high surface areas, porous structures, controlled porosities, structural tunability, crystallinity, and abundant active binding sites make them valuable for capturing a variety of molecules and ions.^[19] Multiple types of MOFs have been utilized in critical metal recovery. For example, Fonseka et al.^[180] prepared a chromium-based MIL MOF modified by

N-(phosphonomethyl)iminodiacetic acid (PMIDA) to recover Eu from a zinc mine ore leachate. The sorbent showed high selectivity of Eu³⁺ over several other transition metal ions, which was ascribed to the binding between Eu³⁺ and the carboxylate, phosphonic groups, and residual amine groups of the PMIDA probes. By adjusting the pH, they were able to recover the captured Eu³⁺ without losing much sorbent material.

Zr(IV) species have been reported to demonstrate an affinity for various anions, making Zr-based MOF a powerful sorbent for reclaiming precious metal anions like $\mathrm{PdCl_4}^{2-}$, $\mathrm{PtCl_6}^{2-}$, and $\mathrm{AuCl_4}^-$ (Figure 5e). $^{[102,120]}$ Zr-based MOFs can also been applied for the capture and in situ reduction of metal cations. Li et al. $^{[181]}$ synthesized UiO-66 that selectively captured Pd(II) ions and reduced them into Pd nanoparticles in situ that were uniformly distributed in the MOF support within 5 min without any extra reductant or capping agent. The as-synthesized Pd@UiO-66 demonstrated catalytic ability toward Suzuki cross-coupling reactions. Other MOF materials like zeolitic imidazolate frameworks (ZIFs), Zn-based, and Cu-based materials have also been reported for recovering precious metals. $^{[105]}$

To gain P-capturing ability, MOFs have been often modified with La, [182] Zr, [183] and Fe, [184] which provide specific binding sites for P. Du et al.[121] pointed out the microporous structures of most MOFs might limit the diffusion of targets into the sorbents. Modification strategies such as reintroducing defects, adding additional bonding sites, and exposing introduced holes could be effective ways to create hierarchical porous MOFs to improve the adsorption performance. Yang et al.[185] summarized the application of MOFs for uranium recovery and identified chemical stability, selectivity, kinetics, mechanistic study, and processibility as challenges for this field. The high synthetic cost and poor processibility of MOFs due to their microcrystalline nature and powdery shape have hindered their application in industry. To address this challenge, research has been done to incorporate MOFs into substrate materials like polymers, magnetic nanoparticles, graphene oxide, or metal foams to impart simple operation and efficient separation.[105]

COFs are similar to MOFs, but instead of having metal-based nodes linked with organic ligands, the structure is fully comprised of covalent bonds to form pores in a cyclic manner. Metals like gold, [186] palladium, [187] and uranium [188] are typical targets for COF-based sorbents. Yue et al. [187] synthesized a new sp² carbon-conjugated covalent organic framework containing a selenodiazole structure for selective Pd removal and achieved an ultrahigh adsorption capacity of 4578.6 mg g $^{-1}$. Zhao et al. [189] demonstrated that the adsorption capacities of bipyridine-based COFs could be optimized by tuning the pore microenvironment, emphasizing the importance of choosing the right building blocks and surface functional groups for optimal adsorption performance.

3.5. Biological Materials

Biomass derived from plants, animals, or biodegradable waste products can not only be processed into biochar or zeolite materials^[190] but can also be used directly as sorbents for critical resource recovery. Biomass materials possess several advantages including natural abundance, simple processing, and



ADVANCED MATERIALS

biodegradability. Recycling waste or sludge as sorbents presents a sustainable strategy for resource recovery. Various examples of using domestic waste like fruit and vegetable peels, [191] agricultural waste like plant seeds, shells, and husks, [192] industrial waste like blast furnace slag [193] and fly ash, [194] animal waste like bones, [195] and marine waste like seaweed, brown algae, and peat moss [196] can be found in the literature. [197] Special care should be taken when selecting appropriate industrial by-products as sorbents as some of these materials may pose the risk of secondary pollution by potentially releasing toxic elements. [198] Some living or recently living organisms like fungi [199] and algae [200] have also been used for resource recovery.

Microorganisms like bacteria represent another class of biological materials that have been explored for recovering critical metals and nutrients.^[201-204] Cheng et al.^[205] studied the mechanism of adsorption and biomineralization of Ce³⁺ by a bacteria strain called Bacillus licheniformis. They found that Ce3+ was adsorbed onto the bacterial surface through binding with phosphate and carboxylic groups to form Ce(OH)3, which was subsequently transformed to CePO₄ and CeO₂ through biomineralization. By engineering E. coli bacteria, Xie et al.[204] designed a cascaded induction system to regulate terbium adsorption and recovery. The major drawbacks of microorganism-based sorbents are the strict requirements of operation and recovery conditions^[206] that limit their industrial applications.^[125] Won et al.^[207] discussed the requirements of applying biosorbents for metal recovery, such as process applicability, high adsorption capacity, fast kinetics, selectivity, and stability. They also proposed potential strategies to enhance resource recovery performance, such as pretreatment, increasing binding sites, eliminating the interfering sites, coating with ionic polymers, and genetic cell surface modification.

3.6. Composite Materials

Instead of using a single material, many sorbent designs combine two or more materials together to synergistically enhance the performance for resource recovery. Ramasamy et al. [208] fabricated a series of 1-(2-pyridylazo)-2-naphthol-grafted sorbents based on activated carbon and nanosilica to extract REEs from acid mine drainage. The hybrid sorbents showed better removal efficiency for 16 REEs and better selectivity in the presence of interferents ions (Na+, Ca2+, and Mg2+) compared to sorbents made solely from activated carbon or nanosilica. Making sorbents from composite materials can also improve their adsorption kinetics. Vicente-Martínez et al.[209] prepared silver-functionalized graphene oxides (GO@AgNPs) as sorbents to remove phosphates from water. Compared to pristine GO, GO@AgNPs showed instant removal of phosphate at nearly 100% removal efficiency while GO required >10 min to reach adsorption equilibrium at <80% removal efficiency.

Composite materials can also be designed to improve adsorption selectivity. Bui et al. [210] embedded nanoscale zirconium molybdate into an anion exchange resin to improve the selectivity of phosphate capture in the presence of sulfate interferents. Li et al. [211] combined two Li-selective materials (hollow ${\rm TiO_2}$ -based LIS and ZIF-8) together to enhance the overall Li selectivity by using ZIF-8 to regulate the hydration structure of ions, resulting in faster Li+ transport over other competing

ions. By incorporating magnetic nanoparticles into other material systems, efficient magnetic removal can be achieved. [212] By mixing with supporting scaffold such as polymers, the aggregation issue of nanoparticles, [87] poor processibility of MOF-based materials, [105] and immobilization of microorganism sorbents can be addressed.

Despite so many advantages of making hybrid materials, being practical and not overusing this strategy is important. Some researchers try to make multifunctional composites aiming to simultaneously remove two or more targets, or to achieve multimodal applications with a single sorbent like simultaneous catalysis and recovery. However, a careful evaluation of the manufacturing and real-world performance of such hybrid sorbents should be considered as they may not exceed the performance of a single material that targets a specific analyte in a resource recovery process.

3.7. Outlook

When assessing sorbent materials for specific resource targets and water sources, several factors aside from adsorption performance must be considered including cost, sustainability, reapplication strategy, and potential effects on other parts of multistage resource recovery systems.[17,172,213] Depending on the materials and applications, surface modifications, bulk material treatments, or designing composite materials may be necessary to develop an effective sorbent. Achieving high selectivity is a grand challenge for all sorbent materials and can be improved by grafting target-specific ligands, such as amidoxime groups for uranium capture, [214] or by exploiting ion-imprinted technology. [134] The development of cost-effective, nontoxic materials, as well as methods to efficiently recover both resources and sorbents are just as important as adsorption performance and are often overlooked in lab-scale research. The unintentional release of toxic species from sorbent materials can pollute water reservoirs and damage natural ecosystems, necessitating more scrupulous monitoring of sorbent loss and material leaching during resource recovery processes. Overall, sorbent materials offer a promising pathway to recover critical resources from water, but there is still a need for more emphasis on developing practical materials and fabrication processes that are viable for industrial scale-up.

4. Catalysts

Catalysis has emerged as a promising strategy for resource recovery from wastewater and seawater that has been studied and used in both lab-scale and field-scale applications. Catalytic processes have potential to exhibit high selectivity, activity, and reusability compared to some other conventional resource recovery strategies. Catalytic processes are mainly divided into two classes based on the form of energy input: electrocatalysis (electrical energy driven) and photocatalysis (optical energy driven). In some cases, electrocatalysis and photocatalysis can occur simultaneously via a process called photoelectrocatalysis, in which a semiconducting material absorbs photons and creates electron/hole pairs to carry out electrochemical reactions.



ADVANCED MATERIALS

4.1. Electrocatalysts

For electrocatalysis, the applied electric potential or current can be tuned to control yield and product selectivity. This has made electrocatalysis an attractive process for the recovery of a variety of different resources. Electrocatalysts have been applied most often for the extraction of metals such as REEs and uranium.

Phosphate (PO_4^{3-}), as an indispensable fertilizer component with limited supplies, is under increasing threat with rising food production demand. In recent years, electrochemical phosphate recovery has attracted attention because such processes are amenable to more facile control of the pH compared with traditional methods. [215] Electrochemical phosphate recovery is sometimes coupled with water electrochemical reduction. As the water reduction reaction occurs, phosphate precipitation takes place at or near the cathode. [216] Different advanced electrocatalysts designed for hydrogen evolution have the potential to be used for the purpose of phosphate recovery in the future.

Metal extraction from water has attracted more attention to date. For example, uranium, a vital resource for nuclear power generation, exists in seawater as a highly stable complex $Ca_{2}[UO_{2}(CO_{3})_{3}]$ at a concentration of 3.3 µg L^{-1} . [217] The quantity of uranium from seawater is sufficient to ensure sustained power generation for thousands of years, motivating the development of sustainable and economic technologies for its extraction.^[218] As described in the previous section, several sorbents have been developed with binding sites for uranyl ions (UO22+) such as amidoxime, polyphenol, and phosphate groups. However, the relatively sluggish kinetics have hindered practical application of the adsorption method for uranium extraction from seawater. Electrochemical methods coupled with adsorption have been pursued. In a recent contribution from Cui and co-workers, an electrochemical method was developed for the efficient extraction of uranium from seawater based on an amidoximefunctionalized carbon electrode. The amidoxime functionalization enables surface-specific binding to hexavalent uranyl ions, and uranyl ions were reduced to the insoluble tetravalent UO₂ on the electrode surface at the voltage of -5 to 0 V.[219] The amidoxime groups impart hydrophilicity and a high binding affinity to uranyl ions. The amidoxime functional group in the cathode serves as the chelation site, which is operated at -5 V.

In addition to the sorption applications described above, TMD monolayers offer potential catalytic applications in resource recovery. Recently, Zhu and co-workers developed MoS $_2$ nanosheets for both electrochemical binding and reduction of uranium. They demonstrated that the S edge sites in Sterminated MoS $_2$ nanosheets served as highly efficient active sites for the electrocatalytic extraction of uranium, the extraction capacity of which reached 1823 mg g $^{-1}$ at $-3~\rm V.^{[220]}$

Metal–nitrogen–carbon (M–N–C) nanomaterials have been applied as electrocatalysts in many applications. The single atom serves as the active site for selective catalytic reactions. Recently, Ma and co-workers reported a hollow nitrogen-doped carbon capsule supporting iron single-atom sites (Fe–N $_x$ –C) functionalized with amidoxime groups. The isolated iron centers (FeN $_x$) reduce the U(VI) to U(V). The uranium uptake capacity of this Fe–N $_x$ –C–R (R represents amidoxime groups) catalyst is 128 mg g⁻¹. Based on the same strategy, Ma and co-workers recently developed another metal–nitrogen–carbon nanoma-

terial for catalytic uranium extraction. They synthesized an indium–nitrogen–carbon catalyst, which was also functionalized with amidoxime groups for effective uranyl ion adsorption from seawater. The uranium uptake capacity of this $\rm In-N_x-C-R$ reached 335.4 mg g $^{-1}.^{[221]}$ Such adsorbent–electrocatalysis strategies exhibit efficient extraction of uranium from seawater and can likely be applied to recover other resources of interest as well.

Nonmetallic catalysts, although demonstrated for other aqueous electrocatalytic transformations such as nitrate reduction, have not yet been explored for recovery of critical resources from water. This area represents fertile ground for future research.

4.2. Photocatalysts

Photocatalysis is considered a promising approach to alleviate environmental pollution and simultaneously realize resource recovery from wastewater because of the possible utilization of solar energy as the energy input. Since the pioneering work from Fujishima and Honda utilizing n-type TiO2 photo-electrochemical cells to generate hydrogen from water in 1972,[222] chemical reactions initiated by photocatalysis have attracted much attention. Photocatalytic reactions normally occur at the surface of semiconductors and are induced by redox energy bands. The semiconductor is excited via transfer of reductive electrons from the valence band to the conduction band, leaving positively charged holes in the valence band. The excited electrons and holes afterward are separated and diffuse to the surface of the photocatalyst. Finally, the electrons initiate reduction reactions while the holes participate in oxidation.[222-224] Photocatalytic degradation of various pollutants in wastewater is typically an exothermic reaction, which is merely accelerated by the catalyst. This is in contrast to most reduction reactions, especially water splitting and CO₂ reduction, where the processes have $\Delta G > 0$ and require photochemical energy input to proceed. [225] Compared to degradation, recovery is likely the rate-determining step in synergistic photocatalytic systems. Thus, most efforts have been devoted to accelerating the kinetics of the catalytic process.

Early efforts began with the modifications of ${\rm TiO}_2$. For example, flame pyrolysis synthesis of P25 ${\rm TiO}_2$ resulted in a minority rutile phase fraction with enhanced photocatalytic activity. [226] Several methods to lower energy wavelengths, extending the photoactivity to the visible range, were realized by incorporation of transition metals [227] or introducing nonmetal dopants [228,229] to create oxygen vacancies or low-lying interband states. [230] Beyond modified ${\rm TiO}_2$, some other semiconductors that have been evaluated as substitute photocatalysts with visible light activity include ${\rm WO}_3$, [231] ${\rm C}_3{\rm N}_4$, [232] and perovskites. [233]

Heavy-metal ions accumulated in water circulation systems are a significant challenge, but also represent a potential resource to be recovered. Numerous methods have been developed for effective heavy-metal-ion removal and recovery from wastewater. Among them, photocatalysis has become a promising technology since the redox reaction induced by charge at the solid/liquid interface is often straightforward. Qu and co-workers simultaneously photoelectrocatalytically oxidized Cu-ethylenediamine triacetic acid (EDTA) at a $\rm TiO_2$ film electrode and reductively recovered Cu²+ at a stainless-steel cathode (**Figure 6**). The Cu²+ recovery ratio reached 67% after 3 h in this experiment. [234]

ADVANCED MATERIALS

www.advmat.de

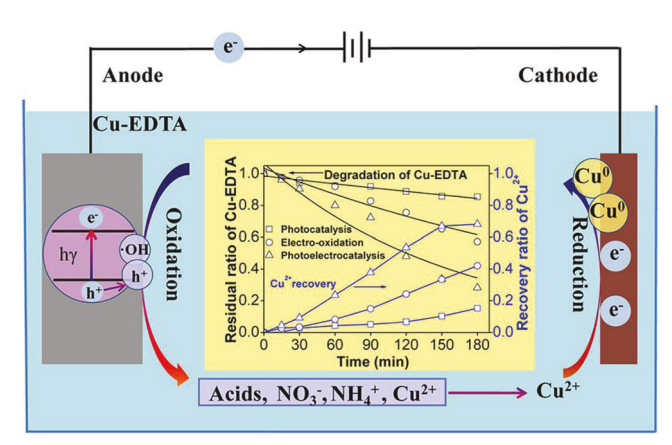


Figure 6. Photoelectrocatalytic oxidation of Cu–EDTA at the TiO₂ electrode and simultaneous recovery of Cu²⁺ by electrodeposition. Reproduced with permission. [234] Copyright 2013, American Chemical Society.

4.3. Outlook

The development of systems for photo- and electrocatalytic extraction of valuable metals from seawater and other water sources is still at an early stage and at this point is eclipsed by adsorption as the dominant mechanism of extraction. The mechanisms of catalytic extraction of targeted metal ions often remain elusive, and there is a need for more standardized methods to evaluate and compare the performance of catalyst materials. Considering the abundance of resources available in seawater and geothermal brines and the success of photo- and electrocatalysts in other industries, we anticipate that increasingly efficient catalysts for resource extraction will be discovered and developed in the near future.

5. Electrodes

Electrochemical processes have the capability to recover valued ionic species from unconventional sources such as seawater, wastewater, and brine.[219,235-237] By applying an electrical potential or current, ions in the source water can migrate toward specific electrode surfaces to chemically react or change valence. Recovery can be achieved by reducing cations and depositing them on the cathode surface (electrodeposition),^[235] or by storing them on the electrode surface (electrosorption) $^{[238]}$ or crystal structure (intercalation) and subsequently releasing them in a small amount of clean water by reversing the current direction. In all of these processes, electrode materials play important roles in determining the mechanism, rate, and selectivity of resource recovery. In this section, we introduce several electrode materials used to recover valued species, including emerging lithium intercalation electrodes, carbon-based electrodes, conventional mixed metal oxide electrodes, and their associated electrochemical processes.

5.1. Lithium Intercalation Electrodes

In the early 1990s, Kanoh et al. $^{[239]}$ reported an electrochemical system that achieved Li $^+$ insertion with a working electrode made

of λ -manganese dioxide (λ -MnO₂). Meanwhile, the same electrode showed no insertion response to K⁺ and Na⁺ in a mixed alkali metal ion chloride solution. Although selective insertion and extraction of Li+ was successfully demonstrated, water splitting taking place at the counter electrode (platinum, Pt) increased energy consumption, which hindered the further development of the system. In recent years, with soaring lithium demand due to the increasing need for lithium-ion batteries, new Li-extraction methods have been developed with the goals of improving recovery rate and selectivity while reducing cost and energy consumption. An electrochemical ion pumping method proposed by Pasta et al.[240] has attracted much attention as the process consumes less energy per kilogram of lithium recovered than the method reported by Kanoh et al. Electrochemical ion pumping generally takes place in electrochemical cells consisting of a lithium-containing electrolyte (e.g., oil and gas produced water, geothermal brine), a working electrode, and a counter electrode (Figure 7a). First, an electrical current is applied to the cell, causing Li⁺ ions to migrate from the electrolyte to the lithium intercalation electrode. The Li⁺ ions are then dehydrated and inserted in between the layers of the working electrode (Figure 7b). Next, the electrolyte solution is exchanged with a recovery solution with a reduced volume where Li⁺ is released by reversing the current direction. Finally, the Li-containing brine is flushed again in the cell and the cycle repeats itself multiple times to increase the Li concentration and purity of the recovery solution.

5.1.1. Lithium Iron Phosphate (LiFePO₄/FePO₄)

LiFePO₄ (LFP) is a common cathode material for Li-ion batteries. It was first introduced for battery applications in the 1990s as a cathode material in aqueous Li-ion batteries and possesses an ordered olivine structure shown by its characteristic X-ray diffraction (XRD) peaks.^[244] LFP has been used as a working electrode for lithium recovery from brines due to its stability in aqueous solution, appropriate working potential, and ability to store large quantities of ions per unit volume. It possesses 1D diffusion channels (Figure 7c) that grant facile Li⁺ ion insertion into octahedral sites via the reaction

$$FePO_4 + Li^+ + e^- \leftrightarrow LiFeO_4$$
 (1)

The ion-insertion process is governed by both thermodynamic and kinetic parameters. That is, limited by the channel dimensions of the FePO₄ host, ions first need to be fully dehydrated before intercalation. Next, ions migrate in the crystalline host materials and are stored in the interstitial sites. LFP demonstrates a low energy barrier for Li⁺ migration and a strong bonding energy with Li⁺ ions, making it a suitable candidate for selective Li⁺ ion insertion over competitor ions (e.g., Na⁺, K⁺, Mg²⁺, and Ca²⁺). The selectivity of Li⁺ intercalation over multivalent competitor ions like Mg²⁺ and Ca²⁺ is also enhanced by the lower energy requirement to dehydrate Li⁺.

Using FePO₄ as the working electrode, Yan et al.^[242] demonstrated the effect of solution composition on lithium selectivity and electrode stability. The authors compared the Faradic efficiency (i.e., the percentage of the charge flow that is effectively used to extract Li⁺) in binary solutions with Li⁺ and other cations

15214959, D. Downloaded from https://onlinelibbary.wie/.com/doi/10.1002/adma.2023090913by University of Chicago Litary, Wiley Online Library on [1708/2023]. See the Terms and Conditions (https://onlinelibrary.wie/.com/terms-and-conditions) on Wiley Online Library for rules of use; OA articles are governed by the applicable Creative Commons.

www.advmat.de

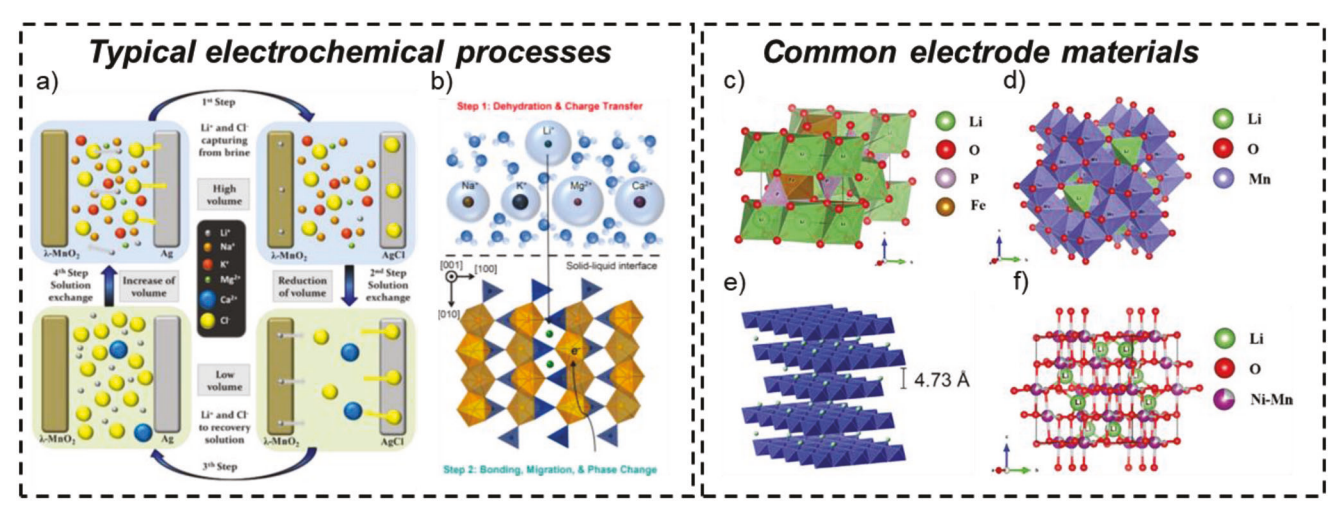


Figure 7. a) Steps to extract lithium from brine using a lithium-ion pumping method. The schematic utilizes a λ-MnO₂ lithium intercalation electrode as the working electrode and a Ag anion capturing electrode as the counter electrode. Reproduced with permission.^[241] Copyright 2016, Wiley-VCH. b) A schematic showing the solid–liquid interface during an ion intercalation process using FePO₄ as the working electrode. Reproduced with permission.^[242] Copyright 2022, The Authors, published by National Academy of Sciences USA. c–f) Crystal structure of: c) olivine LiFePO₄; d) spinel LiMn₂O₄; e) Li_{0.70}CoO₂; f) spinel LiNi_{0.5}Mn_{1.5}O₄. c,d,f) Reproduced with permission.^[18] Copyright 2020, The Authors, published by Wiley-VCH. e) Reproduced with permission.^[243] Copyright 2021, Elsevier.

(Na+, K+, Mg2+, and Ca2+) and showed consistently high efficiency (>93%) when K+, Mg²⁺, or Ca²⁺ are present with Li⁺ but lower efficiency when Na+ is present. This result identified Na+ as the primary competitor that lowers the selectivity of Li⁺ intercalation while K+, Mg2+, and Ca2+ are spectators that do not directly compete for host storage sites. Additionally, the long-term process stability in a simulated brine source was demonstrated over 100 cycles of intercalation and deintercalation, maintaining a Faradic efficiency of $100 \pm 2.5\%$ without significant selectivity decay. Furthermore, the authors pointed out that improving the Li⁺ to Na⁺ selectivity could allow the FePO₄ electrode to be used for more diverse source electrolytes with lower Li+ concentrations and Li⁺ molar ratios. In another example, Trócoli et al.^[245] also studied the effect of cations and current density on the ion selectivity of LFP hosts. They demonstrated that the selectivity was not only controlled by the intrinsic properties of the material but also by mass transport. Specifically, it was shown that the selectivity of Li⁺ over Na⁺ and Mg²⁺ depended on both concentration and current density. At high concentrations of Li+ in equimolar solutions with competitor ions, Li+ was recovered with a high selectivity independent of the concentration of other cations. However, in a simulated brine solution with lower concentrations of Li⁺ than competitor ions, the intercalation process was controlled by Li⁺ diffusion. Due to the high concentration of Na⁺, its cointercalation with Li+ was unavoidable at high current densities, leading to a decrease in Li/Na selectivity. Thus, it was concluded that lower current densities can yield better Li⁺ selectivity at the expense of a slower rate of extraction.

5.1.2. Lithium Manganese Oxide (LiMn₂O₄/ λ -MnO₂)

 $LiMn_2O_4$ (LMO) is a cathode material that possesses a spinel structure corresponding with the Fd3m space group. The spinel structure consists of 3D pores that can exclude large ions by steric

hinderance effects during the intercalation process (Figure 7d). These small pores favor Li⁺ transport, enabling the selective recovery of Li⁺ from brines. LiMn₂O₄ has tetrahedral 8a sites for Li⁺, octahedral 16d sites for Mn³⁺ and Mn⁴⁺, and face-centered cubic 32e sites for O²⁻. Intercalation phenomena in the electrochemical lithium recovery system can be described by the following redox mechanism. At the electrochemical reduction step, the valence of the manganese cations is changed from +4 to +3 and Li⁺ intercalates in the tetrahedral 8a sites. This process can be described as

$$2\lambda - \text{MnO}_2 + 0.5\text{Li}^+ + 0.5\text{e}^- \leftrightarrow \text{Li}_{0.5}\text{Mn}_2\text{O}_4$$

 $\text{Li}_{0.5}\text{Mn}_2\text{O}_4 + 0.5\text{Li}^+ + 0.5\text{e}^- \leftrightarrow \text{LiMn}_2\text{O}_4$
(2)

where ${\rm Li}_{0.5}{\rm Mn}_2{\rm O}_4$ serves as a partially lithiated transition composition.

At the electrochemical oxidation step, the valence of the manganese cations is changed from +3 to +4 and Li⁺ deintercalates. While both LFP and LMO have sufficient Li⁺ reactivity with and electrochemical stability windows for lithium recovery, the LMO electrode shows a much higher stability for repeated cycles and higher selectivity factors for Li⁺/Mg²⁺ separation. [246–248] As a result, LMO-based electrochemical lithium recovery systems have been studied more intensively than LFP.

 λ -MnO $_2$ was first used for lithium recovery from water as a working electrode to selectively react with Li $^+$ in the presence of oxygen evolution at the counter electrode surface (Pt), as reported by Kanoh et al. $^{[249]}$ The authors proposed a redox mechanism for Li $^+$ insertion into λ -MnO $_2$ accompanying a reduction of Mn $^{4+}$ to Mn $^{3+}$. In the 2010s, the use of electrochemical systems for lithium recovery based on the operating principles of batteries was first explored. For example, Lee et al. $^{[250]}$ used a rechargeable battery that consisted of a λ -MnO $_2$ positive electrode to capture lithium and a silver negative electrode to capture chloride anions. While this method demonstrated high lithium selectivity



ADVANCED MATERIALS

on the electrode have not been a focus in many studies, Battistel et al. [18] pointed out that both LFP and LMO could experience some problems in long-term cycling, as LFP's specific charge can degrade quickly while LMO suffers from structural instability due to unavoidable Mn dissolution. Other Li-intercalation electrodes such as NMC and LNMO have been less commonly studied for aqueous lithium recovery, as NMC has the lowest Li selectivity compared to the other electrodes discussed and LNMO is limited by a low maximum theoretical Li extraction capacity (12.66 mg g $^{-1}$).

and low energy consumption, further improvement can be made to increase the long-term stability and to design a more inexpensive chloride capturing electrode. Kim et al.[251] developed a flow system to recover lithium using λ -MnO₂ as the Li-intercalation electrode and activated carbon as the counter electrode to remove anions. The design also utilized an anion exchange membrane to prevent cation insertion at the activated carbon electrode. In a 30 mm equimolar solution containing chlorinated Li⁺, Na⁺, K⁺, Ca²⁺, and Mg²⁺, the Li⁺ concentration fluctuated by 5–6 mм during 30 min cycles of discharging/charging at 0.5 mA cm⁻² while the concentration changes of other ions were negligible, indicating the selective intercalation of Li⁺. High selectivity was also observed in a synthetic brine based on the composition of the Atacama brine, where the Li⁺ concentration increased by 60 mм after three cycles while the concentration changes of other ions were <1 mм.

5.1.3. Other Transition Metal Oxides

While LFP and LMO are two of the most commonly used lithium interaction electrodes for lithium recovery, other types of materials have been reported with excellent performance. Recently, a layered cobalt oxide electrode was studied to extract Li. Lithium cobalt oxide has been extensively studied in the Li-ion battery field and is known to favor Li+ intercalation over Na+ due to the large difference in their stabilization energies.^[252] Hill et al.^[243] formed a core-shell structure (Figure 7e), (NaLi)_{1-x}CoO₂, with a $\text{Li}_{0.94}\text{CoO}_2$ core, and $\text{Na}_{0.51}\text{CoO}_2$ shell when $\text{Li}_{1-x}\text{CoO}_2$ was submerged into an aqueous NaCl solution. It was further demonstrated that the Li phase restricted large layer spacing expansion and promoted Li intercalation over Na. LiNi, Co, Mn_{1-x-v}O₂ (NCM/NMC) represents another promising family of cathodes for lithium intercalation due to their high discharge capacity, moderate voltage platform, and high energy density. Within the NCM family, LiNi_{1/3}Co_{1/3}Mn_{1/3}O₂ has been drawing specific attention due to its unique structural properties. Specifically, only Ni²⁺ and Co³⁺ are electroactive during the redox reaction while Mn⁴⁺ remains inactive, deterring capacity fading that occurs during electrochemical cycling due to Mn dissolution and Jahn-Teller distortion. [253] LiNi_{0.5}Mn_{1.5}O₄ (LNMO) is another promising electrode material with cubic spinel structure (Figure 7f). It has a high charge/discharge potential (≈4.7 V vs Li/Li⁺), high theoretical specific capacity (≈147 mAh g⁻¹), and is less toxic than cobalt-containing cathodes. During the Li extraction process, Ni²⁺/Ni⁴⁺ and Mn³⁺/Mn⁴⁺ go through redox reactions that facilitate and accelerate the process.[18]

For lithium intercalation electrodes, aspects that should be considered for further development include lithium intercalation capacity, electrode stability in aqueous environments, manufacturing costs, and environmental impacts. Electrochemical process parameters such as energy consumption and counter electrode selection must also be considered. However, a comprehensive comparison between electrode materials is hindered by discrepancies in testing conditions and analysis methods. In general, LFP and LMO are the most widely studied electrodes for electrochemical lithium recovery due to their high selectivity for Li intercalation, although LMO surpasses LFP in Li⁺/Mg²⁺ separation. Additionally, while reusability and the effects of cycling

5.2. Carbon-Based Electrodes

Carbon-based electrodes have been widely used in electrochemical processes to effectively remove and recover ionic species for resource recovery (and desalination). Typical carbon-based electrodes include activated carbon, carbon aerogels, carbon nanotubes, carbon nanofibers, graphene-based materials such as graphene flakes, graphene loaded with metal oxides, and composites of graphene with other carbon-based materials. In general, carbon-based materials are selected as electrodes due to properties such as high specific surface area, porosity, broad poresize distribution, electrical conductivity, chemical stability, and low manufacturing cost. Due to the abovementioned properties, carbon electrodes have been applied in various electrochemical methods to recover valued resources from aqueous environments.

Carbon-based electrodes have been widely used for electrosorption technologies such as capacitive deionization (CDI) to recover heavy-metal ions and nutrients from different sources. The CDI process is operated by the adsorption of ions in the electrical double layer (EDL) of a capacitive electrode via either electrostatic interactions or Faradaic intercalation of ions into the crystal structure of the electrode (Figure 8a).[254] The most conventional CDI flow cell configuration, flow-by CDI, consists of a pair of oppositely charged porous carbon electrodes enabling capacitive ion sorption and a separator in between to prevent short circuit and allow water to flow. To begin with, a potential bias or a constant current is applied to the electrodes, causing ions to migrate toward oppositely charged electrodes. The ions are stored near the electrode surface due to the formation of the EDL, which is described using the Gouy-Chapman-Stern (GCS) model (Figure 8b). [254] It should be noted that the number of ions that can be stored in the EDL is closely related to the accessible electrode area. Therefore, materials with larger surface areas are usually more effective in ion removal and recovery. After the target ions are captured, the electrode can be short circuited or the current direction can be reversed to release the ions into a small volume of solution. In flow-CDI, the electrode material is dispersed in a suspension that circulates a predetermined path over a current collector. Such design further enhances the electrode capacitance, which could be beneficial for resource recovery. Other configurations of CDI include rocking-chair CDI, membrane CDI (MCDI), and flow-electrode CDI (FCDI) (Figure 8a). Interested readers are directed to the referenced reviews that offer more detailed analyses of CDI technologies.[15,254-256]



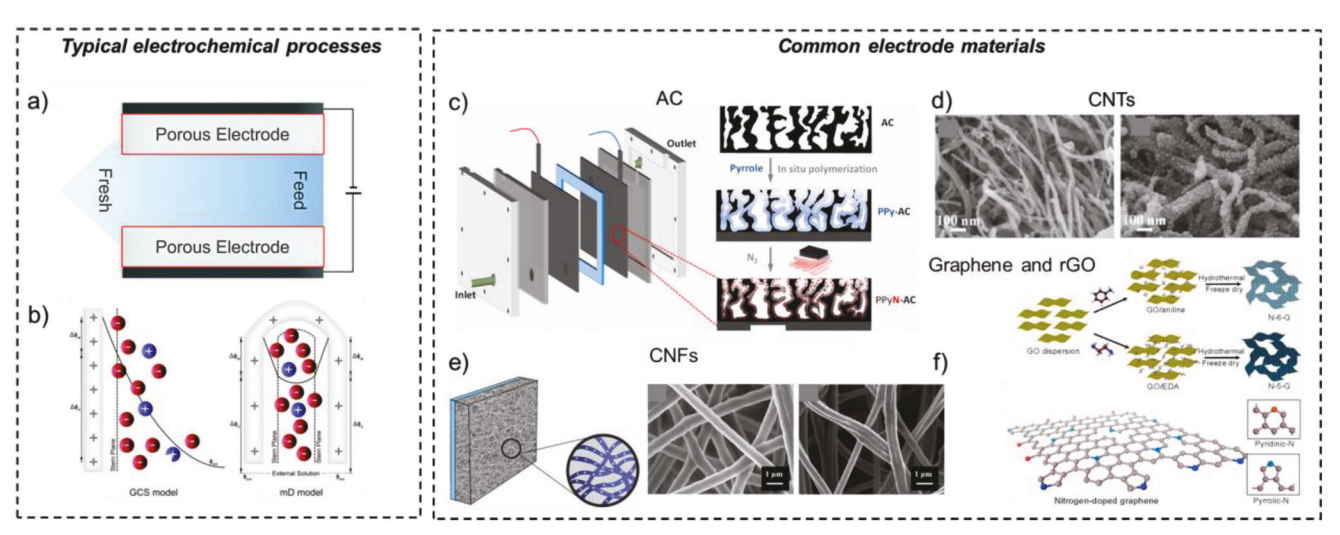


Figure 8. a) A typical flow-by CDI method to remove ions from an aqueous solution. b) Demonstration of an EDL formation on a charged surface based on the GCS model (left) and a modified Donnan (mD) model (right) which describes EDL with a finite pore structure. a,b) Reproduced under the terms of the CC-BY Creative Commons Attribution 3.0 Unported license.^[254] Copyright 2021, Royal Society of Chemistry. c–f) Schematics and SEM images of: c) pyrrolic-N-doped activated carbon electrodes (bottom); d) CNTs (left) and ferrocene–polyaniline-functionalized CNT electrodes (right); e) polyaniline CNF and polyaniline/CNT CNF electrodes; f) synthesis of N-doped graphene electrodes. c) Reproduced with permission.^[257] Copyright 2022, Elsevier. d) Reproduced with permission.^[258] Copyright 2022, American Chemical Society. e) Reproduced with permission.^[259] Copyright 2016, American Chemical Society. f) Reproduced with permission.^[260] Copyright 2018, Elsevier.

5.2.1. Activated Carbon

Various forms of activated carbon have been studied as electrode materials. The material is known for its high surface area, relatively high electrical conductivity (10⁻⁸-10¹⁰ S m⁻¹), and low cost.[261] Surface area of the activated carbon electrode could be as high as 1000-2000 m² g⁻¹ for some synthesized activated carbon fibers, aerogels, and cloths.[262] Activated carbon electrodes can be fabricated by pyrolysis at high temperatures with oxidizing gases or via chemical activation at lower temperatures in the presence of activation agents such as phosphoric acid or potassium hydroxide. Fabrication conditions yield varying pore sizes in the activated electrodes, which are classified as micropores (<2 nm), mesopores (2–50 nm), or macropores (>50 nm). [261] Ion removal and recovery efficiency of a CDI process depends on the capacitance of the electrodes, which is mainly determined by the electrode surface area. However, other properties such as porosity, pore-size distribution, conductivity, and surface functionality also influence the capacitance.

Bao et al. [263] studied the separation and recovery of vanadium (V(V)) from a simulated vanadium-bearing solution in a CDI unit with a resin-activated carbon (RAC) composite electrode. Separation of impurity ions such as Al, P, and Si from V(V) was achieved as the impurity ions were adsorbed in the EDLs of the RAC electrodes while V(V) was adsorbed by the resin. The adsorbed impurity ions could be removed by eluting with H_2SO_4 followed by V(V) recovery by eluting with NaOH.

Activated carbon can also be applied as a suspended electrode in a FCDI process, where a carbon suspension can be pumped through electrode compartments and flowed between the ion-exchange membranes and current collectors. The electrode circulation enables continuous removal and recovery of ions with no need for a discharging step.^[264] Bian et al.^[265] reported a FCDI

process with suspended activated carbon as the electrode material to remove and recover salt (NaCl), $\rm NH_4^+$, nitrate (NO $_3^-$), and $\rm PO_4^{3-}$ from a synthetic wastewater. The authors showed that the salinity removal efficiency increased with increasing carbon loading from 5 to 15 wt%. When a reverse potential was applied, more than 80% of the removed nutrient ions were recovered in the concentrate during discharging operation. Activated carbon could also serve as a support material in a composite electrode. For example, Lin et al. $^{[266]}$ reported a FCDI method using electrodes composed of potassium titanate ($\rm K_2Ti_2O_5$, KTO) mixed with activated carbon powder (KTO–AC). The KTO–AC electrode exhibited a much higher specific gravimetric capacitance in NH $_4$ Cl solution than in NaCl solution, mainly due to the highly favored adsorption of NH $_4^+$ on the KTO compared to that of Na $^+$.

5.2.2. Carbon Nanotubes and Carbon Nanofibers

CNTs are used as capacitive electrodes due to their high electrical and thermal conductivity, mechanical stability, and high porosity stemming from their tubular structure (Figure 8d). However, pure CNT electrodes have limited specific surface area (100–400 m² g⁻¹), which results in relatively low capacitance, making CNT electrodes less attractive for CDI than other carbon-based electrodes. [267] It has been suggested that more structural defects in CNTs can increase the capacitance as the defects can act as active sites for ion adsorption. Hence, one strategy to increase the capacitance is through chemical modification of CNTs with other functionalities. For example, Ren et al. demonstrated that doping CNTs with nitrogen enhances their hydrophilicity and electrosorption capacity for Na⁺ ions in CDI. [268] Moreover, CNTs can act as conductive additives for other functional materials, such as



ADVANCED MATERIALS

www.advmat.de

polymers and metal oxides, or they can be incorporated into carbon/carbon composite materials. [267]

Carbon nanofiber (CNF) can also be used as a capacitive electrode because of its high electrical conductivity, chemical stability, and relatively high specific surface area due to its small fiber diameter ($\approx\!100$ nm) and high porosity (Figure 8e). [269–271] Research on enhancing the capacitance of CNF electrodes has primarily been focused on manipulation of fiber morphology, addition of pseudocapacitive materials, and incorporation of highly conductive materials. [261] For example, several studies showed that the electrochemical capacitance of the CNF can be improved by incorporating redox-active materials. [272,273] Additionally, the electrical conductivity of CNF can be increased by fabricating composite materials with CNF and CNTs.

Gao et al.[258] reported a CDI process using a ferrocenepolyaniline-functionalized CNT (Fc-PANI/CNT) electrode to selectively recover phosphorus from wastewater. PANI was selected as the polymer phase because of its high doping level, electrical conductivity, and environmental stability, whereas Fc amides were embedded in the polymer phase as active moieties. During the CDI test, the phosphate adsorption capacity reached 35 mg PO_4^{3-} g⁻¹ at 1.2 V in a simulated wastewater solution consisting of NaCl, Na₂SO₄, NaNO₃, and NaH₂PO₄. Using activated carbon fiber and a MCDI method, Wang et al.[274] demonstrated the removal and recovery of Cu²⁺ and Zn²⁺ from a single-component solution of 500 mg L⁻¹ CuCl₂ or 500 mg L⁻¹ ZnCl₂. The highest adsorption capacities of Cu^{2+} and Zn^{2+} were reported to be 108.7 and 122.6 mg g^{-1} , respectively. At voltages between 0.4 and 0.6 V, Cu²⁺ adsorption capacities were greater than that of adsorption capacities of Zn²⁺, possibly due to the smaller hydrated radius of Cu^{2+} . At voltages between 0.8 and 1.2 V, the amount of Zn^{2+} adsorbed was greater than that of Cu²⁺, likely due to the reduction and deposition of Cu²⁺ into Cu⁺ and Cu at voltages above 0.6 V. which decreased the active surface area of the electrode. Furthermore, the authors also reported a 42.8% recovery efficiency of Cu/Cu⁺.

5.2.3. Graphene-Based Materials

Graphene and reduced graphene oxide serve as effective capacitive electrodes due to their high electrical conductivity, high surface area, flexibility, excellent mechanical properties, and rich chemistry (Figure 8f). As a parent material, 2D graphene can be fabricated into specific structures with varying characteristic dimensions (e.g., 0D carbon dot, 1D fiber, 2D sheet, and 3D foam), yet the parent is still mostly studied because of the abovementioned merits as well as the small diffusional resistance to ion transport. One challenge that limits further application of graphene is restacking and agglomeration that restricts ion diffusion and results in deteriorated electrochemical performance of the electrode. This issue can be resolved by adding a spacer material (e.g., conductive polymer, transition metal oxides, carbonbased materials) in between the layers of graphene sheets.^[261,275] The spacer can provide a consistent interlayer spacing and recover the internal surface area to enable higher ionic storage within the EDLs and enhance the electrode capacitance.

Liu et al.^[276] developed a direct current/alternating current (AC) technique to remove low-concentration heavy-metal ions

from point-of-use water and recover high-concentration heavymetal ions (Cu²⁺, Cd²⁺, Pb²⁺) from industrial wastewater. Owing to the high specific surface area of graphene oxide, the electrodes fabricated by depositing graphene oxide on carbon felt offered high-density surface functional groups that could anchor the heavy-metal ions to facilitate the nucleation. Additionally, the AC electrochemical technique showed high removal efficiencies for Cu²⁺, Cd²⁺, and Pb²⁺. By tuning the AC frequency and voltage, Pb2+, Cu2+, and Cd2+ could be recovered in a sequential manner. In another example, Liu et al. [277] reported using chemically modified graphene-based electrodes to recover Pb2+ and Na+ from wastewater. Specifically, EDTA was grafted to the surface of a graphene oxide cathode in a CDI process. During the CDI. Pb²⁺ and Na⁺ were adsorbed by chelation and electrostatic interaction, resulting in high removal efficiencies of Pb2+ (99.9%) and Na⁺ (≈98.7%) in a range of Pb²⁺ concentrations between 5 and 100 ppm. To recover the ions, Na+ was first desorbed and recovered by reversing the voltage and short circuiting, followed by regeneration of the CDI electrodes using HNO3 to recover Pb^{2+} .

Like lithium intercalation electrodes, carbon-based electrodes are used widely as a capacitive electrode in CDI processes for resource recovery. It is noted that comparing the electrode performance across varying studies is challenging because metrics such as adsorption capacity are process-dependent and may be calculated using different masses of electrodes. For example, ion uptake values should be reported per mass of active materials in both positive and negative electrodes, but it is sometimes reported based on the total mass of both electrodes or the active material mass of only one electrode. Therefore, unifying calculation performance metrics, and even identifying and using metrics that are independent of individual conditions, is critical to compare electrode performance. [238,262] Furthermore, modifications of carbon electrodes in CDI processes are suggested to yield higher ion selectivity and capacity. Specifically, doping the carbon electrodes with heteroatoms (e.g., sulfur) has been shown to exhibit excellent electrosorption performance.[278]

5.3. Anode Materials

A foundational aspect of electrochemical technology is the combinatory choice of anodic and cathodic materials. The role of anodes is driven by oxidation and is supported by selecting materials with properties such as high oxygen and hydrogen evolution reaction potentials. $^{[279]}$ The leading anodic materials for oxidation processes include lead dioxide (PbO2), iridium-based oxides (IrO2), ruthenium-based oxides (RuO2), Pt, and boron-doped diamond (BDD). More distinguishing characteristics are related to active, nonactive, and mixed metal oxides (MMOs) that have larger potential for oxidation processes and are often a mixture of IrO2 and RuO2 on titanium substrate. $^{[280]}$ These electrode materials have been robustly researched since the 1980s, and many of the promising technologies rely on a subset of the aforementioned materials. $^{[279]}$

Regarding the growing field of resource recovery, the subscripted role of anodes is the oxidation of metal complexes in wastewater to promote heavy metal capture.^[281] Since wastewater



ADVANCED MATERIALS

contains many mixed metal complexes, many of the articles that address anodes for recovery begin at electrochemical oxidation (EO) (Figure 9a). The EO process can be divided into two types: direct and indirect electrooxidation. During a direct electrooxidation process, electrons transport directly between the anode and the reductants. During an indirect electrooxidation process, electrons are lost with the assistance of oxidants while active radicals are generated in situ. Electrooxidation can be used to recover heavy metal ions by oxidizing ion chelates and then subsequently reducing or concentrating them for extraction. [280] By lending EO to the complex degradation of wastewater, this process has been coupled with additional electrochemical processes to create a dual system that recovers metals. [282]

These additional processes include electrodeposition,[290,291] electrosorption (ES), and electro-Fenton (EF)[292] processes. The ED process is governed by the potential-driven migration of metal ions and reduction into solid metal at the cathode surface. Since this process is fueled by charge difference, there is opportunity to improve the selectivity of separation in high pollutant scenarios (Figure 9c).[293] The EF process utilizes a well-known oxidation procedure called the Fenton reaction (Figure 9d). The purpose of this reaction is to produce OH*, which enhances oxidation. However, the classical reaction requires excessive reagent use, which generates waste and poses cost concerns. When incorporating the electrochemical aspect of this reaction, EF can dually control synthesis and catalyze ongoing reactions. Specifically, during the EF process, H₂O₂ is generated by the reduction of oxide with compressed air. Iron is thus added to the solution in a catalytic amount and is continuously reduced at the cathode upon the utilization of H₂O₂ potential.^[292] The mechanism of the ES process was previously explained in Section 5.2 (Figure 9b). ES is a sought-after technology because of its low cost and effective operation under low energy consumption.[237,294]

5.3.1. Pt

Pt is a noble metal that is often used as an anode because it is resistant to corrosion and offers an extended service life. [295] However, due to its high cost and lower affinity toward oxidation, it is not an ideal candidate for large-scale processes in wastewater treatment.[279,295] In a study evaluating a wastewater treatment facility in Indonesia, sludge was analyzed due to its high aluminum resource content during coagulation for treatment of wastewater. Barakwan et al. [296] used a Pt anode and stainless-steel (SS) cathode to recover aluminum. The electrolysis time was 6 h in highly acidic (pH = 3) sludge with large concentration of heavy metals and organic pollutants. The Pt/SS system recovered 52.10% of aluminum at 300 mA with minimal impurities. At 300 mA, 88.14% of the captured content was aluminum while magnesium and iron impurities represented less than 7%. Investigation on the removal of mercury by Tunsu and Wickman^[287] proposed a PtHg4 alloy formed on Pt films. Mercury atoms bound with a population of >88 g cm⁻³ to the Pt electrodes with formation of PtHg₄ (Figure 9g). This technique has significant uptake, a large active surface area, and good stability; similar approaches could likely be utilized to capture other resources of interest from complex wastewater.

5.3.2. PbO₂

Lead and PbO₂ (Pb/PbO₂) anodes have a high oxidation potential, are inexpensive, and are widely applicable in electrochemistry. PbO₂-based materials are sought-after due to their nonactive anodic properties, allowing them to create OH radicals that can be used in organic degradation and mineralization reactions. [297] To improve the electrocatalytic performance of the anode, modifications can be made (Figure 9h).[298] One of the concerning factors during the electrode operation of PbO2 is the leaching of Pb, a toxic element. However, attempts have been made to integrate this anode for oxidation-guided recovery processes like in wastewater from electroplating industries by Wang et al.[299] In this study, a reactor design of a rotating mesh-disk was implemented to enhance destruction rate of Cu, Cr, and Ni metal complexes. In alkaline solutions at current density of 10 mA cm⁻², >97% of each complex was destroyed within 120 min. El-Gayar et al.[300] examined a dual process, oxidation of FeSO₄ and deposition of Cu via an electrocatalytic cell of oscillating vertical electrodes. The technique increased oxidation (from 35% to 92%) and deposition (from 52% to 98%) enhanced by rotational speed. Additionally, energy consumption was decreased in this system for both processes. This is a prime example in the recovery of critical resources from mixed wastewater and perhaps can be of interest to the field with less toxic materials.

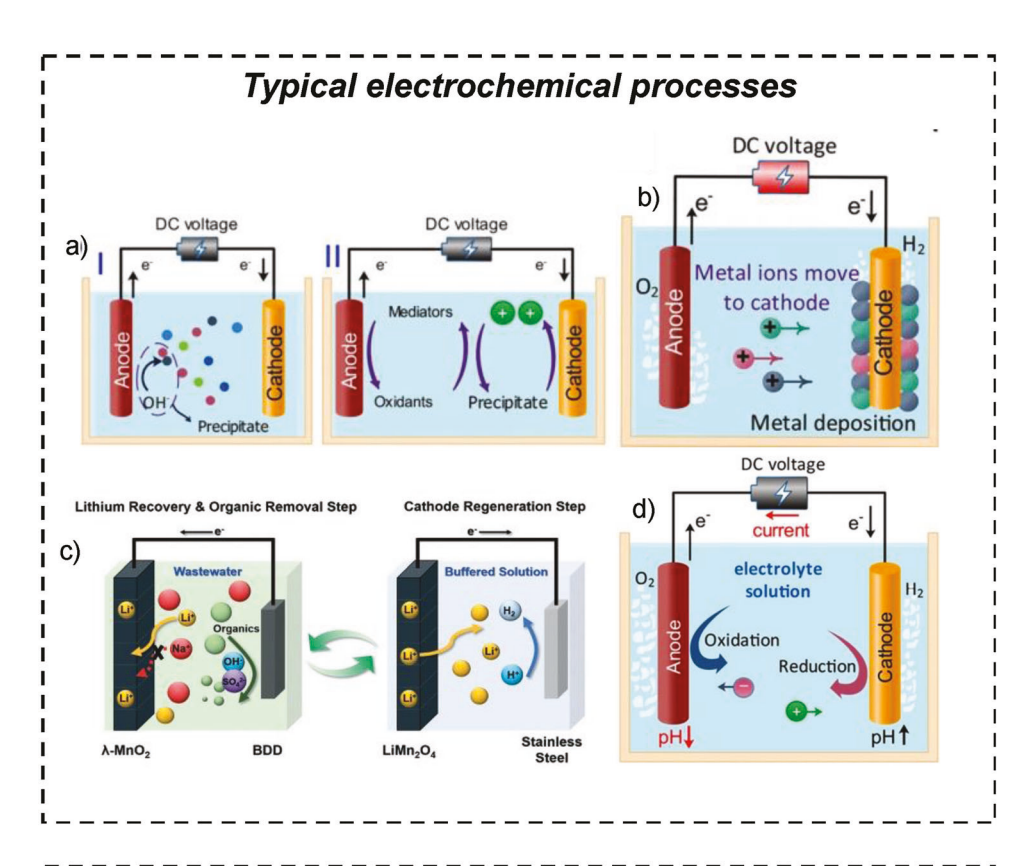
5.3.3. IrO_2 and RuO_2

RuO2 and IrO2 are classified as active anodes because of their low oxygen evolution overpotentials that hinder the complete oxidation of pollutants in EO.[301,302] However, these materials have undergone modifications that improve serviceable lifetimes (i.e., stability and resistance to corrosion).[301] Reports of improving stability while decreasing dependence on IrO2 and or RuO2 for synthesis and improving electrode integrity are ongoing. [303] Several studies have explored modifications such as IrO_2 -Ta O_5 , [304] (Ir, W) O_x , [302] (Sn, Sb, Ir) O_x , [302] and RuO₂/CoO_x^[285] (Figure 9e,f). These anodes are commonly used in wastewater treatment due to their stability, corrosion resistance, and integration with Ti substrates to increase cost efficiency and conductivity.[279] In regard to resource recovery, Du et al.[305] recovered liquid Hg via electrochemical oxidation using a Ti cathode and IrO₂/Ti anode. For the duration of a 30 minute reaction, there was an observable "silver-gray" deposit. A current density of ≤10 mA cm⁻³ demonstrated the highest removal rate at roughly 90% during the first four hours of the reaction, and after three complete runs, the electrochemical reduction exhibited the same efficiency.

To recover Cu from cyanide-contaminated wastewater, Pombo and Dutra^[306] created an electrocatalytic cell comprised of a stainless-steel cathode and ruthenium-oxide-layered titanium anode. At a current of 1.0 A, a potential drop was observed that was attributed to complete CuO deposition on the anode. In this case, the electrode became a catalyst for remaining cyanide oxidation. SEM images depicted the difference in morphology at the beginning and end of the reaction. Images indicate that after three hours of electrolysis, there was increased roughness on the surface of the anode. Copper and oxygen peaks observed by

15214095, 0, Downloaded from https://onlinelibrary.wiley.com/doi/10.1002/adma.202300913 by University Of Chicago Library, Wiley Online Library on [17.08/2023]. See the Terms

www.advancedsciencenews.com



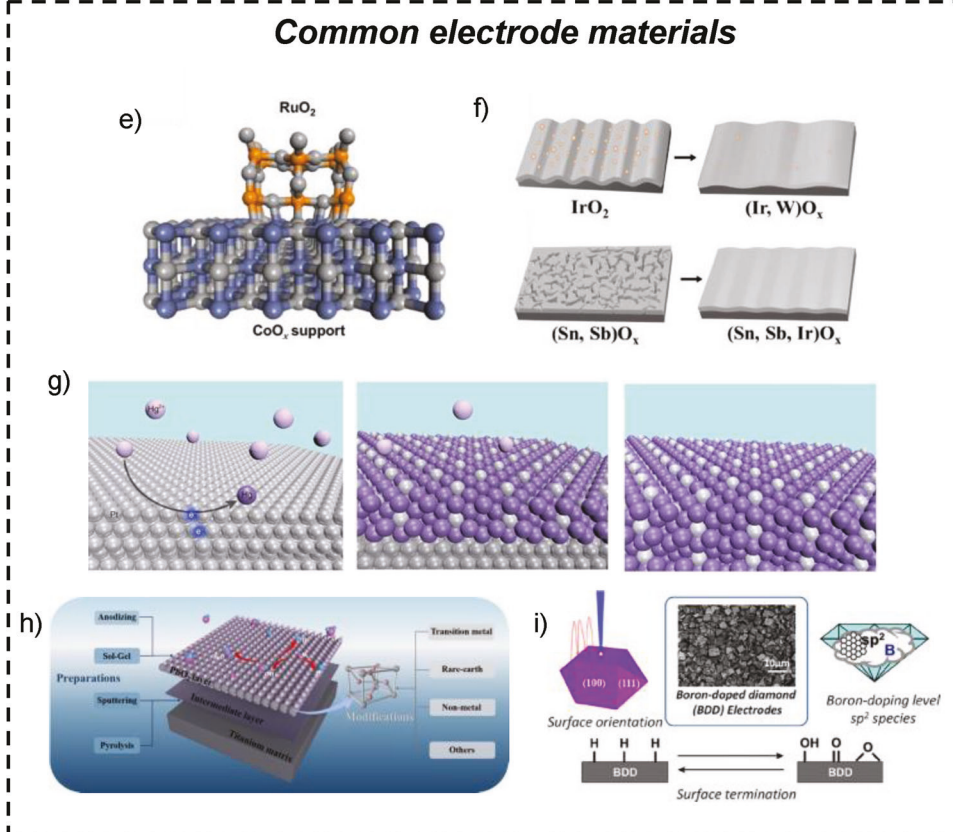


Figure 9. a-d) Schematic of: a) typical electrochemical processes direct (I) and indirect (II) electrochemical oxidation processes; b) electrosorption process; c) electrodeposition; d) electro-Fenton process. a,b,d) Reproduced under the terms of the CC-BY Creative Commons Attribution 4.0



ADVANCED MATERIALS

energy-dispersive X-ray spectroscopy (EDS) confirmed that the surface coverage was CuO. Under favorable conditions related to temperature, current density, and flow rate, copper ions were recovered at 0.70 mg L^{-1} and cyanide ions 0.08 mg L^{-1} . Kim and Bael 307 also investigated the use of Ti/Ir–Ru anode for copper recovery via ED. The electrodes were fabricated via spin-coating and over a six hour reaction period, there was complete removal of Cu with starting concentrations at two cases of 1 and 10 g L^{-1} . High potential and low concentration of copper in solution showed an increase in recovery. On the cathode, there were visible dark powder deposits that could be easily recovered by scraping the surface

There is potential to expand the study conducted by Wang et al., [308] where the team successfully combined electrodialysis (anode) and electrodeposition (cathode) for the removal of nickel ions in wastewater. It was reported that there was successful removal of Ni²⁺ concentrations over a nine hour reaction time with a low pH, 50 mL min⁻¹ flow rate, and 2.2 V cell voltage. The anode played a significant role on the reduction of nickel concentrations; however, analysis of anode/cathode postreaction was not in the scope of this research. Similar conditions associated with this electrochemical system with analysis much like that on the morphological and sedimentation changes on anode and cathode can move this research into the realm of recovery studies.

Out of the MMO electrodes, IrO2 and RuO2 dominate resource recovery applications. Electrochemical recovery of critical resources still has much room for future exploration with MMO anodes widely used in electrooxidation. Historically, the focus of electrochemical technologies in water treatment has trended toward the electrochemical oxidation of organic pollutants. This technique is important in treatment processes but overlooks another valuable opportunity in water treatment: the recovery of critical resources. The judicious selection of an anode material to couple with a functional cathode is critical to develop efficient electrochemical resource recovery processes. Thus, this review evaluates anode materials that have been established for electrochemical oxidation for wastewater, and their consequent coupling with cathodes to develop optimal systems for resource recovery from mixed aqueous solutions. Furthermore, studies that reveal the possibilities of heavy metal removal offer valuable insights to the field of resource recovery. Similar frameworks can be applied for critical-resource-dominant aqueous environments for which optimal conditions can be determined not only for removal, but also consequent resource retrieval.

5.3.4. BDD

The starting point of BDD is the robust mineral diamond. Diamonds are a fascinating material that provide chemical inertness, extreme hardness, high charge carrier mobility, and sp³

hybridization with tetrahedral bonding. Although these characteristics set diamonds apart for their stability and functionality, for this material to be applicable into the field of electrochemistry, it must undergo modification to decrease its wide bandgap and improve conductivity. A popular modification is increasing boron content to contribute to sp² impurities, which can improve the conductivity of the material and change the anodic behavior (Figure 9i).[309] The effectiveness of BDD is primarily governed by its synthesis, substrate, boron content, hybridization ratio, morphology, and O₂/H₂ evolution overpotential. [309,310] The routes to BDD electrode materials are typically by chemical vapor deposition or high-pressure/high-temperature processing. Like many other electrodes, the combination of working electrode and substrate is critical. For BDD, the most important substrate for improvement of activity is Ti because of stability, conductivity, low cost, and reliable use in other anodic materials. The doping level of boron can dictate the ratio of hybridization and impurities to the BDD.[311,312]

Several studies have applied BDD electrodes to the recovery of metals. In the chemical-mechanical planarization/polishing industry, the wastewater produced is an area for the recovery of copper has thus been investigated by Tamilmani et al.[291] They used a BDD cathode and BDD anode for the simultaneous electrodeposition of copper and electrooxidation of organics observed by deposition as discrete clusters on the BDD surface by SEM. Zhuo et al.[313] similarly used a BDD cathode and Ti anode to electrooxidize Ni(II) citrate and recover the Ni²⁺ via electrodeposition. By utilizing high current densities and acidic conditions, they recovered 72.6% of the Ni at >95% purity. Sludge is an important byproduct of wastewater treatment processes where suspension of particles can harbor additional hazardous contaminants and critical resources. Burgos-Castillo et al.[314] examined the leaching of critical resources from wastewater treatment sludge. Upon acidification of urban sludge with applied EF processes, Fenton's reaction via oxidation of organic metal complexes favored the recovery of metals Cd, Cu, and Zn. For Li recovery, Kim et al. $^{[284]}$ proposed a LMO/BDD system that electrooxidized organics at the BDD anode and captured Li⁺ ions (with 98.6 mol% purity) at the λ-MnO₂ cathode in wastewater that contained organic compounds and Li⁺. Use of BDD electrodes in resource recovery systems is still in its infancy, as its high cost is a restricting factor for practical applications. Further work must be done to develop competitive materials that complement the robustness of the BDD while also taking into consideration the potential for industrial scale-up.

5.4. Outlook

Intercalation and carbonaceous electrodes are both adopted as capacitive electrodes to recover valued species such as Li⁺, heavy

International license (https://creativecommons.org/licenses/by/4.0). [283] Copyright 2022, The Authors, published by Springer Nature. c) Reproduced with permission. [284] Copyright 2018, Royal Society of Chemistry. e-i) Common electrode materials. e) Modified structure of RuO2/CoOx. Reproduced under the terms of the CC-BY Creative Commons Attribution 4.0 International license (https://creativecommons.org/licenses/by/4.0). [285] Copyright 2022, The Authors, published by Springer Nature. f) Diagram of surface changes on modified IrO2 anode. Reproduced with permission. [286] Copyright 2022, Elsevier. g) Alloying process for Pt anode with PtHg4. Reproduced under the terms of the CC-BY Creative Commons Attribution 4.0 International license (https://creativecommons.org/licenses/by/4.0). [287] Copyright 2018, The Authors, published by Springer Nature. h) Schematic diagram of PbO2 preparation and modifications. Reproduced with permission. [288] Copyright 2022, Elsevier. i) Overview of BDD anode structure, morphology, and boron doping. Reproduced with permission. [289] Copyright 2022, American Chemical Society.



ADVANCED MATERIALS

metals, and nutrients in processes where ions are stored either via intercalation or within the EDL. As a group of materials, lithium intercalation electrodes are favored for Li⁺/Mg²⁺ separation with greater Li⁺ selectivity and Li⁺ recovery rate. Further work should focus on Li+/Na+ selectivity, as Na+ is also a competitor ion coexisting with Li+ in many sources (e.g., geothermal brine). It is also important to include cycling studies (i.e., reusability) for these electrodes since they are only economically viable (i.e., produced lithium with higher cost than the cost of active materials on the electrodes) after a certain number of cycles (e.g., 8-30).[18] Carbon-based electrodes are often favored due to their comparatively low cost. Similar to intercalation materials, reusability of carbonaceous electrode has also limited applications to date. For example, AC electrodes typically show significant capacity loss in large number of cycle tests.[315] MMO and BDD are both considered charge-transfer electrodes, and they are commonly applied in electrochemical processes due to their resistance to corrosion and dissolution. For MMO electrodes, the catalytic efficiency is highly dependent on the fabrication method. Therefore, identifying suitable preparation methods that generate stable and consistent resource-recovering performance is critical. For BDD electrodes, future work should focus on lowering the material cost per area and identifying suitable substrate that can provide stable support of the electrode.

6. Interfacial Solar Steam Generators

ISSGs have recently emerged as a promising alternative to conventional distillation processes to harness solar energy for water treatment and resource recovery. By utilizing a porous photothermal material that absorbs light across the solar spectrum and converts it to heat, heat transfer can be localized at the air/water interface to substantially improve the energy efficiency of evaporation. In most ISSGs, the photothermal material is designed to be buoyant and floated at the surface of the water to be purified (i.e., a 2D configuration), although other system architectures have also been explored to imbue desirable heat and mass transport properties. The evaporated water can then be condensed onto a transparent, hydrophobic surface suspended above the system and collected for reuse.

In addition to generating clean water, ISSGs can also simultaneously concentrate and extract critical resources from wastewaters and brines. For example, solar evaporation ponds are currently used to extract lithium salts from high-salinity brines, which contain many ions such as Na⁺ and K⁺ that must be precipitated out to obtain usable concentrations of lithium carbonate.[316] This process is intrinsically slow, in part due to water's poor absorption of light across the solar spectrum. Thus, ISSGs could potentially accelerate the rate of this process by several fold. Likewise, ISSGs could also be used to concentrate streams to more desirable concentrations of resources for postprocessing, such as nitrates and phosphates in municipal wastewater. These same principles can be extended to recover resources from a variety of feed streams, although different resource concentrations and environmental conditions necessitate strategic design of material properties for optimal performance.

The two primary metrics that must be considered when evaluating the performance of an ISSG are evaporation efficiency and antifouling performance. The evaporation efficiency η is directly calculated from the equation $\eta = \dot{m}h_{\rm vap}/P_{\rm sun}$ where \dot{m} is the evaporation rate due to sunlight, h_{vap} is the specific enthalpy of vaporization of the solution, and $P_{\rm sun}$ is the incident solar irradiance. [317] Typically, \dot{m} is calculated by subtracting the evaporation rate in dark conditions from the evaporation rate under the specified solar irradiance. This decouples the evaporation that occurs naturally from that which is directly powered by sunlight in the efficiency metric. It is conventional for evaporation efficiencies to be reported under 1-sun irradiance (1 kW m⁻²) using a calibrated solar simulator, although in practical use, the natural solar irradiances will vary based on time and weather conditions. A higher evaporation efficiency (and, in effect, evaporation rate) is desirable to make ISSGs that function at viable timescales for water treatment and resource recovery applications. To achieve high evaporation efficiencies, it is important for photothermal materials to be efficient absorbers of light across the solar spectrum, as well as for the overall ISSG to be thermally insulated from heat loss to the bulk water or the surrounding environment. It is not uncommon for ISSGs to surpass 100% efficiency by exploiting phenomena such as latent heat recycling or evaporative cooling, which can extract more thermal energy from the environment.[318,319]

As is the case with membranes, fouling can severely inhibit the performance and lifetime of ISSGs by clogging the pores via salt crystallization, particulate adsorption, or biofilm formation. In addition to restricting the transport of water, if the surface of the photothermal material is covered by a foulant such as salt crystals, light absorption can also be severely restricted, causing evaporation efficiencies to decrease over time. Thus, it is important to evaluate the ability of an ISSG to maintain its evaporation efficiency over extended periods of time in an environment containing foulants. Active techniques could potentially be borrowed from conventional membrane cleaning strategies such as sonication, washing, and/or targeted chemical treatments.[320] However, imbuing antifouling character via control of material surface properties such as morphology, hydrophilicity, and surface charge can also passively enhance ISSG performance and reduce operating costs associated with fouling mitigation.[321] The aggregation of foulants is inevitable in most ISSGs, as dissolved species begin to saturate due to the concentration of the aqueous system via evaporation. However, in the context of resource recovery, ISSGs could be designed to spatially direct the adsorption or crystallization of resources for separation and collection.

Material properties play a vital role in governing the performance of ISSGs, and a broad range of photothermal materials have been demonstrated as viable candidates across a variety of architectures. This includes carbonaceous, metallic, semiconductor, organic, and hybrid organic–inorganic materials. Several published reviews have discussed photothermal materials and architectures for ISSGs. [322-325] However, most of this literature is solely focused on designing materials for water purification. In this section, we will summarize some of the pertinent photothermal materials and architectural designs that have been reported and highlight their potential applications in critical resource recovery.

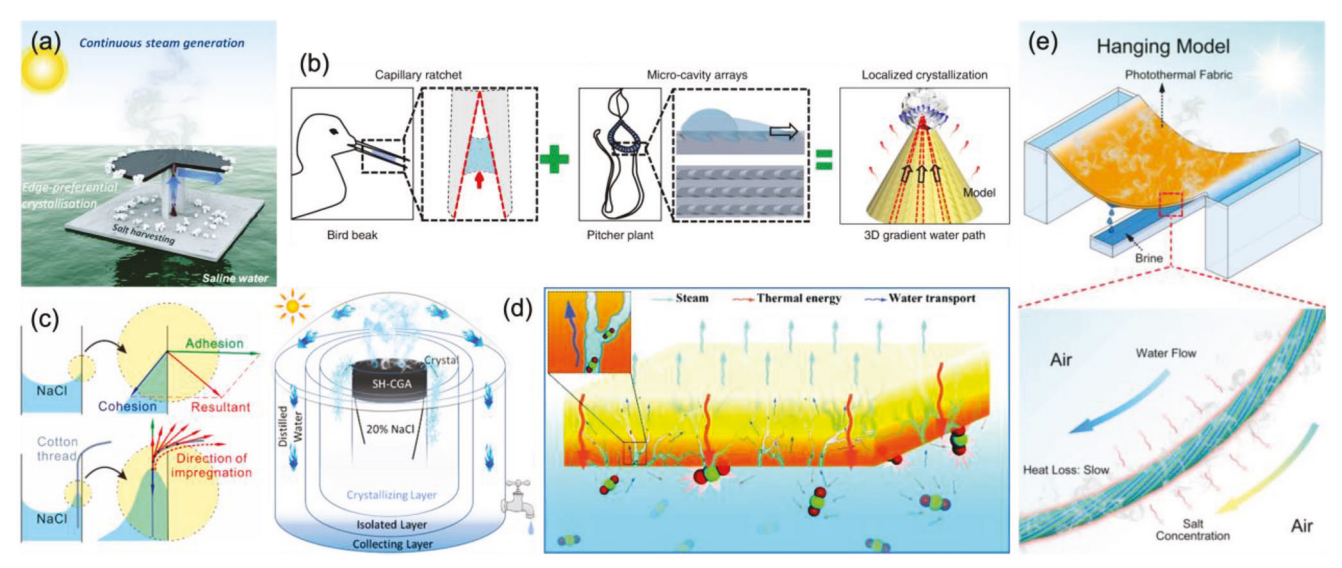


Figure 10. a) Schematic of CNT evaporator for edge-preferential salt crystallization and harvesting. Reproduced with permission.^[331] Copyright 2019, Royal Society of Chemistry. b) Structure of biomimetic 3D printed evaporator for localized salt crystallization. Reproduced under the terms of the CC-BY Creative Commons Attribution 4.0 International license (https://creativecommons.org/licenses/by/4.0).^[332] Copyright 2020, The Authors, published by Springer Nature. c) Schematic of carbonized algae evaporator with cotton threads for control of salt crystallization. Reproduced with permission.^[333] Copyright 2020, American Chemical Society. d) Schematic of simultaneous steam generation and UO₂²⁺ adsorption using a graphene aerogel with bayberry tannin. Reproduced with permission.^[334] Copyright 2021, published by Royal Society of Chemistry. e) Schematic of hanging photothermal fabric submerged in two tanks of seawater for brine concentration. Reproduced with permission.^[335] Copyright 2019, Wiley-VCH.

6.1. Carbon Materials

6.1.1. Carbon Nanomaterials

Xia et al. [331] coated superhydrophilic cellulose filter paper with CNTs and placed it on a polystyrene foam insulator with a cotton thread sewn through for vertical water transport via capillary action. This design enabled localized salt crystallization at the edges of the filter paper by continuously transporting saline solution through the hydrophilic medium while water simultaneously evaporated from the surface (Figure 10a). This enables the continuous harvesting of valuable salts from water, as the salt crystallization does not obstruct the evaporation surface and can easily be collected by gravity forcing salt crystals to fall off the edges. Wu et al. [332] similarly achieved localized salt crystallization by 3D printing a biomimetic evaporator from a UV resin loaded with CNTs (Figure 10b). By mimicking the structure of the asymmetric capillary ratchet of a bird beak and the micro-

cavity arrays from the surface of a pitcher plant, the evaporator could transport a thin film of liquid water much faster than a conventional porous filter paper could via capillary wicking. The engineered water transport pathway produces a salinity gradient across the continuously evaporating liquid film, resulting in localized salt crystallization at the apex, which can easily be collected.

6.1.2. Natural Carbon-Based Materials

Natural carbon-based biomass materials have also been demonstrated to serve as inexpensive and effective photothermal materials for ISSGs.[336-338] One of the earliest reports of biomass photothermal materials being used for ISSGs came from Xu et al.[339] who used a carbonized umbrella-shaped shiitake mushroom as an evaporator. The carbonized mushroom was able to absorb about 96% of the solar spectrum while also effectively supplying water through its hydrophilic surface and porous microstructure. A variety of other natural materials have been carbonized for direct utilization in ISSGs including wood, [340,341] bamboo, [342] sunflower heads,[343] algae,[333,344] and several more. For example, Li et al.[333] fabricated an evaporator from carbonized green algae coated with polyacrylic acid for superhydrophilicity. By also integrating cotton threads to the edges of the evaporator, salt crystallization could be localized along the threads due to their stronger adhesion to NaCl than the algae-based evaporator or the container (Figure 10c). Like other designs for directed crystallization, this could be used as a simple mechanism for harvesting valuable salt resources from brines and wastewaters. An alternate mechanism for recovery of metal ions is to design a material to simultaneously function as a photothermal material and a sorbent.



www.advmat.de

Hou et al. $^{[345]}$ chemically treated and etched carbonized basswood to introduce more pores and oxygen-rich functional groups along the pores for simultaneous steam generation and Pb^{2+} adsorption. The concentration gradient of metal ions due to evaporation coupled with the localized heating of the carbonized surface results in enhanced adsorption of Pb^{2+} by the wood structure, making this design useful for recovering metal ions from wastewater.

Natural biomass materials can also be integrated into ISSGs as substrates for other photothermal materials to offer unique transport properties. For example, wood has commonly been used as a substrate material for ISSGs due to its low thermal conductivity and porous structure for capillary water transport. Yang et al. coated basswood with Chinese ink, a photothermal material made from carbon soot and animal glue, to achieve a higher evaporation rate than could be achieved by coating a PVDF membrane with the same ink.^[346] Biomass materials can also be integrated into ISSGs as functional additives for resource recovery. Wu et al.[334] integrated bayberry tannin, which is typically water soluble, into a porous graphene aerogel for simultaneous steam generation and uranium extraction. The bayberry tannin is immobilized in the aerogel by hydrogen bonding with reduced GO, allowing it to chelate with UO22+ ions in the water. The movement of UO₂²⁺ and its interaction with the bayberry tannin is further enhanced by the high temperature of the evaporator under solar illumination, offering a new pathway to extracting uranium from seawater (Figure 10d).

6.2. Metals and Semiconductors

Certain metals and semiconductors can act as photothermal materials by dissipating energy through surface plasmon interactions when light is absorbed. A surface plasmon refers to the oscillation of electrons at a metal–dielectric interface caused by photonic excitation, which can either propagate along the interface as a surface plasmon polariton or localize around specific surface geometries (denominated as localized surface plasmon resonance, LSPR). The energy dissipated by the oscillation of surface plasmons is mostly released as thermal energy, therein generating the photothermal effect desired for ISSGs.[347,348] The light-to-heat conversion efficiency of a plasmonic material can be tailored by modulating its geometry or morphology. Intrinsic differences in the dielectric constants of various materials also play a role in governing light absorption and scattering, making material selection for ISSG applications important.[349]

6.2.1. Metallic Materials

Metallic nanoparticles are a class of plasmonic materials that have frequently been studied for photothermal applications. One of the earliest reports of solar steam generation using photothermal materials came from Neumann et al., [350] who fabricated SiO₂ core—Au shell nanoparticles and dispersed them in solution. Similar dispersed configurations have also been reported using pure gold [351] and silver [352] nanoparticles. However, this configuration for steam generation inherently suffers from significant heat loss to the bulk water, as heat transfer is delocalized via conduction by the dispersed nanoparticles. In addition, any water

vapor formed at the surface of the nanoparticles can only escape the solution as bubbles, which could potentially dissolve or reliquefy before reaching the surface. To improve the evaporation efficiency, metallic nanoparticles can instead be fixed onto a buoyant, porous substrate that localizes heat transfer at the air/water interface. For example, Zhou et al.^[353] coated a nanoporous anodic aluminum oxide membrane with aluminum nanoparticles that exhibited >96% absorption of light across the solar spectrum. Similar design strategies have been demonstrated across other plasmonic nanoparticles and substrates, such as copper on cellulose membranes^[354] or palladium on wood^[355] and bamboo.^[356]

Metallic nanoparticles tend to have narrow absorption spectra, which can limit their efficacy for solar energy harvesting. Thus, it can be more effective to design specific surface morphologies for plasmonic materials that can broaden their absorption spectra and curtail reflective losses.[357] Zhang et al.[358] processed gold into a highly porous film consisting of gold nanowires that broadened the range of light absorption due to the length scale of the spacings between the nanowires. In addition, the porous structure enhanced light absorption through the increased surface area for electron collisions and through light trapping within the pores. Another approach that has improved broadband absorption is the use of a composite material in which each constituent material has a different absorption spectrum. Yang et al.[359] fabricated hybrid plasmonic nanoparticles made of nickel and carbon, where nickel offered a high light absorption ratio and carbon served as a broadband absorber. They also incorporated these nanoparticles into a hydrogel film to fabricate an ISSG that could increase its surface roughness through the introduction of a magnetic field, which in effect boosted the evaporation rate to as high as $2.25 \text{ kg m}^{-2} \text{ h}^{-1}$.

6.2.2. Semiconductor Materials

A variety of semiconductor materials have also been used for ISSGs including metal chalcogenides, metal oxides, and 2D materials.[360] Plasmonic semiconductors that leverage the LSPR effect for light-to-heat conversion mechanistically function similar to plasmonic metals. The light-absorption properties of semiconductors can also be further tuned via doping, defect engineering, and surface modifications. For example, Huang et al. [361] fabricated a freestanding membrane from MoO_{3-x} , a plasmonic semiconductor, which exhibited an evaporation efficiency of 95% under 1-sun irradiance. By controlling the concentration of oxygen vacancies in MoO_{3-x}, the selective chemisorption of positively charged organic dyes was achieved. This type of design could potentially be used to remove undesirable pollutants from wastewater streams, simultaneously yielding cleaner water for reuse and a purer concentrate of critical nutrients like phosphates for recovery. Other plasmonic semiconductors that have been reported to be used in ISSGs include $Cu_{2-x}S$,[362,363] Cu_2ZnSnS_4 , [364,365] and WO_{3-x} . [366]

In addition to the LSPR effect, semiconductors can also generate heat through the nonradiative relaxation of electrons excited by photons with energies exceeding the material's bandgap energy. Some photothermal materials that demonstrate this effect include MoS_2 , [367,368] TiO_x , [369] Fe_3O_4 , [370] and MXenes. [371] Zhao et al. [371] fabricated a photothermal membrane from 2D Ti_3C_2

ADVANCED MATERIALS

nanosheets (a type of MXene) modified with a fluoroalkylsilane to produce a hydrophobic surface for salt rejection. This design could be of value to prevent salt crystallization on the evaporation surface in ISSG brine concentration systems for critical resource recovery. Hu et al. [370] hierarchically assembled a magnetically responsive conical array of graphene-coated Fe₃O₄ nanoparticles that demonstrated a high evaporation rate of 5.9 kg m⁻² h⁻¹ by harvesting environmental energy and dynamically improving water vapor diffusion by magnetic movement of the conical array. This ISSG also showed high resistance to salt crystallization and could redissolve precipitated salts at night due to the high rate of water transport, making it promising for concentrating high-salinity streams.

6.3. Organic and Hybrid Organic-Inorganic Materials

Synthetic organic and polymer materials have also been widely reported as suitable photothermal materials for ISSGs. PDA has been used as a coating for many water treatment materials because of the simplicity of its self-polymerization process for conformal depositions and its versatility for surface chemical modifications.^[48] In addition to these properties, PDA also serves as an effective photothermal material for ISSGs due to its broadband light absorption and adhesive characteristic for coating porous substrates. Wu et al.[319] coated polypropylene membranes with PDA and suspended them in water in a pyramidal geometry to boost evaporation rates by harvesting environmental energy. The superhydrophilicity of PDA also inhibits fouling of the evaporation surface from oily pollutants during steam generation, which can be useful for concentrating oily wastewater streams for resource recovery. A suspended ISSG configuration was also implemented by Liu et al.[335] using a cotton fabric coated with polyaniline nanorods as the photothermal absorber. The two ends of the fabric are immersed in saline water while the middle droops, allowing concentrated brines to drip from the fabric to a tank below for collection (Figure 10e). In addition to resisting salt crystallization on the absorber surface, the design reduces thermal losses to the bulk water experienced in conventional ISSGs and allows water to evaporate from both faces of the photothermal material. Polypyrrole is another organic photothermal material that has been integrated into ISSGs using substrates such as polyvinyl alcohol hydrogels^[372] and polystyrene/cellulose.^[373]

COFs have also been integrated into ISSGs for photothermal evaporation and resource adsorption. Xia et al.^[374] developed a broadband absorbing porphyrin COF that could easily be coated onto a variety of substrates via a one-pot synthesis. Qiu and co-workers^[375,376] developed COFs that could bind with UO₂²⁺ ions and integrated them into microporous hydrogels to achieve simultaneous photothermal evaporation and UO₂²⁺ adsorption. Hybrid organic—inorganic materials have also been reported as efficient photothermal materials for ISSGs including ferric tannate^[377] and several MOF materials.^[378–380]

6.4. Outlook

Overall, ISSGs hold great promise as materials that can passively and simultaneously recover critical resources and generate clean water. There is little room left to improve the light harvesting capabilities of photothermal materials, as many different materials have been reported to achieve near 100% absorption of the solar spectrum. Thus, it is important to utilize technoeconomic and life cycle analyses to quantitatively assess and compare the costs and environmental impacts of different materials for ISSGs. These metrics should be taken into consideration in conjunction with performance metrics to design inexpensive and sustainable ISSGs. Organic and carbon-based materials are particularly promising in this regard due to their low cost and simple processing techniques compared to metallic and semiconductor materials that can achieve similar light-to-heat conversion efficiencies. There is also still a need for more investigation to elucidate the roles of surface and transport properties of materials for specific resource recovery applications (e.g., Li, U, N/P) such as hydrophilicity, surface charge, porosity, and adsorption kinetics. There is also much left to be explored in 3D ISSG architectures to harvest environmental energy for enhanced evaporation and to exploit physical transport phenomena for antifouling and resource extraction. The field of ISSG research is still in an early stage and has primarily been focused on applications in passive desalination. To advance these technologies for use in critical resource recovery, more emphasis will need to be placed on optimizing ISSGs to concentrate specific resources in the presence of interferents and foulants, as well as evaluating the ability of ISSGs to operate at scale over extended periods of time.

7. Outlook and Conclusion

Securing supplies of critical resources represents a pressing challenge that must be addressed to support the production of chemicals, materials, and technologies that are vital to securing a sustainable and prosperous future. Thus, intelligently engineered material technologies for precise and selective separations are necessary to extract economically viable quantities of critical resources from water. Membranes, sorbents, catalysts, electrodes, and ISSGs all hold great promise as separation technologies for resource recovery applications. However, there are still several technical challenges in material design that must be overcome to improve their performance and practical viability.

Membrane materials represent a mature separation technology that has seen commercialization and utility for water treatment and critical resource recovery. However, there are still barriers that must be surmounted to improve their performance for practical applications. First and foremost, more work must be done to increase the selectivity of membranes toward dissolved resources in the presence of common interferents at realistic and relevant concentration ratios. In particular, the separation of species of like-charge and valence via ion-exchange membranes is crucial for the recovery of metal ions in many relevant streams (e.g., cation/cation separation, monovalent/monovalent ion separation). However, the transport of ions under confinement at the nanoscale is still not fully understood, demanding synergy between fundamental and applied studies to advance this field. Membranes fabricated from polymers and 2D materials are especially of interest for studying and controlling ion transport. Progresses in fabrication and self-assembly techniques have enabled the fabrication of membranes with narrow poresize distributions as platforms to study precision separations at



ADVANCED MATERIALS

www.advmat.de

the nanoscale. [381,382] The tunability of the surface functionalization and interlayer spacing in stacked 2D materials also offers an interesting platform under which to study ion transport and separations. [383] The developments of more mechanically robust membranes and membrane surfaces that resist fouling are also necessary for separation processes to operate continuously and cost-effectively. The problems of fouling and membrane stability are further exacerbated by the concentration polarization phenomena in highly selective membranes, which may require the use of active intervention techniques to subdue the formation of parasitic concentration gradients.

Sorbent materials likewise require more research and development to achieve higher selectivities for critical resource uptake in the presence of interferents. There is promise in research focused on developing new sorbents via the synthesis of supramolecular receptors or by designing and grafting resource-selective ligands onto surfaces for inner-sphere chemisorption of critical resources. Further investigation is also required to develop facile and sustainable mechanisms of elution or desorption for sorbents that can be regenerated and recycled (e.g., electrically, chemically). The design of sorbents that can directly be used in end products after adsorbing resources can also be useful and promote a more circular resource economy, such as the use of natural sorbent materials (e.g., biochar) in fertilizer mixes after adsorbing nutrients.

The use of catalysts for the extraction of critical resources from water via chemical reactions is not yet widely adopted, primarily due to an existing barrier in understanding the fundamental kinetics and interaction phenomena that occur at the heterogeneous solid-liquid interface, particularly in complex and/or confined environments. The same problems have hindered progress in the use of catalysis for other water treatment applications such as pollutant degradation. [384] Thus, there is a need for a concerted effort of both computational modeling and experimental exploration to develop answers to these critical questions and consequently advance the development of catalytic resource recovery technologies. Using these tools to probe the structure and conversion mechanisms of molecules at interfacial catalytic sites will be important to learn how to design more efficient and selective catalysts for practical applications. While these questions linger, there is a great opportunity space for further research attention to be directed into studying catalytic materials and processes for critical resource recovery and this field can be expected to grow in the future. The design of electrocatalysts that can be integrated into multistep or hybrid electrochemical water treatment systems to achieve higher selectivities or novel separations is one interesting avenue. The design of solar-powered photocatalysts also holds promise to design sustainable resource recovery systems. There still exists a large parameter space of novel photocatalytic materials to be explored beyond conventional semiconductors like TiO₂, including the design of novel MOFs and COFs.[385]

The design of electrode materials for electrochemical resource recovery processes is a rapidly growing field. In particular, this topic has garnered attention for lithium recovery due to the existing knowledge and library of available materials for Li⁺ intercalation from the battery field. However, more work must be done to improve the selectivity of these electrodes for Li⁺ over Na⁺, which is typically present in much higher concentrations, as well as the overall Li⁺-storage capacity. Additionally, there is still much room

to expand these studies toward the intercalation of other metal ions and REEs using various transition metal oxide structures. Inspiration could also be drawn from the novel concept of dualion electrochemical systems, in which both cations and anions of interest can be intercalated into opposing electrodes.^[386,387] Aside from intercalation, there is also room to improve the selectivity and uptake capacity of carbon-based electrodes for CDI and electrosorption processes via functional modifications such as doping. There is also a large parameter space to be explored for designing and optimizing anodic materials for resource recovery, which has been less discussed in the literature than cathodes. Research into more cost-effective fabrication techniques or superior alternatives to conventional materials for electrochemical redox reactions such as MMOs and BDD are still needed. For all of these electrode materials, more study must be done on their performance over many cycles to determine and reduce the causes of capacity fade in order for these systems to be more practical for usage in critical resource recovery.

Although the development of ISSG technology is still in a nascent stage, it has received tremendous research attention and is rapidly growing as a promising strategy for inexpensive offgrid operations in water treatment and resource recovery. As it was previously discussed, many different photothermal materials have been proven to be effective for ISSG applications in controlled settings. Thus, technoeconomic and life cycle analysis should be used to determine the most economical and sustainable material options, with low-cost natural materials like biochar likely to be the most promising. One of the major goals for ISSGs is to improve the evaporation rates to reduce the land area requirements and to operate at practical timescales. This will require the design of highly hydrophilic materials with porous structures optimized to boost the rates of capillary water transport for continuous evaporation. Hydrogels have shown strong promise on this frontier, reporting some of the highest evaporation rates in the ISSG literature. [324,372] Another major challenge to address is the design of surfaces with antifouling or localized precipitation properties for continuous evaporation and resource concentration. There is still room to explore new surface morphologies and functionalizations to minimize the impact of solute precipitation on evaporation rates, and more longterm experimental studies are needed to fully evaluate their performance. There is also a vast design space in ISSG architectures, with more research needed in novel 3D architectures to boost evaporation rates and modulate fluid, heat, and solute transport pathways. Most of the current ISSG technologies are limited to applications in the nonselective concentration of resourcecontaining solutions; more research must be conducted in designing ISSG materials that can perform selective separations or integrate hybrid-functional materials (e.g., catalysts, sorbents) to imbue resource selectivity.

One of the major obstacles to evaluating and comparing the performance of different materials for resource recovery applications is the lack of any standard methodology in the reported experimental conditions and quantitative metrics. Even within the context of a single technological basis, there are a variety of relevant quantitative metrics that may not always be consistently reported across the literature. For example, in the case of electrodes for electrosorption, the selectivity, gravimetric uptake capacity, capacity fading (i.e., desorption efficiency), and

specific energy consumption would all be important but may not rial science and engineering will undoubtedly play a significant role in designing the novel materials and separation strategies required to recover critical resources from water and to ensure a secure and sustainable future across the globe.

always be reported in publications. This is further complicated by the diversity of water sources and their respective compositions that are of interest for critical resource recovery. If the context for evaluation is further narrowed down to a single given resource (e.g., lithium), the mixture of interferents and the concentrations of both resources and interferents still varies across different reports in the literature, making results difficult to directly compare. To enhance consistency and transparency in this field, it is important for researchers to provide detailed reports of their experimental conditions and methods for quantifying performance. More discourse also needs to be had to determine what concentrations and conditions should be considered as standard for specific streams of interest to critical resource recovery applications (e.g., Li-rich brines, nutrient-rich wastewaters, wastewaters containing REEs). More standardized data are also more conducive to utility by machine learning algorithms that can potentially correlate material properties to quantifiable performance metrics. Due to the myriad of material compositions and hybrid combinations that can be fabricated, machine learning can serve a powerful role to uncover trends in the literature and offer guidance on the direction of future research efforts.

There are still many challenges that must be overcome to make these separation technologies more practical for widespread adoption. Despite the advances that have been made in the synthesis and fabrication of nanomaterials, more work must be done to make these processes more scalable and economical, especially for emerging classes of versatile materials like 2D materials and supramolecular receptors that can enable precise separations. The intrinsic economic value, resource intensiveness, and end-of-life management of the materials that are used to develop resource recovery technologies must also be carefully considered via rigorous life cycle and technoeconomic analyses. For example, there will inherently be tradeoffs in using critical minerals like precious metals to fabricate sorbents or ISSGs compared to inexpensive but less tunable materials like natural carbonaceous materials and biochar. At the process scale, a combination of modeling and technoeconomic analysis can also help to inform which components of a separation system limit its overall performance and cost-effectiveness, which can be used to further guide the directions of research in this field.

The problem of securing critical resource supplies is inextricably linked to the management and treatment of water resources and necessitates the advancement of material-based separation technologies for resource recovery. As this review has demonstrated, each of these technologies can be fabricated from a variety of materials with unique properties, making them useful for different stages and scenarios of critical resource recovery. There is no single material that can efficiently perform all separations; thus, effective resource recovery systems will need to employ dynamic combinations of these materials for different applications. For example, one could employ an ISSG to preconcentrate a stream containing critical resources to concentrations suitable for catalytic or electrochemical recovery processes. Alternatively, one could integrate selective sorbent materials onto the surface of a membrane or ISSG to capture critical resources while simultaneously treating water. New materials and hybrid combinations of technologies will continue to be developed as this field matures and more applied research efforts formulate. Mate-

Acknowledgements

W.C., J.G.E., F.G., Y.L., Y.W., and Z.X. contributed equally to this work. This work was supported as part of the Advanced Materials for Energy-Water-Systems (AMEWS) Center, an Energy Frontier Research Center funded by the U.S. Department of Energy, Office of Science, Basic Energy Sciences at Argonne National Laboratory under Contract No. DE-AC02-06CH11357.

Conflict of Interest

The authors declare no conflict of interest.

Keywords

critical materials, nanomaterials, resource recovery, separation, water

Received: January 30, 2023 Revised: March 22, 2023 Published online:

- [1] "U.S. Geological Survey Releases 2022 List of Critical Minerals," https://www.usgs.gov/news/national-news-release/us-geologicalsurvey-releases-2022-list-critical-minerals (accessed: March 2023).
- [2] Mineral Commodity Summaries: Cobalt, U.S. Geological Survey, Reston, VA, USA 2023.
- L. Gaines, Sustainable Mater. Technol. 2018, 17, e00068.
- [4] D. Schrijvers, A. Hool, G. A. Blengini, W.-Q. Chen, J. Dewulf, R. Eggert, L. van Ellen, R. Gauss, J. Goddin, K. Habib, C. Hagelüken, A. Hirohata, M. Hofmann-Amtenbrink, J. Kosmol, M. Le Gleuher, M. Grohol, A. Ku, M.-H. Lee, G. Liu, K. Nansai, P. Nuss, D. Peck, A. Reller, G. Sonnemann, L. Tercero, A. Thorenz, P. A. Wäger, Resour., Conserv. Recycl. 2020, 155, 104617.
- R. W. Scholz, F.-W. Wellmer, J. Ind. Ecol. 2019, 23, 313.
- B. W. Schipper, H.-C. Lin, M. A. Meloni, K. Wansleeben, R. Heijungs, E. van der Voet, Resour., Conserv. Recycl. 2018, 132, 28.
- S. Lin, M. Hatzell, R. Liu, G. Wells, X. Xie, Resour., Conserv. Recycl. **2021**, 175, 105853.
- [8] R. M. DuChanois, N. J. Cooper, B. Lee, S. K. Patel, L. Mazurowski, T. E. Graedel, M. Elimelech, Nat. Water 2023, 1, 37.
- [9] Mineral Commodity Summaries: Lithium, U.S. Geological Survey, Reston, VA, USA 2023.
- [10] D. Aitken, D. Rivera, A. Godoy-Faúndez, E. Holzapfel, Sustainability **2016**, 8, 128.
- [11] P. Kehrein, M. van Loosdrecht, P. Osseweijer, M. Garfí, J. Dewulf, J. Posada, Environ. Sci.: Water Res. Technol. 2020, 6, 877.
- [12] M. S. Diallo, M. R. Kotte, M. Cho, Environ. Sci. Technol. 2015, 49,
- [13] E. Walling, W. Moerman, W. Verstraete, D. K. V. Gomez, C. Vaneeckhaute, in Resource Recovery from Water: Principles and Application, IWA Publishing, London, UK 2022, pp. 21-45.
- [14] A. Taghvaie Nakhjiri, H. Sanaeepur, A. Ebadi Amooghin, M. M. A. Shirazi, Desalination 2022, 527, 115510.
- [15] S.-Y. Pan, A. Z. Haddad, A. Kumar, S.-W. Wang, Water Res. 2020, 183, 116064.



ADVANCED MATERIALS

- [16] G. Naidu, S. Ryu, R. Thiruvenkatachari, Y. Choi, S. Jeong, S. Vigneswaran, Environ. Pollut. 2019, 247, 1110.
- [17] M. R. Adam, M. H. D. Othman, T. A. Kurniawan, M. H. Puteh, A. F. Ismail, W. Khongnakorn, M. A. Rahman, J. Jaafar, J. Environ. Chem. Eng. 2022, 10, 107633.
- [18] A. Battistel, M. S. Palagonia, D. Brogioli, F. La Mantia, R. Trócoli, Adv. Mater. 2020, 32, 1905440.
- [19] S. Iftekhar, G. Heidari, N. Amanat, E. N. Zare, M. B. Asif, M. Hassanpour, V. P. Lehto, M. Sillanpaa, Environ. Chem. Lett. 2022, 20 3697
- [20] H. Yang, S. Ye, Z. Zeng, G. Zeng, X. Tan, R. Xiao, J. Wang, B. Song, L. Du, M. Qin, Y. Yang, F. Xu, Chem. Eng. J. 2020, 397, 125502.
- [21] S. Guo, Y. Wan, X. Chen, J. Luo, Chem. Eng. J. 2021, 409, 127376.
- [22] P. S. Goh, K. C. Wong, A. F. Ismail, Desalination 2022, 521, 115377.
- [23] T. G. Ambaye, M. Vaccari, F. D. Castro, S. Prasad, S. Rtimi, *Environ. Sci. Pollut. Res.* 2020, 27, 36052.
- [24] C. E. D. Cardoso, J. C. Almeida, C. B. Lopes, T. Trindade, C. Vale, E. Pereira, Nanomaterials 2019, 9, 814.
- [25] X. Li, Y. Mo, W. Qing, S. Shao, C. Y. Tang, J. Li, J. Membr. Sci. 2019, 591, 117317.
- [26] J. P. H. Perez, K. Folens, K. Leus, F. Vanhaecke, P. Van Der Voort, G. Du Laing, Resour., Conserv. Recycl. 2019, 142, 177.
- [27] M. K. Jha, A. Kumari, R. Panda, J. Rajesh Kumar, K. Yoo, J. Y. Lee, Hydrometallurgy 2016, 165, 2.
- [28] D. Puyol, D. J. Batstone, T. Hülsen, S. Astals, M. Peces, J. O. Krömer, Front. Microbiol. 2017, 7, 2106.
- [29] E. Barry, R. Burns, W. Chen, G. X. De Hoe, J. M. M. De Oca, J. J. de Pablo, J. Dombrowski, J. W. Elam, A. M. Felts, G. Galli, J. Hack, Q. He, X. He, E. Hoenig, A. Iscen, B. Kash, H. H. Kung, N. H. C. Lewis, C. Liu, X. Ma, A. Mane, A. B. F. Martinson, K. L. Mulfort, J. Murphy, K. Mølhave, P. Nealey, Y. Qiao, V. Rozyyev, G. C. Schatz, S. J. Sibener, et al., Chem. Rev. 2021, 121, 9450.
- [30] K. Hayamizu, Y. Chiba, T. Haishi, RSC Adv. 2021, 11, 20252.
- [31] C. Lu, C. Hu, C. L. Ritt, X. Hua, J. Sun, H. Xia, Y. Liu, D.-W. Li, B. Ma, M. Elimelech, J. Qu, J. Am. Chem. Soc. 2021, 143, 14242.
- [32] D. Xu, Z. Shah, G. Sun, X. Peng, Y. Cui, Miner. Eng. 2019, 139, 105861
- [33] J. Kim, J. Kim, S. Hong, Water Res. 2018, 129, 447.
- [34] H. Yan, W. Li, Y. Zhou, M. Irfan, Y. Wang, C. Jiang, T. Xu, *Membranes* **2020**. *10*. 135.
- [35] H. Zangeneh, A. A. Zinatizadeh, S. Zinadini, M. Feyzi, D. W. Bahnemann, Sep. Purif. Technol. 2019, 209, 764.
- [36] T.-Z. Jia, J.-P. Lu, X.-Y. Cheng, Q.-C. Xia, X.-L. Cao, Y. Wang, W. Xing, S.-P. Sun, J. Membr. Sci. 2019, 580, 214.
- [37] P. Li, H. Lan, K. Chen, X. Ma, B. Wei, M. Wang, P. Li, Y. Hou, Q. J. Niu, Sep. Purif. Technol. 2022, 280, 119949.
- [38] L. Shi, S. Liu, W.-S. Hung, W. Shi, X. Lu, C. Wu, J. Membr. Sci. 2023, 668, 121252.
- [39] A. Pérez-González, R. Ibáñez, P. Gómez, A. M. Urtiaga, I. Ortiz, J. A. Irabien, J. Membr. Sci. 2015, 473, 16.
- [40] K. Gu, S. Wang, Y. Li, X. Zhao, Y. Zhou, C. Gao, J. Membr. Sci. 2019, 581, 214.
- [41] Y. Hao, Q. Li, B. He, B. Liao, X. Li, M. Hu, Y. Ji, Z. Cui, M. Younas, J. Li, J. Mater. Chem. A 2020, 8, 5275.
- [42] Y. Liang, Y. Zhu, C. Liu, K.-R. Lee, W.-S. Hung, Z. Wang, Y. Li, M. Elimelech, J. Jin, S. Lin, Nat. Commun. 2020, 11, 2015.
- [43] X. You, K. Xiao, H. Wu, Y. Li, R. Li, J. Yuan, R. Zhang, Z. Zhang, X. Liang, J. Shen, Z. Jiang, iScience 2021, 24, 102369.
- [44] Y. Xiao, D. Guo, T. Li, Q. Zhou, L. Shen, R. Li, Y. Xu, H. Lin, Appl. Surf. Sci. 2020, 515, 146063.
- [45] C. Zhou, X. Gao, S. Li, C. Gao, Desalination 2013, 317, 67.
- [46] J. Ding, H. Wu, P. Wu, Chem. Eng. J. 2020, 396, 125199.
- [47] H.-C. Yang, R. Z. Waldman, M.-B. Wu, J. Hou, L. Chen, S. B. Darling, Z.-K. Xu, Adv. Funct. Mater. 2018, 28, 1705327.

- [48] Z. Wang, H.-C. Yang, F. He, S. Peng, Y. Li, L. Shao, S. B. Darling, Matter 2019, 1, 115.
- [49] Y. Wu, R. Lin, F. Ma, W. Xing, J. Pan, J. Colloid Interface Sci. 2021, 587, 703.
- [50] X. Q. Cheng, Z. X. Wang, Y. Zhang, Y. Zhang, J. Ma, L. Shao, J. Membr. Sci. 2018, 554, 385.
- [51] Q. Li, Z. Liao, X. Fang, D. Wang, J. Xie, X. Sun, L. Wang, J. Li, J. Membr. Sci. 2019, 584, 324.
- [52] C. Zhou, T. Segal-Peretz, M. E. Oruc, H. S. Suh, G. Wu, P. F. Nealey, Adv. Funct. Mater. 2017, 27, 1701756.
- [53] L. Xing, J. Song, Z. Li, J. Liu, T. Huang, P. Dou, Y. Chen, X.-M. Li, T. He, J. Membr. Sci. 2016, 520, 596.
- [54] J. Kloos, N. Joosten, A. Schenning, K. Nijmeijer, J. Membr. Sci. 2021, 620, 118849.
- [55] G. M. Bögels, J. A. M. Lugger, O. J. G. M. Goor, R. P. Sijbesma, Adv. Funct. Mater. 2016, 26, 8023.
- [56] J. Vander Linden, R. F. De Ketelaere, J. Membr. Sci. 1998, 139, 125.
- [57] A. Surucu, V. Eyupoglu, O. Tutkun, J. Ind. Eng. Chem. 2012, 18, 629.
- [58] I. Van de Voorde, L. Pinoy, R. F. De Ketelaere, J. Membr. Sci. 2004, 234, 11.
- [59] G. Zante, M. Boltoeva, A. Masmoudi, R. Barillon, D. Trébouet, Sep. Purif. Technol. 2020, 252, 117477.
- [60] F. Radmanesh, T. Rijnaarts, A. Moheb, M. Sadeghi, W. M. de Vos, J. Colloid Interface Sci. 2019, 533, 658.
- [61] W. Ye, R. Liu, X. Chen, Q. Chen, J. Lin, X. Lin, B. Van der Bruggen, S. Zhao, J. Membr. Sci. 2020, 608, 118182.
- [62] F. Sheng, N. U. Afsar, Y. Zhu, L. Ge, T. Xu, Membranes 2020, 10, 114.
- [63] A. Gilles, M. Barboiu, J. Am. Chem. Soc. 2016, 138, 426.
- [64] H.-C. Yang, Y. Xie, H. Chan, B. Narayanan, L. Chen, R. Z. Waldman, S. K. R. S. Sankaranarayanan, J. W. Elam, S. B. Darling, ACS Nano 2018, 12, 8678.
- [65] Q. Chen, P. Yu, W. Huang, S. Yu, M. Liu, C. Gao, J. Membr. Sci. 2015, 492, 312.
- [66] Z. Yang, W. Fang, Z. Wang, R. Zhang, Y. Zhu, J. Jin, J. Membr. Sci. 2021, 620, 118862.
- [67] Q. Wen, D. Yan, F. Liu, M. Wang, Y. Ling, P. Wang, P. Kluth, D. Schauries, C. Trautmann, P. Apel, W. Guo, G. Xiao, J. Liu, J. Xue, Y. Wang, Adv. Funct. Mater. 2016, 26, 5796.
- [68] T. Ma, Y. Su, Y. Li, R. Zhang, Y. Liu, M. He, Y. Li, N. Dong, H. Wu, Z. Jiang, J. Membr. Sci. 2016, 503, 101.
- [69] J. Zhang, L. Yang, Z. Wang, S. Yang, P. Li, P. Song, M. Ban, J. Membr. Sci. 2019, 587, 117159.
- [70] M. Velický, P. S. Toth, Appl. Mater. Today 2017, 8, 68.
- [71] K. Huang, G. Liu, J. Shen, Z. Chu, H. Zhou, X. Gu, W. Jin, N. Xu, Adv. Funct. Mater. 2015, 25, 5809.
- [72] L. Qin, Y. Zhao, J. Liu, J. Hou, Y. Zhang, J. Wang, J. Zhu, B. Zhang, Y. Lvov, B. Van der Bruggen, ACS Appl. Mater. Interfaces 2016, 8, 34914.
- [73] X. Shi, A. Xiao, C. Zhang, Y. Wang, J. Membr. Sci. 2019, 576, 116.
- [74] J. Zhu, M. Tian, J. Hou, J. Wang, J. Lin, Y. Zhang, J. Liu, B. V. der Bruggen, J. Mater. Chem. A 2016, 4, 1980.
- [75] Y. Guo, Y. Ying, Y. Mao, X. Peng, B. Chen, Angew. Chem., Int. Ed. 2016, 55, 15120.
- [76] W. Zhang, L. Zhang, H. Zhao, B. Li, H. Ma, J. Mater. Chem. A 2018, 6, 13331.
- [77] L. Sun, Y. Ying, H. Huang, Z. Song, Y. Mao, Z. Xu, X. Peng, ACS Nano 2014, 8, 6304.
- [78] W. Hu, X. Cui, L. Xiang, L. Gong, L. Zhang, M. Gao, W. Wang, J. Zhang, F. Liu, B. Yan, H. Zeng, J. Colloid Interface Sci. 2020, 560, 177.
- [79] K. Fu, X. Liu, D. Yu, J. Luo, Z. Wang, J. C. Crittenden, Environ. Sci. Technol. 2020, 54, 16212.
- [80] P. Xu, J. Hong, Z. Xu, H. Xia, Q.-Q. Ni, Sep. Purif. Technol. 2021, 270, 118796.



- [81] A. Pendse, S. Cetindag, M.-H. Lin, A. Rackovic, R. Debbarma, S. Almassi, B. P. Chaplin, V. Berry, J. W. Shan, S. Kim, Small 2019, 15, 1904590.
- [82] G. P. S. Ibrahim, A. M. Isloor, A. Moslehyani, A. F. Ismail, J. Water Process Eng. 2017, 20, 138.
- [83] Z. Xia, W. Chen, R. Shevate, Y. Wang, F. Gao, D. Wang, O. A. Kazi, A. U. Mane, S. S. Lee, J. W. Elam, S. B. Darling, ACS Nano 2022, 16, 18266.
- [84] M. O. Daramola, P. Hlanyane, O. O. Sadare, O. O. Oluwasina, S. E. Iyuke, Membranes 2017, 7, 14.
- [85] Y.-H. Li, Z. Di, J. Ding, D. Wu, Z. Luan, Y. Zhu, Water Res. 2005, 39, 605.
- [86] P. Loganathan, S. Vigneswaran, J. Kandasamy, N. S. Bolan, Crit. Rev. Environ. Sci. Technol. 2014, 44, 847.
- [87] A. Othman, E. Dumitrescu, D. Andreescu, S. Andreescu, ACS Sustainable Chem. Eng. 2018, 6, 12542.
- [88] L. Wang, L. Yang, Y. Li, Y. Zhang, X. Ma, Z. Ye, Chem. Eng. J. 2010, 163, 364.
- [89] R. Yang, K. B. Aubrecht, H. Ma, R. Wang, R. B. Grubbs, B. S. Hsiao, B. Chu, *Polymer* **2014**, *55*, 1167.
- [90] P. Singhal, B. G. Vats, V. Pulhani, J. Ind. Eng. Chem. 2020, 90, 17.
- [91] L. I. Bowden, A. P. Jarvis, P. L. Younger, K. L. Johnson, *Environ. Sci. Technol.* 2009, 43, 2476.
- [92] M. I. A. Abdel Maksoud, A. M. Elgarahy, C. Farrell, A. H. Al-Muhtaseb, D. W. Rooney, A. I. Osman, *Coord. Chem. Rev.* 2020, 403, 213096.
- [93] P. Lodeiro, R. Herrero, M. E. Sastre de Vicente, J. Hazard. Mater. 2006, 137, 1649.
- [94] G. P. Rao, C. Lu, F. Su, Sep. Purif. Technol. 2007, 58, 224.
- [95] S. Petzet, B. Peplinski, P. Cornel, Water Res. 2012, 46, 3769.
- [96] A. Drenkova-Tuhtan, K. Mandel, A. Paulus, C. Meyer, F. Hutter, C. Gellermann, G. Sextl, M. Franzreb, H. Steinmetz, Water Res. 2013, 47 5670
- [97] F. Seidi, M. R. Saeb, Y. Huang, A. Akbari, H. Xiao, Chem. Rec. 2021, 21, 1876.
- [98] W. C. Fowler, C. Deng, G. M. Griffen, T. Teodoro, A. Z. Guo, M. Zaiden, M. Gottlieb, J. J. de Pablo, M. V. Tirrell, J. Am. Chem. Soc. 2021, 143, 4440.
- [99] J. L. Lopes, K. L. Marques, A. V. Girão, E. Pereira, T. Trindade, J. Colloid Interface Sci. 2016, 475, 96.
- [100] X. Xu, Y. Chen, P. Wan, K. Gasem, K. Wang, T. He, H. Adidharma, M. Fan, Prog. Mater. Sci. 2016, 84, 276.
- [101] B. Wu, C. Liu, C. Fu, P. Wu, C. Liu, W. Jiang, Chem. Eng. J. 2019, 373, 1030.
- [102] S. Lin, D. H. K. Reddy, J. K. Bediako, M.-H. Song, W. Wei, J.-A. Kim, Y.-S. Yun, J. Mater. Chem. A 2017, 5, 13557.
- [103] B. Yan, C. Ma, J. Gao, Y. Yuan, N. Wang, Adv. Mater. 2020, 32, 1906615.
- [104] T. M. Huggins, A. Haeger, J. C. Biffinger, Z. J. Ren, Water Res. 2016, 94, 225.
- [105] Z. Chang, L. Zeng, C. Sun, P. Zhao, J. Wang, L. Zhang, Y. Zhu, X. Qi, Coord. Chem. Rev. 2021, 445, 214072.
- [106] C. W. Purnomo, E. P. Kesuma, I. Perdana, M. Aziz, Waste Manage. 2018, 79, 454.
- [107] D. Luo, L. Wang, H. Nan, Y. Cao, H. Wang, T. V. Kumar, C. Wang, Environ. Chem. Lett. 2023, 21, 497.
- [108] L. Zhang, L. Wan, N. Chang, J. Liu, C. Duan, Q. Zhou, X. Li, X. Wang, J. Hazard. Mater. 2011, 190, 848.
- [109] M. Carboni, C. W. Abney, K. M. L. Taylor-Pashow, J. L. Vivero-Escoto, W. Lin, Ind. Eng. Chem. Res. 2013, 52, 15187.
- [110] "Biochar," https://biochar-international.org/biochar/ (accessed: March 2023).
- [111] M. M. Rossi, L. Silvani, N. Amanat, M. P. Papini, *Materials* 2021, 14, 1776.

- [112] P. Yuan, J. Wang, Y. Pan, B. Shen, C. Wu, Sci. Total Environ. 2019, 659, 473.
- [113] L. Fang, J. Li, S. Donatello, C. R. Cheeseman, C. S. Poon, D. C. W. Tsang, J. Cleaner Prod. 2020, 244, 118853.
- [114] Y. Yao, B. Gao, J. Chen, L. Yang, Environ. Sci. Technol. 2013, 47, 8700.
- [115] B. Sarkar, S. Mandal, Y. F. Tsang, P. Kumar, K.-H. Kim, Y. S. Ok, Sci. Total Environ. 2018, 612, 561.
- [116] D. Huang, J. Wu, L. Wang, X. Liu, J. Meng, X. Tang, C. Tang, J. Xu, Chem. Eng. J. 2019, 358, 1399.
- [117] W. Liu, Z. Tao, D. Wang, Q. Liu, Y. Zhang, Y. Zhang, A. Dong, J. Hazard. Mater. 2021, 410, 124601.
- [118] R. Hai, Y. Wang, X. Wang, Z. Du, Y. Li, PLoS One 2014, 9, e107345.
- [119] W. Yu, L. Sisi, Y. Haiyan, L. Jie, RSC Adv. 2020, 10, 15328.
- [120] Y. Chen, H. Shang, Y. Ren, Y. Yue, H. Li, Z. Bian, ACS ESQT Engg 2022, 2, 1039.
- [121] M. Du, Y. Zhang, Z. Wang, M. Lv, A. Tang, Y. Yu, X. Qu, Z. Chen, Q. Wen, A. Li, Chem. Eng. J. 2022, 442, 136147.
- [122] G. Salfate, J. Sánchez, Polymers 2022, 14, 4786.
- [123] B. Sniatala, T. A. Kurniawan, D. Sobotka, J. Makinia, M. H. D. Othman, Sci. Total Environ. 2023, 856, 159283.
- [124] V. Rychkov, E. Kirillov, S. Kirillov, G. Bunkov, M. Botalov, V. Semenishchev, D. Smyshlyaev, A. Malyshev, A. Taukin, A. Akcil, Sep. Purif. Rev. 2022, 51, 468.
- [125] T. Liu, J. Chen, Sep. Purif. Technol. 2021, 276, 119263.
- [126] H. Du, C. Y. K. Lung, T.-C. Lau, Environ. Sci.: Water Res. Technol. 2018, 4, 421.
- [127] B. N. Kumar, S. Radhika, B. Ramachandra Reddy, Chem. Eng. J. 2010, 160. 138.
- [128] B. Clark, G. Gilles, W. A. Tarpeh, ACS Appl. Mater. Interfaces 2022, 14, 22950.
- [129] W. Wang, R. Narain, H. Zeng, in Polymer Science and Nanotechnology (Ed: R. Narain), Elsevier, Amsterdam, The Netherlands 2020, pp. 203–244.
- [130] M. Khan, I. M. C. Lo, Water Res. 2016, 106, 259.
- [131] S. Wang, K. Xiao, Y. Mo, B. Yang, T. Vincent, C. Faur, E. Guibal, J. Hazard. Mater. 2020, 386, 121637.
- [132] B. Aguila, Q. Sun, H. C. Cassady, C. Shan, Z. Liang, A. M. Al-Enizic, A. Nafadyc, J. T. Wright, R. W. Meulenberg, S. Ma, Angew. Chem., Int. Ed. 2020, 59, 19618.
- [133] M. M. Yusoff, N. R. N. Mostapa, M. S. Sarkar, T. K. Biswas, M. L. Rahman, S. E. Arshad, M. S. Sarjadi, A. D. Kulkarni, J. Rare Earths 2017, 35, 177.
- [134] L. Baudino, C. Santos, C. F. Pirri, F. L. Mantia, A. Lamberti, Adv. Sci. 2022, 9, 2201380.
- [135] Z. Dong, X. Yang, Q. Pan, Y. Ao, J. Du, M. Zhai, L. Zhao, Cellulose 2020, 27, 3249.
- [136] H. Siwek, A. Bartkowiak, M. Włodarczyk, K. Sobecka, Water, Air, Soil Pollut. 2016, 227, 427.
- [137] M. H. Mahaninia, L. D. Wilson, J. Appl. Polym. Sci. 2016, 133, 42949.
- [138] K. Venkiteshwaran, E. Wells, B. K. Mayer, Water Environ. Res. 2021, 93, 1173.
- [139] M. Gurung, B. B. Adhikari, H. Kawakita, K. Ohto, K. Inoue, S. Alam, Ind. Eng. Chem. Res. 2012, 51, 11901.
- [140] Y. Wang, S. B. Darling, J. Chen, ACS Appl. Mater. Interfaces 2021, 13,
- [141] M. Zelzer, R. V. Ulijn, in Smart Polymers and Their Applications (Eds: M. R. Aguilar, J. San Román), Woodhead Publishing, Cambridge, UK 2014, pp. 166–203.
- [142] G. Yang, Y. Liu, H. Li, X. Tian, J. Pan, Sep. Purif. Technol. 2021, 266, 118540.
- [143] A. Alsbaiee, B. J. Smith, L. Xiao, Y. Ling, D. E. Helbling, W. R. Dichtel, Nature 2016, 529, 190.
- [144] J. V. Gavette, N. S. Mills, L. N. Zakharov, C. A. Johnson II, D. W. Johnson, M. M. Haley, Angew. Chem., Int. Ed. 2013, 52, 10270.



- [145] W. Zhao, B. Qiao, C.-H. Chen, A. H. Flood, Angew. Chem., Int. Ed. 2017, 56, 13083.
- [146] E. M. Fatila, M. Pink, E. B. Twum, J. A. Karty, A. H. Flood, Chem. Sci. 2018, 9, 2863.
- [147] S. M. Harris, J. T. Nguyen, S. L. Pailloux, J. P. Mansergh, M. J. Dresel, T. B. Swanholm, T. Gao, V. C. Pierre, Environ. Sci. Technol. 2017, 51, 4540
- [148] E. D. Doidge, I. Carson, P. A. Tasker, R. J. Ellis, C. A. Morrison, J. B. Love, Angew. Chem., Int. Ed. 2016, 55, 12436.
- [149] H. Wu, L. O. Jones, Y. Wang, D. Shen, Z. Liu, L. Zhang, K. Cai, Y. Jiao, C. L. Stern, G. C. Schatz, J. F. Stoddart, ACS Appl. Mater. Interfaces 2020, 12, 38768.
- [150] H. Wu, Y. Wang, L. O. Jones, W. Liu, L. Zhang, B. Song, X.-Y. Chen, C. L. Stern, G. C. Schatz, J. F. Stoddart, Angew. Chem., Int. Ed. 2021, 60, 17587.
- [151] H. Yu, G. Naidu, C. Zhang, C. Wang, A. Razmjou, D. S. Han, T. He, H. Shon, Desalination 2022, 539, 115951.
- [152] W. Yao, F. J. Millero, Environ. Sci. Technol. 1996, 30, 536.
- [153] E. Yavuz, Ş. Tokalıoğlu, H. Şahan, Ş. Patat, *Talanta* **2014**, *128*, 31.
- [154] Y. Su, W. Yang, W. Sun, Q. Li, J. K. Shang, Chem. Eng. J. 2015, 268, 270.
- [155] A. Uheida, M. Iglesias, C. Fontàs, M. Hidalgo, V. Salvadó, Y. Zhang, M. Muhammed, J. Colloid Interface Sci. 2006, 301, 402.
- [156] Y. Qing, Y. Hang, R. Wanjaul, Z. Jiang, B. Hu, Anal. Sci. 2003, 19, 1417.
- [157] B. Feng, C. Yao, S. Chen, R. Luo, S. Liu, S. Tong, Chem. Eng. J. 2018, 350, 692.
- [158] C. Yao, S. Chen, L. Wang, H. Deng, S. Tong, Chem. Eng. J. 2019, 373, 1168.
- [159] Z. Qin, X. Tang, Y. Su, Z. He, Y. Qu, S. Tong, ACS Appl. Nano Mater. 2020. 3, 4102.
- [160] L. Wang, K. Wang, R. Huang, Z. Qin, Y. Su, S. Tong, Chemosphere 2020, 252, 126578.
- [161] T.-H. Kim, L. Lundehøj, U. G. Nielsen, Appl. Clay Sci. 2020, 189, 105521.
- [162] J. Y. Park, J. Lee, G.-M. Go, B. Jang, H.-B. Cho, Y.-H. Choa, Appl. Surf. Sci. 2021, 548, 149157.
- [163] S. C. N. Tang, I. M. C. Lo, Water Res. 2013, 47, 2613.
- [164] D. Weng, H. Duan, Y. Hou, J. Huo, L. Chen, F. Zhang, J. Wang, Prog. Nat. Sci.: Mater. Int. 2020, 30, 139.
- [165] W. Chouyyok, R. J. Wiacek, K. Pattamakomsan, T. Sangvanich, R. M. Grudzien, G. E. Fryxell, W. Yantasee, *Environ. Sci. Technol.* 2010, 44, 3073.
- [166] C. Zeng, P. Liu, Z. Xiao, Y. Li, L. Song, Z. Cao, D. Wu, Y.-F. Zhang, ACS Sustainable Chem. Eng. 2022, 10, 1103.
- [167] S. Iftekhar, V. Srivastava, M. Sillanpää, Chem. Eng. J. 2017, 320, 151.
- [168] A. Amaria, N. Nuryono, S. Suyanta, Orient. J. Chem. 2017, 33, 384.
- [169] P. Vassileva, D. Voikova, J. Hazard. Mater. 2009, 170, 948.
- [170] M. A. M. Khraisheh, Y. S. Al-degs, W. A. M. Mcminn, Chem. Eng. J. 2004, 99, 177.
- [171] H. Wang, X. Wang, P. Xia, J. Song, R. Ma, H. Jing, Z. Zhang, X. Cheng, J. Zhao, Appl. Clay Sci. 2017, 135, 418.
- [172] H. Wu, C. Vaneeckhaute, Chem. Eng. J. 2022, 433, 133664.
- [173] S. Wang, Y. Peng, Chem. Eng. J. 2010, 156, 11.
- [174] M. S. Onyango, D. Kuchar, M. Kubota, H. Matsuda, *Ind. Eng. Chem. Res.* 2007, 46, 894.
- [175] A. B. Đukić, K. R. Kumrić, N. S. Vukelić, M. S. Dimitrijević, Z. D. Baščarević, S. V. Kurko, L. L. Matović, Appl. Clay Sci. 2015, 103, 20.
- [176] O. V. Eremin, E. S. Epova, R. A. Filenko, O. S. Rusal', V. A. Bychinsky, J. Min. Sci. 2017, 53, 915.
- [177] Q. Zhou, Y. Fu, X. Zhang, T. Luo, W. Luo, Mater. Sci. Eng., B 2018, 227, 89.
- [178] J. Xie, L. Lai, L. Lin, D. Wu, Z. Zhang, H. Kong, J. Environ. Sci. Health, Part A: Toxic/Hazard. Subst. Environ. Eng. 2015, 50, 1298.

- [179] M. Ibrahim, M. Labaki, J.-M. Giraudon, J.-F. Lamonier, J. Hazard. Mater. 2020, 383, 121139.
- [180] C. Fonseka, S. Ryu, Y. Choo, M. Mullett, R. Thiruvenkatachari, G. Naidu, S. Vigneswaran, ACS Sustainable Chem. Eng. 2021, 9, 16896.
- [181] Y. Li, H. Zhong, Y. Jin, B. Guan, J. Yue, R. Zhao, Y. Huang, ACS Appl. Mater. Interfaces 2022, 14, 40408.
- [182] H. Liu, W. Guo, Z. Liu, X. Li, R. Wang, RSC Adv. 2016, 6, 105282.
- [183] M. Li, Y. Liu, F. Li, C. Shen, Y. V. Kaneti, Y. Yamauchi, B. Yuliarto, B. Chen, C.-C. Wang, Environ. Sci. Technol. 2021, 55, 13209.
- [184] Q. Xie, Y. Li, Z. Lv, H. Zhou, X. Yang, J. Chen, H. Guo, Sci. Rep. 2017, 7, 3316.
- [185] W. Yang, Q. Pan, S. Song, H. Zhang, Inorg. Chem. Front. 2019, 6, 1924.
- [186] S. Yang, T. Li, Y. Cheng, W. Fan, L. Wang, Y. Liu, L. Bian, C.-H. Zhou, L.-Y. Zheng, Q.-E. Cao, ACS Sustainable Chem. Eng. 2022, 10, 9719.
- [187] J.-Y. Yue, X.-L. Ding, Y.-T. Wang, Y.-X. Wen, P. Yang, Y. Ma, B. Tang, J. Mater. Chem. A 2021, 9, 26861.
- [188] G. Cheng, A. Zhang, Z. Zhao, Z. Chai, B. Hu, B. Han, Y. Ai, X. Wang, Sci. Bull. 2021, 66, 1994.
- [189] Y. Zhao, C. Xu, Q. Qi, J. Qiu, Z. Li, H. Wang, J. Wang, Chem. Eng. J. 2022, 446, 136823.
- [190] Y. Li, G. Liang, L. Chang, C. Zi, Y. Zhang, Z. Peng, W. Zhao, Energy Sources, Part A 2021, 43, 1745.
- [191] L. Massimi, A. Giuliano, M. L. Astolfi, R. Congedo, A. Masotti, S. Canepari, *Materials* 2018, 11, 334.
- [192] A. Bhatnagar, M. Sillanpää, A. Witek-Krowiak, Chem. Eng. J. 2015, 270, 244.
- [193] H. S. Vinith, Int. J. Civ. Eng. Technol. 2017, 8, 837.
- [194] H. Cho, D. Oh, K. Kim, J. Hazard. Mater. 2005, 127, 187.
- [195] F. Banat, S. Al-Asheh, F. Mohai, Sep. Purif. Technol. 2000, 21, 155.
- [196] I. Ali, M. Asim, T. A. Khan, J. Environ. Manage. 2012, 113, 170.
- [197] D. S. S, V. Vishwakarma, Chemosphere 2021, 273, 129677.
- [198] A. V. Baskar, N. Bolan, S. A. Hoang, P. Sooriyakumar, M. Kumar, L. Singh, T. Jasemizad, L. P. Padhye, G. Singh, A. Vinu, B. Sarkar, M. B. Kirkham, J. Rinklebe, S. Wang, H. Wang, R. Balasubramanian, K. H. M. Siddique, Sci. Total Environ. 2022, 822, 153555.
- [199] A. Kapoor, T. Viraraghavan, Bioresour. Technol. 1995, 53, 195.
- [200] Y. Cao, P. Shao, Y. Chen, X. Zhou, L. Yang, H. Shi, K. Yu, X. Luo, X. Luo, Resour., Conserv. Recycl. 2021, 169, 105519.
- [201] W. D. Bonificio, D. R. Clarke, Environ. Sci. Technol. Lett. 2016, 3, 180.
- [202] P. R. Yaashikaa, B. Priyanka, P. Senthil Kumar, S. Karishma, S. Jeevanantham, S. Indraganti, Chemosphere 2022, 287, 132230.
- [203] M. Aryal, M. Liakopoulou-Kyriakides, Colloids Surf., A 2011, 387, 43.
- [204] X. Xie, X. Tan, Y. Yu, Y. Li, P. Wang, Y. Liang, Y. Yan, J. Hazard. Mater. 2022, 424, 127642.
- [205] Y. Cheng, T. Zhang, L. Zhang, Z. Ke, L. Kovarik, H. Dong, J. Hazard. Mater. 2022, 426, 127844.
- [206] N. Das, D. Das, J. Rare Earths 2013, 31, 933.
- [207] S. W. Won, P. Kotte, W. Wei, A. Lim, Y.-S. Yun, Bioresour. Technol. 2014, 160, 203.
- [208] D. L. Ramasamy, V. Puhakka, E. Repo, S. Ben Hammouda, M. Sillanpää, Chem. Eng. J. 2018, 341, 351.
- [209] Y. Vicente-Martínez, M. Caravaca, A. Soto-Meca, O. De Francisco-Ortiz, F. Gimeno, Sci. Total Environ. 2020, 709, 136111.
- [210] T. H. Bui, S. P. Hong, J. Yoon, Water Res. 2018, 134, 22.
- [211] H. Li, T. Chen, J. Jiang, G. Gao, C. Wang, Z. Lu, Chem. Eng. J. 2023, 451, 138662.
- [212] F. S. A. Khan, N. M. Mubarak, Y. H. Tan, M. Khalid, R. R. Karri, R. Walvekar, E. C. Abdullah, S. Nizamuddin, S. A. Mazari, J. Hazard. Mater. 2021, 413, 125375.
- [213] V. Gunarathne, A. U. Rajapaksha, M. Vithanage, D. S. Alessi, R. Selvasembian, Mu. Naushad, S. You, P. Oleszczuk, Y. S. Ok, Crit. Rev. Environ. Sci. Technol. 2022, 52, 1022.



- [253] J. Li, S. Xiong, Y. Liu, Z. Ju, Y. Qian, Nano Energy 2013, 2, 1249.
- H. Guo, J. Guo, Y. Zhang, G. Zeng, J. Mater. Chem. A 2020, 8, 7588. [215] N. A. Snyder, C. G. Morales-Guio, Electrochem. Sci. Adv. 2022, Smet, Energy Environ. Sci. 2021, 14, 1095. e2200010.
- [216] Y. Lei, B. Song, R. D. van der Weijden, M. Saakes, C. J. N. Buisman, Environ. Sci. Technol. 2017, 51, 11156.

[214] N. Tang, J. Liang, C. Niu, H. Wang, Y. Luo, W. Xing, S. Ye, C. Liang,

- [217] F. Endrizzi, L. Rao, Chemistry 2014, 20, 14499.
- [218] R. V. Davies, D. J. Kennedy, R. W. McIlroy, D. R. Spence, K. M. Hill, Nature 1964, 203, 1110.
- [219] C. Liu, P.-C. Hsu, J. Xie, J. Zhao, T. Wu, H. Wang, W. Liu, J. Zhang, S. Chu, Y. Cui, Nat. Energy 2017, 2, 17007.
- [220] X. Tang, Y. Liu, M. Liu, H. Chen, P. Huang, H. Ruan, Y. Zheng, F. Yang, R. He, W. Zhu, Nanoscale 2022, 14, 6285.
- [221] X. Liu, Y. Xie, M. Hao, Z. Chen, H. Yang, G. I. N. Waterhouse, S. Ma, X. Wang, Adv. Sci. 2022, 9, 2201735.
- [222] A. Fujishima, K. Honda, Nature 1972, 238, 37.
- [223] D. Wang, S. Chen, S. Lai, W. Dai, L. Yang, L. Deng, M. Suo, X. Wang, J.-P. Zou, S.-L. Luo, Chin. Chem. Lett. 2023, 34, 107861.
- [224] C. A. Martínez-Huitle, S. Ferro, Chem. Soc. Rev. 2006, 35, 1324.
- [225] F. E. Osterloh, ACS Energy Lett. 2017, 2, 445.
- [226] D. C. Hurum, A. G. Agrios, K. A. Gray, T. Rajh, M. C. Thurnauer, J. Phys. Chem. B 2003, 107, 4545.
- [227] W. Choi, A. Termin, M. R. Hoffmann, J. Phys. Chem. 1994, 98, 13669.
- [228] S. Banerjee, S. C. Pillai, P. Falaras, K. E. O'Shea, J. A. Byrne, D. D. Dionysiou, J. Phys. Chem. Lett. 2014, 5, 2543.
- [229] H. Zhang, A. U. Mane, X. Yang, Z. Xia, E. F. Barry, J. Luo, Y. Wan, J. W. Elam, S. B. Darling, Adv. Funct. Mater. 2020, 30, 2002847.
- [230] S. K. Loeb, P. J. J. Alvarez, J. A. Brame, E. L. Cates, W. Choi, J. Crittenden, D. D. Dionysiou, Q. Li, G. Li-Puma, X. Quan, D. L. Sedlak, T. D. Waite, P. Westerhoff, J.-H. Kim, Environ. Sci. Technol. **2019**, *53*, 2937.
- [231] M. Liao, L. Su, Y. Deng, S. Xiong, R. Tang, Z. Wu, C. Ding, L. Yang, D. Gong, J. Mater. Sci. 2021, 56, 14416.
- [232] P. Niu, G. Liu, H.-M. Cheng, J. Phys. Chem. C 2012, 116, 11013.
- [233] W. Wang, M. O. Tadé, Z. Shao, Chem. Soc. Rev. 2015, 44, 5371.
- [234] X. Zhao, L. Guo, B. Zhang, H. Liu, J. Qu, Environ. Sci. Technol. 2013, 47.4480
- [235] Y. Liu, Y.-Y. Deng, Q. Zhang, H. Liu, Sci. Total Environ. 2021, 757, 143901.
- [236] B. P. Chaplin, Acc. Chem. Res. 2019, 52, 596.
- [237] W. Jin, Y. Zhang, ACS Sustainable Chem. Eng. 2020, 8, 4693.
- [238] R. Chen, T. Sheehan, J. L. Ng, M. Brucks, X. Su, Environ. Sci.: Water Res. Technol. 2020, 6, 258.
- [239] H. Kanoh, K. Ooi, Y. Miyai, S. Katoh, Langmuir 1991, 7, 1841.
- [240] M. Pasta, A. Battistel, F. L. Mantia, Energy Environ. Sci. 2012, 5, 9487.
- [241] R. Trócoli, C. Erinmwingbovo, F. L. Mantia, ChemElectroChem 2017, 4, 143.
- [242] G. Yan, M. Wang, G. T. Hill, S. Zou, C. Liu, Proc. Natl. Acad. Sci. USA 2022, 119, e2200751119.
- [243] G. T. Hill, F. Shi, H. Zhou, Y. Han, C. Liu, Matter 2021, 4, 1611.
- [244] A. K. Padhi, K. S. Nanjundaswamy, J. B. Goodenough, J. Electrochem. Soc. 1997, 144, 1188.
- [245] R. Trócoli, A. Battistel, F. L. Mantia, Chemistry 2014, 20, 9888.
- [246] Y. Mu, C. Zhang, W. Zhang, Y. Wang, Desalination 2021, 511, 115112.
- [247] L. L. Missoni, F. Marchini, M. del Pozo, E. J. Calvo, J. Electrochem. Soc. 2016, 163, A1898.
- [248] J. Sun, D. Liang, X. Meng, Z. Li, Processes 2022, 10, 2654.
- [249] H. Kanoh, K. Ooi, Y. Miyai, S. Katoh, Sep. Sci. Technol. 1993, 28, 643.
- [250] J. Lee, S.-H. Yu, C. Kim, Y.-E. Sung, J. Yoon, Phys. Chem. Chem. Phys. 2013, 15, 7690.
- [251] S. Kim, J. Lee, J. S. Kang, K. Jo, S. Kim, Y.-E. Sung, J. Yoon, Chemosphere 2015, 125, 50.
- [252] S. P. Ong, V. L. Chevrier, G. Hautier, A. Jain, C. Moore, S. Kim, X. Ma, G. Ceder, Energy Environ. Sci. 2011, 4, 3680.

- [254] J. G. Gamaethiralalage, K. Singh, S. Sahin, J. Yoon, M. Elimelech, M. E. Suss, P. Liang, P. M. Biesheuvel, R. L. Zornitta, L. C. P. M. de
- [255] S. Porada, R. Zhao, A. van der Wal, V. Presser, P. M. Biesheuvel, Prog. Mater. Sci. 2013, 58, 1388.
- [256] W. Xing, J. Liang, W. Tang, D. He, M. Yan, X. Wang, Y. Luo, N. Tang, M. Huang, Desalination 2020, 482, 114390.
- [257] F. Zhao, S. Chen, H. Xiang, T. Gao, D. Wang, D. Wei, M. Sillanpää, Y. Ke, C.-J. Tang, Carbon 2022, 197, 282.
- [258] F. Gao, X. Li, W. Shi, Z. Wang, ACS Appl. Mater. Interfaces 2022, 14, 31962.
- [259] S. K. Simotwo, C. DelRe, V. Kalra, ACS Appl. Mater. Interfaces 2016, 8, 21261.
- [260] Q. Ji, C. Hu, H. Liu, J. Qu, Chem. Eng. J. 2018, 350, 608.
- [261] M. Kumar, P. Sinha, T. Pal, K. K. Kar, in Handbook of Nanocomposite Supercapacitor Materials II, Springer Nature, Cham, Switzerland 2020, pp. 29-70.
- [262] Z.-H. Huang, Z. Yang, F. Kang, M. Inagaki, J. Mater. Chem. A 2017, 5. 470.
- [263] S. Bao, J. Duan, Y. Zhang, Chemosphere 2018, 208, 14.
- [264] S. Yang, J. Choi, J. Yeo, S. Jeon, H. Park, D. K. Kim, Environ. Sci. Technol. 2016, 50, 5892.
- [265] Y. Bian, X. Chen, L. Lu, P. Liang, Z. J. Ren, ACS Sustainable Chem. Eng. 2019, 7, 7844.
- [266] L. Lin, J. Hu, J. Liu, X. He, B. Li, X. Li, Environ. Sci. Technol. 2020, 54, 12723.
- [267] G. Lota, K. Fic, E. Frackowiak, Energy Environ. Sci. 2011, 4, 1592.
- [268] L. Ren, J. Zhou, S. Xiong, Y. Wang, Langmuir 2020, 36, 12030.
- [269] C. S. Sharma, H. Katepalli, A. Sharma, M. Madou, Carbon 2011, 49, 1727.
- [270] S. Maldonado, K. J. Stevenson, J. Phys. Chem. B 2004, 108, 11375.
- [271] C.-S. Lee, S. E. Baker, M. S. Marcus, W. Yang, M. A. Eriksson, R. J. Hamers, Nano Lett. 2004, 4, 1713.
- [272] Y. Cheng, L. Huang, X. Xiao, B. Yao, L. Yuan, T. Li, Z. Hu, B. Wang, J. Wan, J. Zhou, Nano Energy 2015, 15, 66.
- [273] L. Kebabsa, J. Kim, D. Lee, B. Lee, Appl. Surf. Sci. 2020, 511, 145313.
- [274] C. Wang, L. Chen, S. Liu, J. Colloid Interface Sci. 2019, 548, 160.
- [275] M. Zhang, W. Kong, J. Electroanal. Chem. 2020, 878, 114703.
- [276] C. Liu, T. Wu, P.-C. Hsu, J. Xie, J. Zhao, K. Liu, J. Sun, J. Xu, J. Tang, Z. Ye, D. Lin, Y. Cui, ACS Nano 2019, 13, 6431.
- [277] P. Liu, T. Yan, J. Zhang, L. Shi, D. Zhang, J. Mater. Chem. A 2017, 5, 14748.
- [278] Y. Wei, L. Xu, K. Yang, Y. Wang, Z. Wang, Y. Kong, H. Xue, J. Electrochem. Soc. 2017, 164, E17.
- [279] M. Shestakova, M. Sillanpää, Rev. Environ. Sci. Biotechnol. 2017, 16, 223.
- [280] Y. Feng, L. Yang, J. Liu, B. E. Logan, Environ. Sci.: Water Res. Technol. **2016**, 2, 800.
- [281] J. Du, B. Zhang, J. Li, B. Lai, Chin. Chem. Lett. 2020, 31, 2575.
- [282] M. Hu, Z. Sun, J. Hu, H. Lei, W. Jin, Ind. Eng. Chem. Res. 2019, 58,
- [283] N. A. A. Qasem, R. H. Mohammed, D. U. Lawal, npj Clean Water 2021. 4. 36.
- [284] S. Kim, J. Kim, S. Kim, J. Lee, J. Yoon, Environ. Sci.: Water Res. Technol. **2018**, 4, 175.
- [285] K. Du, L. Zhang, J. Shan, J. Guo, J. Mao, C.-C. Yang, C.-H. Wang, Z. Hu, T. Ling, Nat. Commun. 2022, 13, 5448.
- [286] F. Chen, C. Ma, C. Zou, L. Cao, J. Yang, Electrochim. Acta 2022, 404, 139722.
- [287] C. Tunsu, B. Wickman, Nat. Commun. 2018, 9, 4876.
- [288] Q. Zhou, X. Zhou, R. Zheng, Z. Liu, J. Wang, Sci. Total Environ. 2022, 806, 150088.
- [289] Y. Einaga, Acc. Chem. Res. 2022, 55, 3605.



- [290] K. Natsui, C. Yamaguchi, Y. Einaga, ECS Meet. Abstr. 2016, 48, 3578.
- [291] S. Tamilmani, W. H. Huang, S. Raghavan, J. Farrell, IEEE Trans. Semicond. Manuf. 2004, 17, 448.
- [292] N. Oturan, M. A. Oturan, in Electrochemical Water and Wastewater Treatment (Eds: C. A. Martínez-Huitle, M. A. Rodrigo, O. Scialdone), Butterworth-Heinemann, Oxford, UK 2018, pp. 193–221.
- [293] S. Yu, Y. Liu, H. Pang, H. Tang, J. Wang, S. Zhang, X. Wang, in Emerging Nanomaterials for Recovery of Toxic and Radioactive Metal Ions from Environmental Media (Ed: X. Wang), Elsevier, Amsterdam, The Netherlands 2022, pp. 1–47.
- [294] P. Xu, B. Elson, J. E. Drewes, in *Desalination*, John Wiley & Sons, Ltd., Hoboken, NJ, USA 2019, pp. 497–523.
- [295] M. Panizza, in *Electrochemistry for the Environment* (Eds: C. Comninellis, G. Chen), Springer, New York 2010, pp. 25-54.
- [296] R. A. Barakwan, W. B. Pratiwi, Y. Trihadiningrum, A. Y. Bagastyo, J. Mater. Cycles Waste Manage. 2020, 22, 2130.
- [297] A. Rahmani, A. Shabanloo, N. Shabanloo, *Mater. Today Chem.* 2023, 27, 101311.
- [298] Z. Hu, J. Cai, G. Song, Y. Tian, M. Zhou, Curr. Opin. Electrochem. 2021, 26, 100659.
- [299] J. Wang, X. Chen, J. Yao, G. Huang, Int. J. Electrochem. Sci. 2015, 10, 5726.
- [300] D. A. El-Gayar, A. H. El-Shazly, Y. A. El-Taweel, G. H. Sedahmed, Chem. Eng. J. 2010, 162, 877.
- [301] G. R. Salazar-Banda, G. d. O. S. Santos, I. M. Duarte Gonzaga, A. R. Dória, K. I. Barrios Eguiluz, Curr. Opin. Electrochem. 2021, 26, 100663.
- [302] X. Shao, C. Ma, L. Zhu, C. Zou, L. Cao, J. Yang, Environ. Sci. Pollut. Res. 2022, 29, 89156.
- [303] X. Qin, F. Gao, G. Chen, J. Appl. Electrochem. 2010, 40, 1797.
- [304] M. Mehdipour, S. H. Tabaian, S. Firoozi, J. Iran. Chem. Soc. 2021, 18, 233.
- [305] Y. Du, J. Yang, Y. Liu, J. Zhou, L. Cao, J. Yang, Sep. Purif. Technol. 2022, 289, 120808.
- [306] F. R. Pombo, A. J. B. Dutra, Environ. Prog. Sustainable Energy 2013, 32, 52.
- [307] J. Kim, S. Bae, Environ. Eng. Res. 2019, 24, 646.
- [308] C. Wang, T. Li, G. Yu, S. Deng, Chemosphere 2021, 263, 128208.
- [309] P. V. Nidheesh, G. Divyapriya, N. Oturan, C. Trellu, M. A. Oturan, ChemElectroChem 2019, 6, 2124.
- [310] S. Nihongi, A. Otake, J. Du, Y. Einaga, Carbon 2022, 200, 456.
- [311] J. H. T. Luong, K. B. Male, J. D. Glennon, Analyst 2009, 134, 1965.
- [312] K. Muzyka, J. Sun, T. H. Fereja, Y. Lan, W. Zhang, G. Xu, Anal. Methods 2019, 11, 397.
- [313] Q. Zhuo, X. Xu, S. Xie, X. Ren, Z. Chen, B. Yang, Y. Li, J. Niu, J. Environ. Sci. 2022, 116, 103.
- [314] R. Burgos-Castillo, M. Sillanpää, E. Brillas, I. Sirés, Sci. Total Environ. 2018, 644, 173.
- [315] S. Hand, R. D. Cusick, Environ. Sci.: Water Res. Technol. 2020, 6, 925.
- [316] Y. Zhang, Y. Hu, L. Wang, W. Sun, Miner. Eng. 2019, 139, 105868.
- [317] X. Li, G. Ni, T. Cooper, N. Xu, J. Li, L. Zhou, X. Hu, B. Zhu, P. Yao, J. Zhu, *Joule* 2019, 3, 1798.
- [318] Y. Wang, X. Wu, B. Shao, X. Yang, G. Owens, H. Xu, Sci. Bull. 2020, 65, 1380.
- [319] S.-L. Wu, L.-N. Quan, Y.-T. Huang, Y.-T. Li, H.-C. Yang, S. B. Darling, ACS Appl. Mater. Interfaces 2021, 13, 39513.
- [320] J. C.-T. Lin, D.-J. Lee, C. Huang, Sep. Sci. Technol. 2010, 45, 858.
- [321] D. Rana, T. Matsuura, Chem. Rev. 2010, 110, 2448.
- [322] S.-L. Wu, H. Chen, H.-L. Wang, X. Chen, H.-C. Yang, S. B. Darling, Environ. Sci.: Water Res. Technol. 2021, 7, 24.
- [323] J. Zhou, Y. Gu, P. Liu, P. Wang, L. Miao, J. Liu, A. Wei, X. Mu, J. Li, J. Zhu, Adv. Funct. Mater. 2019, 29, 1903255.
- [324] F. Zhao, Y. Guo, X. Zhou, W. Shi, G. Yu, Nat. Rev. Mater. 2020, 5, 388.

- [325] G. Liu, T. Chen, J. Xu, G. Yao, J. Xie, Y. Cheng, Z. Miao, K. Wang, Cell Rep. Phys. Sci. 2021, 2, 100310.
- [326] M. Gao, L. Zhu, C. K. Peh, G. W. Ho, Energy Environ. Sci. 2019, 12, 841.
- [327] H. Ghasemi, G. Ni, A. M. Marconnet, J. Loomis, S. Yerci, N. Miljkovic, G. Chen, Nat. Commun. 2014, 5, 4449.
- [328] X. Li, W. Xu, M. Tang, L. Zhou, B. Zhu, S. Zhu, J. Zhu, Proc. Natl. Acad. Sci. USA 2016, 113, 13953.
- [329] N. Xu, J. Li, Y. Wang, C. Fang, X. Li, Y. Wang, L. Zhou, B. Zhu, Z. Wu, S. Zhu, J. Zhu, Sci. Adv. 2019, 5, eaaw7013.
- [330] Y. Wang, L. Zhang, P. Wang, ACS Sustainable Chem. Eng. 2016, 4, 1223.
- [331] Y. Xia, Q. Hou, H. Jubaer, Y. Li, Y. Kang, S. Yuan, H. Liu, M. W. Woo, L. Zhang, L. Gao, H. Wang, X. Zhang, Energy Environ. Sci. 2019, 12, 1840.
- [332] L. Wu, Z. Dong, Z. Cai, T. Ganapathy, N. X. Fang, C. Li, C. Yu, Y. Zhang, Y. Song, Nat. Commun. 2020, 11, 521.
- [333] J. Li, X. Zhou, J. Zhang, C. Liu, F. Wang, Y. Zhao, H. Sun, Z. Zhu, W. Liang, A. Li, ACS Appl. Energy Mater. 2020, 3, 3024.
- [334] F. Wu, D. Liu, G. Li, L. Li, L. Yan, G. Hong, X. Zhang, Nanoscale 2021, 13, 5419.
- [335] Z. Liu, B. Wu, B. Zhu, Z. Chen, M. Zhu, X. Liu, Adv. Funct. Mater. 2019, 29, 1905485.
- [336] I. Ibrahim, V. Bhoopal, D. H. Seo, M. Afsari, H. K. Shon, L. D. Tijing, Mater. Today Energy 2021, 21, 100716.
- [337] T. Arunkumar, H. W. Lim, D. Denkenberger, S. J. Lee, Renewable Sustainable Energy Rev 2022, 158, 112121.
- [338] R. Fillet, V. Nicolas, V. Fierro, A. Celzard, Sol. Energy Mater. Sol. Cells 2021, 219, 110814.
- [339] N. Xu, X. Hu, W. Xu, X. Li, L. Zhou, S. Zhu, J. Zhu, Adv. Mater. 2017, 29, 1606762.
- [340] S. He, C. Chen, Y. Kuang, R. Mi, Y. Liu, Y. Pei, W. Kong, W. Gan, H. Xie, E. Hitz, C. Jia, X. Chen, A. Gong, J. Liao, J. Li, Z. J. Ren, B. Yang, S. Das, L. Hu, *Energy Environ. Sci.* 2019, 12, 1558.
- [341] Y. Kuang, C. Chen, S. He, E. M. Hitz, Y. Wang, W. Gan, R. Mi, L. Hu, Adv. Mater. 2019, 31, 1900498.
- [342] Y. Bian, Q. Du, K. Tang, Y. Shen, L. Hao, D. Zhou, X. Wang, Z. Xu, H. Zhang, L. Zhao, S. Zhu, J. Ye, H. Lu, Y. Yang, R. Zhang, Y. Zheng, S. Gu, Adv. Mater. Technol. 2019, 4, 1800593.
- [343] P. Sun, W. Zhang, I. Zada, Y. Zhang, J. Gu, Q. Liu, H. Su, D. Pantelić, B. Jelenković, D. Zhang, ACS Appl. Mater. Interfaces 2020, 12, 2171.
- [344] L. Yang, G. Chen, N. Zhang, Y. Xu, X. Xu, ACS Sustainable Chem. Eng. 2019, 7, 19311.
- [345] Q. Hou, H. Zhou, W. Zhang, Q. Chang, J. Yang, C. Xue, S. Hu, Sci. Total Environ. 2021, 759, 144317.
- [346] H.-C. Yang, Z. Chen, Y. Xie, J. Wang, J. W. Elam, W. Li, S. B. Darling, Adv. Mater. Interfaces 2019, 6, 1801252.
- [347] J. Liang, H. Liu, J. Yu, L. Zhou, J. Zhu, Nanophotonics 2019, 8, 771.
- [348] A. O. Govorov, H. H. Richardson, *Nano Today* **2007**, *2*, 30.
- [349] J. Chen, Z. Ye, F. Yang, Y. Yin, Small Sci. 2021, 1, 2000055.
- [350] O. Neumann, A. S. Urban, J. Day, S. Lal, P. Nordlander, N. J. Halas, ACS Nano 2013, 7, 42.
- [351] H. Jin, G. Lin, L. Bai, A. Zeiny, D. Wen, Nano Energy 2016, 28, 397.
- [352] H. Wang, L. Miao, S. Tanemura, Sol. RRL **2017**, *1*, 1600023.
- [353] L. Zhou, Y. Tan, J. Wang, W. Xu, Y. Yuan, W. Cai, S. Zhu, J. Zhu, Nat. Photonics 2016, 10, 393.
- [354] Y. Lin, Z. Chen, L. Fang, M. Meng, Z. Liu, Y. Di, W. Cai, S. Huang, Z. Gan, *Nanotechnology* 2018, 30, 015402.
- [355] M. Zhu, Y. Li, F. Chen, X. Zhu, J. Dai, Y. Li, Z. Yang, X. Yan, J. Song, Y. Wang, E. Hitz, W. Luo, M. Lu, B. Yang, L. Hu, Adv. Energy Mater. 2018, 8, 1701028.
- [356] C. Sheng, N. Yang, Y. Yan, X. Shen, C. Jin, Z. Wang, Q. Sun, Appl. Therm. Eng. 2020, 167, 114712.



- [357] Y. Cui, K. H. Fung, J. Xu, H. Ma, Y. Jin, S. He, N. X. Fang, Nano Lett. 2012, 12, 1443.
- [358] Y. Zhang, Y. Wang, B. Yu, K. Yin, Z. Zhang, Adv. Mater. 2022, 34, 2200108.
- [359] F. Yang, J. Chen, Z. Ye, D. Ding, N. V. Myung, Y. Yin, Adv. Funct. Mater. 2021, 31, 2006294.
- [360] I. Ibrahim, D. H. Seo, A. M. McDonagh, H. K. Shon, L. Tijing, Desalination 2021, 500, 114853.
- [361] S. Huang, Y. Long, H. Yi, Z. Yang, L. Pang, Z. Jin, Q. Liao, L. Zhang, Y. Zhang, Y. Chen, H. Cui, J. Lu, X. Peng, H. Liang, S. Ruan, Y.-J. Zeng, Appl. Surf. Sci. 2019, 491, 328.
- [362] C. Zhang, C. Yan, Z. Xue, W. Yu, Y. Xie, T. Wang, Small 2016, 12, 5320.
- [363] Q. Zhang, X. Yin, C. Zhang, Y. Li, K. Xiang, W. Luo, X. Qiao, Small 2022, 18, 2202867.
- [364] C. Mu, Y. Song, K. Deng, S. Lin, Y. Bi, F. Scarpa, D. Crouse, Adv. Sustainable Syst. 2017, 1, 1700064.
- [365] J. Zhang, Y. Yang, J. Zhao, Z. Dai, W. Liu, C. Chen, S. Gao, D. A. Golosov, S. M. Zavadski, S. N. Melnikov, *Mater. Res. Bull.* 2019, 118, 110529.
- [366] Z. Li, M. Zheng, N. Wei, Y. Lin, W. Chu, R. Xu, H. Wang, J. Tian, H. Cui, Sol. Energy Mater. Sol. Cells 2020, 205, 110254.
- [367] Z. Guo, W. Zhou, N. Arshad, Z. Zhang, D. Yan, M. S. Irshad, L. Yu, X. Wang, *Carbon* **2022**, *186*, 19.
- [368] P. Liu, Y. Hu, X.-Y. Li, L. Xu, C. Chen, B. Yuan, M.-L. Fu, Angew. Chem., Int. Ed. 2022, 61, e202208587.
- [369] M. Ye, J. Jia, Z. Wu, C. Qian, R. Chen, P. G. O'Brien, W. Sun, Y. Dong, G. A. Ozin, Adv. Energy Mater. 2017, 7, 1601811.
- [370] Y. Hu, H. Ma, M. Wu, T. Lin, H. Yao, F. Liu, H. Cheng, L. Qu, Nat. Commun. 2022, 13, 4335.
- [371] J. Zhao, Y. Yang, C. Yang, Y. Tian, Y. Han, J. Liu, X. Yin, W. Que, J. Mater. Chem. A 2018, 6, 16196.

- [372] F. Zhao, X. Zhou, Y. Shi, X. Qian, M. Alexander, X. Zhao, S. Mendez, R. Yang, L. Qu, G. Yu, Nat. Nanotechnol. 2018, 13, 489.
- [373] X. Wu, Y. Wang, P. Wu, J. Zhao, Y. Lu, X. Yang, H. Xu, Adv. Funct. Mater. 2021, 31, 2102618.
- [374] Z.-J. Xia, H.-C. Yang, Z. Chen, R. Z. Waldman, Y. Zhao, C. Zhang, S. N. Patel, S. B. Darling, Adv. Mater. Interfaces 2019, 6, 1900254.
- [375] W.-R. Cui, C.-R. Zhang, R.-P. Liang, J.-D. Qiu, J. Mater. Chem. A 2021, 9. 25611.
- [376] C.-R. Zhang, W.-R. Cui, C.-P. Niu, S.-M. Yi, R.-P. Liang, J.-X. Qi, X.-J. Chen, W. Jiang, L. Zhang, J.-D. Qiu, Chem. Eng. J. 2022, 428, 131178.
- [377] C. Zhang, Z. Chen, Z. Xia, R. Z. Waldman, S.-L. Wu, H.-C. Yang, S. B. Darling, Environ. Sci.: Water Res. Technol. 2020, 6, 911.
- [378] S. Ma, W. Qarony, M. I. Hossain, C. T. Yip, Y. H. Tsang, Sol. Energy Mater. Sol. Cells 2019, 196, 36.
- [379] P. He, L. Hao, N. Liu, H. Bai, R. Niu, J. Gong, Chem. Eng. J. 2021, 423, 130268.
- [380] G. Chen, Z. Jiang, A. Li, X. Chen, Z. Ma, H. Song, J. Mater. Chem. A 2021, 9, 16805.
- [381] V. Abetz, Macromol. Rapid Commun. 2015, 36, 10.
- [382] R. Z. Waldman, F. Gao, W. A. Phillip, S. B. Darling, J. Membr. Sci. 2021, 633, 119389.
- [383] J. Wang, H. Zhou, S. Li, L. Wang, Angew. Chem., Int. Ed. 2023, e202218321.
- [384] V. I. Parvulescu, F. Epron, H. Garcia, P. Granger, Chem. Rev. 2022, 122, 2981.
- [385] A. López-Magano, A. Jiménez-Almarza, J. Alemán, R. Mas-Ballesté, Catalysts 2020, 10, 720.
- [386] X. Zhou, Q. Liu, C. Jiang, B. Ji, X. Ji, Y. Tang, H.-M. Cheng, Angew. Chem., Int. Ed. 2020, 59, 3802.
- [387] L. Zhang, H. Wang, X. Zhang, Y. Tang, Adv. Funct. Mater. 2021, 31, 2010958



Seth B. Darling is the Chief Science & Technology Officer for the Advanced Energy Technologies Directorate and a Senior Scientist in the Chemical Sciences & Engineering Division at the Argonne National Laboratory. He also serves as the Director of the Advanced Materials for Energy-Water Systems Energy Frontier Research Center and is a Senior Scientist at the Pritzker School of Molecular Engineering at the University of Chicago. His group's research centers around molecular engineering with a current emphasis on advanced materials for cleaning water.